Alma Mater Studiorum · Università di Bologna

Scuola di Scienze
Dipartimento di Fisica e Astronomia
Corso di Laurea in Fisica

Toeplitz Matrices for the Long-Range Kitaev Model

Relatore:
Prof.ssa Elisa Ercolessi

Presentata da:
Sunny Pradhan

Correlatore:
Dott. Davide Vodola

Anno Accademico 2017/18

Abstract

In this thesis we discuss the topological phases of a one-dimensional superconductive quantum chain, the Kitaev model, alongside a couple of its extension: one with long-range pairing and one with coupling at the boundaries. These phases are investigated with the help of the theory of Toeplitz matrices, which simplifies the solution of the spectrum and of the correlation functions. Furthermore, within the theory of Toeplitz matrices we identify a particular winding number, which serves as a tool for detecting topological phases and massless edge states. Based on this identification, and on some numerical analysis of the long-range Kitaev chain, we propose a conjecture about the emergence of massive edge states, and use it to explain a phase transition without closure of the gap that happens in the long-range Kitaev chain.

Sommario

In questa tesi discuteremo delle fasi topologiche di una catena quantistica unidimensionale con accoppiamento superconduttivo, nota anche come catena di Kitaev, insieme a un paio di estensioni di essa: una con accoppiamento a lungo raggio e una con accoppiamento ai bordi della catena. Queste fasi verranno investigate con l'aiuto della teoria delle matrici di Toeplitz, che semplifica sia la risoluzione dello spettro che delle funzioni di correlazione. Inoltre, all'interno della teoria delle matrici di Toeplitz identificheremo un winding number particolare, che potrà essere usato come strumento per rilevare fasi topologiche e edge state non massivi. Sulla base di questa identificazione, insieme ad alcune analisi numeriche eseguite sulla catena di Kitaev a lungo-raggio, proporremo una congettura sulla comparsa di edge state massivi, che verrà usata poi per spiegare una transizione di fase senza chiusura del gap che avviene nella catena di Kitaev a lungo raggio.

Contents

Introduction

This thesis deals mainly with two subjects: topological phases of a quantum system and the theory of Toeplitz matrices. The former are a new kind of states of the quantum world, which have been discovered and studies just in these last decades. The latter is a branch of functional analysis and linear algebra, which has already been applied to different physical problems: from differential equations to random processes.

Topological matter is an ever-growing field of condensed matter physics which, from a theoretical point of view, offers a variety of intersections of different branches of mathematics and theoretical physics; from a more practical viewpoint, it is full of future technological applications, like quantum computing. The novelty of this field is the discovery of phase transitions without any kind of spontaneous symmetry breaking, especially in low-dimensional systems. Moreover, a new plethora of phenomena emerged in these systems, like for example: non-dissipative charge transport, fractional excitations, non-Abelian statistics of quasiparticles and so on [7, 18, 31, 34].

Therefore, it was made necessary to investigate which were the key properties that truly distinguish one state from another. An important hint came from topology, a branch of mathematics concerned with the classification of geometrical objects, like manifolds and surfaces. Briefly speaking, two objects are topologically equivalent if one can be smoothly deformed into the other, without any abrupt changes. This idea of smooth deformation was brought into the field of Physics, as a way to distinguish and categorize the different states. Roughly, two states are in the same topological phase if one can be slowly deformed into the other, by changing its parameters, without going through any phase transitions.

This treatise focuses on a particular one-dimensional model, the *Kitaev chain*, which was introduced for the first time by Kitaev in its seminal work [24]. It is a relatively simple toy model with a rich phase diagram, as it presents both a trivial and a topological phase. One of the main properties of this chain is the presence of *unpaired Majorana fermions* in the latter phase. Majorana fermions are self-conjugated fermions, i.e. they are their own antiparticles, that appears frequently as quasiparticle excitations in topological

systems. Furthermore, this work also focuses on some extension of the Kitaev chain, in particular the introduction of a long-range superconductive pairing or a generalized boundary conditions. These cases possess *massive edge states*, a new kind of quasiparticles excitations, and what looks like a *brand new kind of phase transitions*.

For the investigation of these models we choose to use the theory of Toeplitz matrices, which are constant along the parallels of the main diagonal. Even though they appear to have a simple form, the theory behind is very rich. The reason behind this choice lies in the fact that the equations that describe the spectrum of a fermionic chain, presented for the first time by Lieb et al. [29], can be expressed in the language of Toeplitz matrices. Their application makes the calculation of some important quantities, like the spectrum or the correlation functions, much easier. Furthermore, it also offer some tools that let us characterize the ordinary topological phases, and also gain some intuition about the new kind of phase transition we have in the long-range pairing case.

The present thesis is structured as follows:

- In Chap. 1 we give an introduction to some basic tools and notions used in the field of Topological Matter. We start with the quantum Hall effect, which served as a starting point for topological insulators and topological superconductors. The chapter moves onto the subject of translationally invariant systems (i.e. Bloch theorem) and antiunitary symmetries. Then, adiabatic equivalence and topological invariants are discussed. Subsequently, a toy model is presented, the SSH model, as an applications of all these notions. The chapter closes with a discussion about topological phases and their classification in noninteracting fermionic Hamiltonian.

- In Chap. 2 we present a summary of the subject of Toeplitz matrices. We start with their definition and some of their basic properties. We also introduce the topics of C^*-algebras and Fredholm operators, which are indispensable in the theory of Toeplitz matrices. Large part of the chapter is dedicated to the sequences of Toeplitz matrices and their spectrum. Circulant matrices are also discussed, because they are convenient in the context of periodic systems.

- In Chap. 3, after a brief discussion about the Majorana fermions and superconductive systems, the Lieb-Schultz-Mattis method is presented, and then their solutions for the spectrum and for the correlation functions, with Toeplitz matrices, is carried out. After that, we finally discuss the Kitaev model and its long-range pairing extension, along the solution of the model in terms of spectrum and correlation

function. Most importantly, in the last section, the emergence of massive edge states is discussed.

- in Chap. 4 we presents some qualitative analysis, which also includes numerical analysis, about two extensions of the Kitaev model: the one with coupling the end of the chain, and the one with long-range superconductive pairing. We will see that these models seems to present phases with massive edge states. In the latter case, we will provide a conjecture, that involves the theory of Toeplitz matrices, that may explain the emergence of massive edge states.

1

Basic notions of Topological Matter

Condensed Matter Physics is concerned with how the different building blocks of matter can rearrange themself, in order to build its different states. In a sense, it deals with the *order* in the quantum world. The main paradigm being used in the field is the Ginzburg-Landau theory, based on the mechanism of *Spontaneous Symmetry Breaking* (SSB), one of the greatest discovery of XX century theoretical physics. It describes systems where the dynamics, specifically the Hamiltonian or the equations of motion, has some special kind of symmetries, as they are invariant under some group of transformation, but the lowest energy solutions, the so-called vacuum solutions or ground states, do not exhibit such properties.

One of the most clear examples of SSB is the phenomenon of ferromagnetism. At a high temperature, a ferrous material exhibits an isotropic behaviour, in the sense that there is no preferred direction in space, which can only be broken by an external magnetic field, due to the fact that such a field aligns the magnetic moments of the sample. From a dynamical point of view, this would mean to introduce some kinds of interaction with the external field that affect the Hamiltonian. Now, suppose we first move the system in a low temperature regime (below some critical value) and then slowly turn off any magnetic field. The result of this process is a spontaneous magnetization of the sample, namely the alignment of the magnetic moments of the sample, even in the absence of any external fields. This magnetization breaks the isotropy of the state without breaking that of the Hamiltonian. Even more exotic cases of SSB are possible, like superconductivity or the Higgs mechanism, where we have a breaking of a more abstract kind of symmetry, the gauge symmetry.

The study of SSB and phase transitions in the Ginzburg-Landau framework relies on *local* order parameter that lets us characterize the different phases and this revealed to be a major limitation. In the last forty years or so, in the field of Condensed Matter a new

kind of order have been found, the *topological order*, for which the Ginzburg-Landau theory is totally ineffective. They were firstly observed in the Quantum Hall Effect (QHE) and through a study of it *topological insulators* and *topological superconductors* were discovered.

The choice of the word "topological" is not random. Topology is used in mathematics as a mean to classify different geometrical objects into broad classes, discarding small details and focusing on fundamental and global proprieties. Moreover, elements of different classes cannot be related by continuous transformations. For example, 2D closed surfaces can be classified by the number of holes in them, called genus, which cannot be altered continuously. The genus is an example of a *topological invariant* and they usually take only integer values.

In the case of quantum systems, topology is used to classify different quantum states that cannot be connected by an *adiabatic transformation* (which will be defined in more detail in 1.4). The QH state was the first state to be discovered that was topologically distinct from all states of the matter known before. The peculiarity of this state is that it shows an insulating behaviour in the bulk but a conductive one along the edges, where charge is carried without dispersion. The quest for topologically equivalent states led to the discovery of topological insulators which, roughly speaking, present the same kind of behaviour but are not restricted to the same symmetries and interactions of the QHE. An example is the Quantum Spin Hall Effect, which does not utilize large magnetic fields but spin-orbit coupling.

Furthermore, another important ingredient for the study of topological matter is the bulk-edge correspondence. This means that the bulk's properties and the edges states are linked together, in the sense that the topology of the bulk strongly determines the state at the edges and also the converse is true.

In the following we will give some useful basic notions about these new subjects and try to underline which are the key concepts involved.

1.1 The quantum Hall effect

As have it been said before, a prime example of topological order is the QHE, the quantum-mechanical counterpart of the classical Hall Effect but in two dimensions and strong magnetic field, at extremely low temperature. The discovery of the QHE dates back to the 1980, when Klitzing et al. [26] observed an anomalous behavior for the Hall conductivity σ_H in a silicon MOSFET, at the previously mentioned conditions. It was observed that it had fixed values, dependent only on fundamental constants, and it was

insensitive to the geometry of the device, which can be interpreted in hindsight as a first hint towards topology. Furthermore, it was found that the Hall conductivity forms certain plateaus on which its value is quantized with an integer ν as

$$\sigma_H = \frac{e^2}{2\pi\hbar}\nu\,, \qquad \nu \in \mathbb{Z}.$$

Given the fact that we are dealing with electrons moving in a two-dimensional sample, classically the action of any magnetic field perpendicular to the sample has the effect to constrain the electrons in a circular motion. From its quantization, Landau levels emerge with energy $E_n = \hbar\omega_B(n + 1/2)$, where $\omega_B = eB/m$ is the cyclotron frequency, and a high level of degeneracy [37]. The integer ν of the Hall conductivity coincides with the number of occupied Landau levels n of the sample. With n fully occupied levels, there is a gap between the occupied bands (valence band) and the unoccupied bands (conduction band). This means that from a spectral point of view, the system resembles an insulator. But unlike an ordinary insulator, it's possible to demonstrate that a QH system does not behave like one, because it can carry electrical current with no dissipation.

In this system, something odd happens at the edges, which can be visualized even in a semi-classical picture. As previously mentioned, the orbits are circular and this is true in the bulk. On the edges, due to the fact that the motion can only happen in one direction, the orbits are no more circular but become skipping along the borders as they are bound to bounce back (see Figure 1.1). The finale result is the formation of *edge modes* of *chiral* particles, in the sense that they are restricted to move only along one direction. It's possible to prove that these edge modes are responsible of the dissipation-free transport of charge. To summarize, we have obtained a state which is insulating in the bulk but conductive along the edges.

Furthermore, there is a deep connection between the Hall conductivity and topology. It was discovered by Thouless et al. [36] that the Hall conductance must take integer values and this integer relates to how the wavefunction wraps in the momentum space, which is a topological invariant known as the *Chern number*.

We now proceed by introducing some useful notions involved in the study of topological matter, like the Bloch theorem, the adiabatic connection and the Berry phase.

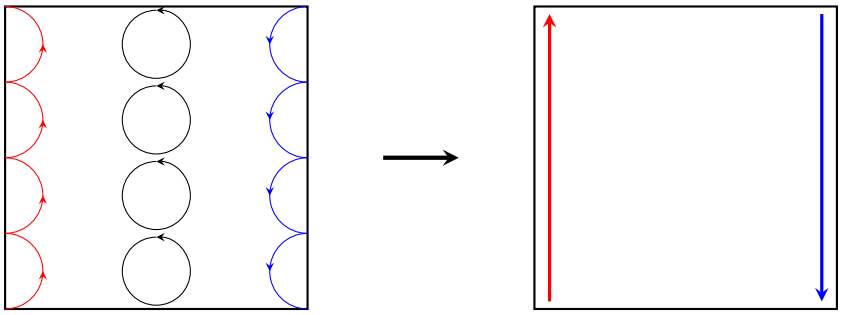

Figure 1.1: The skipping motion along the borders of the system gives rise to chiral particle who can move only in one direction. In this picture the bulk is still an insulator, all current is carried by the edges

1.2 The Bloch theorem

Suppose we have a Hamiltonian in a periodic potential, such that $H(\mathbf{r}) = H(\mathbf{r}+\mathbf{R})$ where $\mathbf{R}$ is the period of the lattice. The Bloch theorem states that the eigenfunction of such a system are in the form

$$\psi_{n,\mathbf{k}}(\mathbf{r}) = e^{i\mathbf{k}\cdot\mathbf{r}} u_{n,\mathbf{k}}(\mathbf{r}) \tag{1.1}$$

where the wavefunction $u_{n,\mathbf{k}}(\mathbf{r})$ is periodic with period $\mathbf{R}$, same as the lattice, $u_{n,\mathbf{k}}(\mathbf{r}) = u_{n,\mathbf{k}}(\mathbf{r}+\mathbf{R})$. This wavefunction is an eigenstate of the *Bloch Hamiltonian*

$$\mathcal{H}(\mathbf{k}) = e^{-i\mathbf{k}\cdot\mathbf{r}} H(\mathbf{r}) e^{i\mathbf{k}\cdot\mathbf{r}} \tag{1.2}$$

thus it satisfies

$$\mathcal{H}(\mathbf{k}) \left| u_{n,\mathbf{k}}(\mathbf{r}) \right\rangle = E_{n,\mathbf{k}} \left| u_{n,\mathbf{k}}(\mathbf{r}) \right\rangle \tag{1.3}$$

where $E_{n,\mathbf{k}}$ is the eigenvalue of the Bloch Hamiltonian and it is periodic in the crystal momentum $\mathbf{k}$: $E_{n,\mathbf{k}} = E_{n,\mathbf{k}+\mathbf{K}}$, where $\mathbf{K}$ is a reciprocal lattice vector.

The eigenvalues depend on two quantum numbers, the band index n and the crystal momentum $\mathbf{k}$. The last one can only take values in the first Brillouin Zone (BZ), namely the first cell of the reciprocal lattice with periodic boundary conditions, due to the periodicity of the energy eigenvalues, while the first one labels the different solutions of the Bloch Hamiltonian for a fixed value of $\mathbf{k}$, Furthermore, n is called band index because the energies $E_{n,\mathbf{k}}$ vary continuously with $\mathbf{k}$, thus forming an *energy band* and different band are usually separated by an *energy gap*. In the end, we see that a crystalline solid, described by a Bloch Hamiltonian, have a band structure of its energy levels. Such a structure can contain a lot of information about its macroscopic behaviour.

Recalling that we are dealing with fermions, the position of the Fermi level let us distinguish two kinds of state: the metallic one and the insulating one. The metallic state has the Fermi level inside an energy band, which means that is only partially filled. When an electric field is applied, the electrons start to shift away from the equilibrium position, as unoccupied states are available for them within the band, gaining momentum and producing an electrical current. On the other hand, insulating states have the Fermi level inside a gap, which means the lower bands are fully occupied. In this case, applying an electric field has no effect on the electrons, as they cannot access new available states, which leads to no electrical current.

1.3 Role of symmetries

A symmetry under a group G in quantum mechanics is usually represented by a family of unitary operators $\{U_i\}$, one for each elements of the group, which each commutes with the Hamiltonian

$$U_i U_i^\dagger = U_i^\dagger U_i = 1 \qquad \text{and} \qquad [U_i, H] = 0. \tag{1.4}$$

which means that it is possible to diagonalize both the Hamiltonian H and the operator U_i simultaneously. This let us partition the Hilbert space of the states into sectors, the eigenspaces of U_i, each one labeled by their eigenvalues. Furthermore, the dynamics of the Hamiltonian in one sector can be treated separately from the other sectors. A clear example of this is a translational invariant Hamiltonian, whose eigenspaces are labeled by the BZ momenta. This is just an application of the Bloch theorem, that let us deals with only Bloch Hamiltonians and to forget the translational symmetry. In conclusion, every unitary symmetry can be made to disappear by restricting our attentions to one eigenspace at a time. It is important to remark that when we refer to the Hamiltonian H, we mean the Hamiltonian of the overall system and not just the single-particle Hamiltonian. For example, as we will see next, the action of a symmetry on H might be different then that on $\mathcal{H}(\mathbf{k})$, the Bloch Hamiltonian, which can be viewed as a single-particle Hamiltonian in momentum space.

A more interesting case is when a symmetry is represented by an *antiunitary* operator, which is an antilinear map that conserve the scalar product up to a complex conjugation, like

$$A[a\alpha(x) + b\beta(x)] = \bar{a}A\alpha(x) + \bar{b}A\beta(x), \qquad \langle A\alpha | A\beta\rangle = \overline{\langle\alpha|\beta\rangle}, \tag{1.5}$$

where the bar stand for complex conjugation.

Time-reversal symmetry A fundamental antiunitary symmetry is the *time-reversal symmetry* (TRS) Θ, that maps t into $-t$. A generic Hamiltonian H is said to be TR-invariant if $\Theta H \Theta^{-1} = H$, so if it commutes with Θ. This operator can be written as a product of an unitary operator T and complex conjugation $\mathcal{K}$ as $\Theta = T\mathcal{K}$. Given the fact that Θ inverts time, it also inverts the momentum, which means it acts on a Bloch Hamiltonian $\mathcal{H}(\mathbf{k})$ as $\Theta\mathcal{H}(\mathbf{k})\Theta^{-1} = \mathcal{H}(-\mathbf{k})$, if it is TR-invariant.

Particle-Hole symmetry Another important antiunitary symmetry is the so-called *particle-hole symmetry* (PHS) Π, also called charge conjugation, and it maps particles into antiparticle and vice-versa. As in the case of TRS, the operator Π can be written as $\Pi = P\mathcal{K}$, where P is an unitary operator. If we consider a free-fermionic Hamiltonian $H = \sum_{ij} \psi_i^\dagger \mathcal{H}_{ij} \psi_j$ where ψ_j are fermionic operators acting on a lattice site j and $\mathcal{H}$ is a Hermitian matrix representing the single-particle Hamiltonian, we say that H is particle-hole invariant if there exists a unitary matrix U_P such that $U_P \bar{\mathcal{H}} U_P^{-1} = -\mathcal{H}$. Furthermore, the PHS affect the spectrum, namely for every eigenstate $|u_E\rangle$ with energy E there is an eigenstate $\Pi |u_E\rangle = |u_{-E}\rangle$ with energy $-E$.

This kind of symmetry is typical in superconducting systems where the main formalism being used to represent the Hamiltonian is the one of Bogoliubov-de Gennes, which has an intrinsic PHS [7, Sec 16.1].

Chiral symmetry The last relevant symmetry to consider is the *chiral symmetry* Γ, which is product of TRS and PHS, hence $\Gamma = \Theta\Pi$. Unlike the others, it is represented by an unitary operator, because is the product of two antiunitary operators, but it has to anticommute with the Hamiltonian if we want to introduce chiral symmetry. Thus, H is chiral if $\{\Gamma, H\} = 0$ or equivalently $\Gamma H \Gamma^{-1} = -H$. Lastly, we remark that a system can have chiral symmetry but without necessarily satisfying TRS or PHS.

1.4 Adiabatic equivalence and topological invariants

A Hamiltonian is *gapped* if the bulk spectrum has an energy gap between the ground state and all the other excited states. Such a Hamiltonian is said to be *adiabatic deformed* if:

- its parameters — e.g. hopping strength, chemical potential — are slowly and continuously changed

- the important symmetries — e.g. chiral symmetry, time-reversal — are respected
- the bulk gap remains open.

Two Hamiltonians are said to be *adiabatically equivalent* if they can be connected by an adiabatic deformation. A *topological invariant* of a gapped Hamiltonian is a quantity, generally an integer, which cannot be modified by an adiabatic deformation. We see immediately that two equivalent Hamiltonians share the same topological invariants, hence they belongs to the same topological class.

Examples of the topological invariants are the *Chern number* or the *winding number*, which are topological invariants associated to the parameter space of the model and to its bulk. Another example of topological invariant is the number of edge states, which are special states that appear only in topologically non-trivial phases and it is clear, as the name says, that they are excitations at the edge of the system (which, we remark, disappears in the thermodynamic limit).

Even though these examples of topological invariants are very different in character, they are related by what is called the *bulk-edge correspondence*, or *bulk-boundary* correspondence. Briefly stated, suppose we have an interface between two topologically distinct phases, so with different Chern numbers, then the boundary supports a certain number of edge modes. By the bulk-edge correspondence

$$N_L - N_R = \Delta n \tag{1.6}$$

where $N_L - N_R$ is the difference between the left-moving and right moving edge modes and Δn is the difference in the Chern numbers across the interface [22]. Thus, we have a bridge that connects the topology of the bulk to the excitations on the boundary, a crucial ingredient for the study of topological matter.

1.5 Berry phase and Chern numbers

To start, consider the Bloch basis $|u_{n,\mathbf{k}}\rangle$. It is unique up to a phase factor. That means it is possible to change the phase by means of an arbitrary function $f(\mathbf{k})$

$$|u_{n,\mathbf{k}}\rangle \mapsto e^{if(\mathbf{k})} |u_{n,\mathbf{k}}\rangle \tag{1.7}$$

This is a manifestation of an $U(1)$ gauge symmetry that characterize the Hilbert space of the system. It has important consequences for the topological classification of states because is a geometrical feature of the Hilbert space.

First of all, a gapped Hamiltonian $H(\mathbf{R})$ is considered, where $\mathbf{R}$ belongs to the parameter space $\mathcal{P}$ (they can be, for example, the chemical potential, the magnetic field etc...). In the case of a Bloch Hamiltonian, the parameters are taken to be the BZ momenta $\mathbf{k}$. Suppose now that the parameters change *slowly* with time, that is $t \in [0, T] \mapsto \mathbf{R}(t) \equiv \mathbf{R}_t \in \mathcal{P}$ in the *adiabatic approximation*. Hence, the Hamiltonian $H(\mathbf{R}_t)$ that varies along a path C in $\mathcal{P}$, that we are going to assume to be closed, such that $\mathbf{R}(0) = \mathbf{R}(T)$. In this situation, an instantaneous orthogonal basis for the instantaneous eigenstates of $H(\mathbf{R}_t)$ at time t, also called a *snapshot basis*, can be introduced [3]

$$H(\mathbf{R}_t)\,|u_n(\mathbf{R}_t)\rangle = E_n(\mathbf{R}_t)\,|u_n(\mathbf{R}_t)\rangle \tag{1.8}$$

The presence of a gap between the initial state's energy and the rest of the spectrum is required, because, combined with the slow evolution, it guarantees that the system will remain in an instantaneous eigenstate at the end of the cycle, if it started from one. This is the reason why gapped Hamiltonians are considered, it is the class of systems for which the notion of adiabatic evolution is meaningful. The adiabatic approximation requires the time evolution of the parameters to be slow, in the sense that the rate of variation of $\mathbf{R}(t)$ has to be slow compared to the frequencies corresponding to the energy gap [3]. This means that the system must have enough time to adjust to the new configuration. We will also require the wavefunctions to be single-valued and smooth along the curve C. In the classification of topological phases, the ground state is usually chose to be the initial state.

Another requirement is that the states must be non-degenerate. If they are in fact degenerate then the Ansatz (1.10) is no more valid, because the phase factor has to be substituted with an unitary transformation. This leads to the notion of non-Abelian Berry phase, which resembles, instead, a non-Abelian gauge theory, but we are will not going to treat it here.

Berry Connection The equation (1.8) does not describe the time evolution of the state. This is achieved by the time-dependent Schrödinger equation

$$i\hbar\partial_t\,|\Phi(t)\rangle = H(\mathbf{R}(t))\,|\Phi(t)\rangle \tag{1.9}$$

If $|\Phi(t=0)\rangle = |u_n(\mathbf{R}_{t=0})\rangle$ then, by the adiabatic theorem, the state will only acquire a phase during time evolution, so we can take as an Ansatz the state [3, 34]

$$|\Phi(t)\rangle = e^{i\gamma_n(t)} e^{-\frac{i}{\hbar}\int_0^t \mathrm{d}t' E_n(\mathbf{R}_{t'})}\,|u_n(\mathbf{R}_t)\rangle \tag{1.10}$$

The second exponential is just the dynamical phase and it can be removed with a gauge transformation. On the other hand, the first phase $\gamma(t)$ cannot be removed because it depends on the geometry of the parameter space $\mathcal{P}$. This phase is called the *Berry phase* and can be calculated as a contour integral along the path C

$$\gamma_n = i \int_C \mathrm{d}\mathbf{R} \, \langle u_n(\mathbf{R}_t) | \nabla_{\mathbf{R}} | u_n(\mathbf{R}_t) \rangle = \int_C \mathrm{d}\mathbf{R} \cdot \mathbf{A}_n(\mathbf{R}) \tag{1.11}$$

of the *Berry connection* (or *Berry potential*)

$$\mathbf{A}_n(\mathbf{R}) = i \, \langle u_n(\mathbf{R}_t) | \nabla_{\mathbf{R}} | u_n(\mathbf{R}_t) \rangle \tag{1.12}$$

The index n refer to the n-th energy band, separated from the other energy bands by a gap. Following the example of the vector potential in electrodynamics, which also emerges from a $U(1)$-gauge invariance, the connection $\mathbf{A}_n$ is not gauge invariant. In fact, applying a gauge transformation on the basis vectors, that is changing the phases with an arbitrary function $\chi(\mathbf{R})$ such that $|u_n(\mathbf{R})\rangle \mapsto e^{i\chi(\mathbf{R})} |u_n(\mathbf{R})\rangle$, then the Berry connection transforms as

$$\mathbf{A}_n(\mathbf{R}) \mapsto \mathbf{A}_n(\mathbf{R}) - \nabla_{\mathbf{R}} \chi \tag{1.13}$$

which means that the Berry phase varies as

$$\Delta\gamma_n = \chi(\mathbf{R}(T)) - \chi(\mathbf{R}(0)). \tag{1.14}$$

Thus, if C is a closed path then γ_n is gauge invariant.

Berry Curvature Recalling that the contour integral of the electromagnetic vector potential A^μ can be expressed as a surface integral of a gauge-invariant quantity, the electromagnetic tensor $F^{\mu\nu}$, likewise, the same can be done for the Berry connection $\mathbf{A}_n$. Its contour integral (1.10) in 3D parameter space can be expressed as a surface integral, thanks to the Stokes theorem, as

$$\gamma_n = \oint_C \mathrm{d}\mathbf{R} \cdot \mathbf{A}_n(\mathbf{R}) = \int_{\mathcal{F}} \mathrm{d}\mathbf{S} \cdot \mathbf{F}_n \tag{1.15}$$

where $\mathcal{F}$ is a surface whose boundary is C. This equation defines the *Berry curvature* $\mathbf{F}_n$ as

$$\mathbf{F}_n = \nabla_{\mathbf{R}} \times \mathbf{A}_n(\mathbf{R}) \tag{1.16}$$

This definition resembles the magnetic field of the vector potential A^μ. The limitation of this formula is that it only works if the parameter space is three-dimensional, on the other hand no condition has been imposed on the dimensionality of the parameter space, when the Berry connection has been defined. A more dimension-agnostic definition is possible by means of differential forms, as it can be seen in [6] for Bloch Hamiltonians. The Berry connection is defined as a 1-form over a fibre bundle, whose base manifold is the BZ and the fibres are the Hilbert space spanned by the basis $u_n(\mathbf{k})$, and the Berry curvature is its the exterior derivative of the connection. It will later be seen that the Berry curvature is the generalization of the notion of Gaussian curvature.

For our scopes, in a d-dimensional space the curvature $\mathbf{F}_n$ can be generalized to an antisymmetric tensor $F^n_{\mu\nu}$

$$F_{\mu\nu} = \partial_\mu A_\nu - \partial_\nu A_\mu = i\left(\langle \partial_\mu u | \partial_\nu u \rangle - \langle \partial_\nu u | \partial_\mu u \rangle\right) \tag{1.17}$$

where $\mu = 1, \ldots, d$ labels the coordinates of the parameter space, $\partial_\mu = \partial/\partial R_\mu$ and the index n and the argument $\mathbf{R}$ have been suppressed for more clarity. It is immediate to see that the quantity $F_{\mu\nu}$ is gauge-invariant. It is important to remark that the different states $|u_n(\mathbf{R})\rangle$ have been assumed to be non-degenerate.

As Berry himself showed [8], it is possible to arrive to a simpler expression for the Berry curvature, that shifts the derivative from the states (which is generally not an easy task) to the Hamiltonian, known as the Berry formula. In fact, from the completeness relation

$$\sum_n |u_n(\mathbf{R})\rangle\langle u_n(\mathbf{R})| = 1 \tag{1.18}$$

and the fact that

$$\langle u_m(\mathbf{R})|\nabla_\mathbf{R}|u_n(\mathbf{R})\rangle = \frac{\langle u_m(\mathbf{R})|\nabla_\mathbf{R} H(\mathbf{R})|u_n(\mathbf{R})\rangle}{E_n - E_m}, \qquad m \neq n \tag{1.19}$$

it is possible to obtain the following formula:

$$\mathbf{F}_n(\mathbf{R}) = \mathrm{Im} \sum_{m\neq n} \frac{\langle u_n(\mathbf{R})|\nabla_\mathbf{R} H(\mathbf{R})|u_m(\mathbf{R})\rangle \times \langle u_m(\mathbf{R})|\nabla_\mathbf{R} H(\mathbf{R})|u_n(\mathbf{R})\rangle}{(E_n - E_m)^2} \tag{1.20}$$

where $\times$ stands for the vector product ($\nabla_\mathbf{R} H$ is a vector in $\mathbf{R}$-space). This expression is easier to calculate than (1.16) or (1.17) and it also makes it clear that the monopoles of the Berry curvature are the point of degeneracy of the spectrum, just by inspection of the denominator. Thus, the points of degeneracy in the $\mathbf{R}$-space acts like magnetic

monopoles.

Two-level System In the following, we are going to analyze the Berry curvature for a two-level system. Such a system can represent, for example, a toy model of an insulator or the dynamics of a spin-$\frac{1}{2}$ system. A generic two-level Hamiltonian can be written in term of Pauli matrices σ_i, $i = x, y, z$, as

$$H(\mathbf{R}) = \frac{1}{2}\begin{pmatrix} Z & X - iY \\ X + iY & -Z \end{pmatrix} = \frac{1}{2}(X\sigma_x + Y\sigma_y + Z\sigma_z) = \frac{1}{2}\mathbf{R}\cdot\boldsymbol{\sigma} \tag{1.21}$$

where $\mathbf{R} = (X, Y, Z)$ and $\boldsymbol{\sigma} = (\sigma_x, \sigma_y, \sigma_z)$

$$\sigma_x = \begin{pmatrix} 0 & 1 \\ 1 & 0 \end{pmatrix} \qquad \sigma_y = \begin{pmatrix} 0 & -i \\ i & 0 \end{pmatrix} \qquad \sigma_z = \begin{pmatrix} 1 & 0 \\ 0 & -1 \end{pmatrix} \tag{1.22}$$

and any constant term proportional to the identity has been ignored, as it just shifts the energy levels and does not affect the dynamics. The energies $E_\pm$ of a two-level Hamiltonian depends just on the modulus of the vector $\mathbf{R}$, namely

$$E_\pm(\mathbf{R}) = \pm\frac{1}{2}\sqrt{X^2 + Y^2 + Z^2} = \pm\frac{|\mathbf{R}|}{2} \tag{1.23}$$

which means they are separated by a gap $|\mathbf{R}|$, hence the only point of degeneracy is $\mathbf{R} = 0$.

Given the eigenstates $|\pm\mathbf{R}\rangle$ with eigenvalues $E_\pm(\mathbf{R})$, we can now use the Berry formula (1.20) for the curvature. For the upper level it reduces to

$$\mathbf{F}_+(\mathbf{R}) = \mathrm{Im}\,\frac{\langle +\mathbf{R}|\nabla H(\mathbf{R})|-\mathbf{R}\rangle \times \langle -\mathbf{R}|\nabla H(\mathbf{R})|+\mathbf{R}\rangle}{|\mathbf{R}|^2} \tag{1.24}$$

and for the lower level is just $\mathbf{F}_- = -\mathbf{F}_+$. Given the fact that $\nabla_{\mathbf{R}} H = \frac{1}{2}\boldsymbol{\sigma}$, we are left with the task of calculating the vector product of expectation values of Pauli matrices. This can be easily achieved by aligning the z-axis along $\mathbf{R}$, such that

$$\sigma_z|\pm\rangle = \pm|\pm\rangle \qquad \sigma_x|\pm\rangle = |\mp\rangle \qquad \sigma_y|\pm\rangle = \pm i|\mp\rangle$$

Immediately, one finds $F_{+x} = F_{+y} = 0$ because $\langle\pm|\sigma_z|\mp\rangle = 0$. So the only non-vanishing

component is along the z-axis

$$\begin{aligned} F_{+z} &= \mathrm{Im}\,\frac{\langle +|\sigma_x|-\rangle\,\langle -|\sigma_y|+\rangle - \langle +|\sigma_y|-\rangle\,\langle -|\sigma_x|+\rangle}{4R^2} \\ &= \mathrm{Im}\,\frac{\langle +|+\rangle\,\langle -|+i|-\rangle - \langle +|-i|+\rangle\,\langle -|-\rangle}{4R^2} \\ &= \mathrm{Im}\,\frac{2i}{4R^2} = \frac{1}{2R^2} \end{aligned} \tag{1.25}$$

where we have suppressed the index $\mathbf{R}$ for convenience and used the notation $R = |\mathbf{R}|$. We see that the monopole is in $\mathbf{R} = 0$.

Because the coordinate system has been rotated, using rotational invariance we can deduce the following general result for two-level systems [7]

$$\mathbf{F}_+ = \frac{\mathbf{R}}{2R^3} \tag{1.26}$$

Thus, the Berry phase is

$$\gamma_+(C) = \int_S \mathrm{d}\mathbf{S}\cdot\frac{\mathbf{R}}{2R^3}, \qquad \exp(i\gamma_+(C)) = \exp\left(i\frac{1}{2}\Omega(S)\right) \tag{1.27}$$

where S is surface with boundary C, $\gamma_+(C)$ the Berry phase of the closed path C and $\Omega(S)$ the solid angle under the surface S.

This will also work for two-band insulators, where parameter is the BZ and the Bloch Hamiltonian can be taken in the form

$$H(\mathbf{k}) = \mathbf{d}(\mathbf{k})\cdot\boldsymbol{\sigma} \tag{1.28}$$

The same formulas apply, we only need to substitute $\mathbf{R}$ with $\mathbf{d}(\mathbf{k})$.

Gauss-Bonnet Theorem Let's consider for a moment two-dimensional manifolds, or surfaces. An important result in this field of topology is the Gauss-Bonnet theorem, which is a bridge between geometry (local properties) and topology (global properties) of compact 2D Riemannian manifolds. It states that the integral over the whole manifold M of its Gaussian curvature $F(\mathbf{x})$ is equal to the Euler characteristic

$$\chi = \frac{1}{2\pi}\int_M \mathrm{d}^2x F(\mathbf{x}) \tag{1.29}$$

which is just $\chi = 2(1-g)$, where g is the genus, intuitively the number of holes of the surface M. For example $g = 0$ for a sphere (which has no holes) but $g = 1$ for a torus (which has one hole). The Gaussian curvature is defined by means of parallel transport of vectors living on the tangent planes, which there is one for each point of M, in this way defining a fibre bundle over M.

Chern Numbers and Winding Numbers The main point of the Gauss-Bonnet theorem is the possibility to relate local properties, like curvature, to global properties, like the genus. It is possible to make the same argument for the Berry phase. It is defined on a manifold, the BZ (a d-dimensional torus) but in general a parameter space $\mathcal{P}$, through a local function, the Berry curvature. It is defined in a similar way to the Gaussian curvature but in this case the different fibres are Hilbert spaces attached at every point of the BZ, generated by the set of eigenstates $\{|u_n(\mathbf{k})\rangle\}$, ending up with a curvature-like structure.

In the case of a two-dimensional BZ, the Berry curvature is a scalar function and, by generalizing the Gauss-Bonnet theorem, its integral over all the BZ defines the *Chern number*.

$$n = \frac{1}{2\pi}\int_{BZ} \mathrm{d}^2k F(\mathbf{k}) = \frac{1}{2\pi}\int_{BZ} \mathrm{d}^2k \left(\frac{\partial A_y}{\partial k_x} - \frac{\partial A_x}{\partial k_y}\right) \tag{1.30}$$

1.6 Su-Schrieffer-Heeger Model

To illustrate now some example of topological properties, we are going to introduce, briefly, the SSH (Su-Schrieffer-Heeger) model. It is is a one-dimensional tight-binding model of polyacetylene, a dimerized chain with Peirels instability, which is made up of elementary cells with two atomic sites (labeled A and B). We are also going to suppose the electrons are spinless for simplicity [3, 22]

The Hamiltonian of the model is [3, 22]

$$H = \sum_{i=1}^{N} (t+\delta t) c^\dagger_{A,i} c_{B,i} + (t-\delta t) c^\dagger_{A,i+1} c_{B,i} + \text{h.c.} \tag{1.31}$$

where the index i runs over all the cells, t is the hopping amplitude and δt is the dimerization factor (which leads to an energy gap). The operators $c_{A,i}, c^\dagger_{A,i}$ and $c_{B,i}, c^\dagger_{B,i}$ are

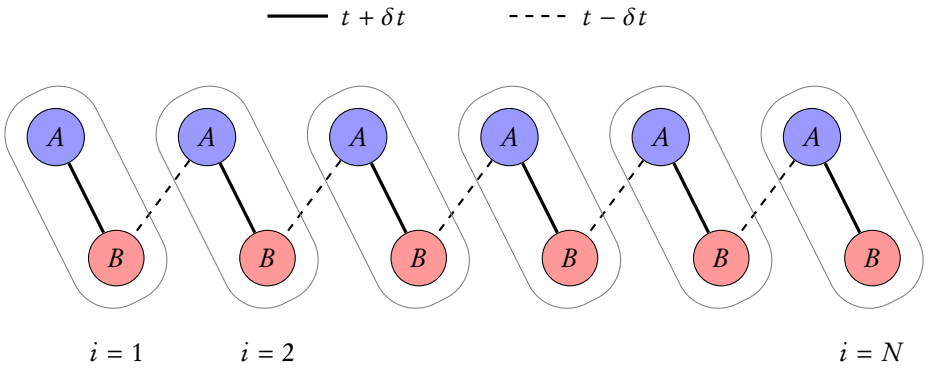

Figure 1.2: Picture of the SSH Model. Every elementary cell has two sites A and B. The cells are labeled by the index $i = 1, \ldots, N$, so the 1d chain is made of two different sublattices. We have two types of hopping: an intra-cell hopping between sites in the same cell of strength $t + \delta t$ and an inter-cell hopping between sites of neighbouring cells of strength $t - \delta t$. We notice that there is no hopping between sites of the same sublattice.

Fermi operators for which the following is true ($\alpha, \beta = A, B$)

$$\{c_{\alpha,i}, c_{\beta,j}\} = 0 \qquad \{c^\dagger_{\alpha,i}, c^\dagger_{\beta,j}\} = 0 \qquad \{c^\dagger_{\alpha,i}, c_{\beta,i}\} = \delta_{\alpha\beta}\delta_{ij} \tag{1.32}$$

If we assume periodic boundary conditions then we are allowed to pass to momentum space with a *Fourier transform*:

$$c_{\alpha,j} = \frac{1}{\sqrt{N}} \sum_k e^{ikj} \tilde{c}_{\alpha,k} \tag{1.33}$$

where $k = 2\pi l/N$ ($l = 0, \ldots, N-1$) is the wave-number. This let us express the Hamiltonian as

$$H = \sum_k \tilde{c}^\dagger_{a,k} H_{ab}(k) \tilde{c}_{b,k} = \sum_k \begin{pmatrix} \tilde{c}^\dagger_{A,k} & \tilde{c}^\dagger_{B,k} \end{pmatrix} H(k) \begin{pmatrix} \tilde{c}_{A,k} \\ \tilde{c}_{B,k} \end{pmatrix} \tag{1.34}$$

where the Bloch Hamiltonian $H(k)$ can be written as

$$H(k) = \mathbf{d}(k) \cdot \boldsymbol{\sigma}, \qquad \mathbf{d}(k) = \begin{pmatrix} (t + \delta t) + (t - \delta t)\cos k \\ (t - \delta t)\sin k \\ 0 \end{pmatrix} \tag{1.35}$$

where we have set the lattice spacing a to 1. We note that d_z is zero which means that

our system has chiral symmetry, because $\Pi = \sigma_z$ anticommutes with the Hamiltonian $\{\Pi, H\} = 0$. The consequence of this is that for every eigenstate $|u_E\rangle$ with energy E there is an eigenstate $\Pi|u_E\rangle = |u_{-E}\rangle$ with energy $-E$. This is analogous to particle-hole symmetry. To be more specific though, the SSH model has all the three antiunitary symmetries listed in Sec. 1.3.

Consider now the Berry phase. The Bloch Hamiltonian (1.35) resembles a two-band system with eigenvalues $\pm|\mathbf{d}(k)|$, which means the only point of degeneracy is $\mathbf{d}(k) = 0$. The map $k \mapsto \hat{\mathbf{d}}(k) = \mathbf{d}(k)/|\mathbf{d}(k)|$ can be thought of as a map from the BZ of the chain (the unit circle S^1) to the two-sphere S^2. Thus, the whole image of the BZ onto S^2 is a closed curve. Moreover, the problem can be simplified because d_z vanishes identically, hence the simpler map from the BZ to the (d_x, d_y)-plane can be considered instead. Then, the Berry phase is going to be half of the angle swept by the vector $\mathbf{d}(k)$ in the plane, with respect to the origin $\mathbf{d} = 0$, and we are interested in how the Berry phase changes when the parameter δt is varied.

Now, there are two different cases that represent two different phases of the model

- $\delta t > 0$, in this case the component d_x is always positive so $\mathbf{d}(k)$ sweeps no angle and the Berry phase is zero. We are gonna call this case the trivial phase
- $\delta t < 0$, here $d_x(k \sim \pi/a) < 0$ and as a result by varying k across the BZ the vector $\mathbf{d}$ rotates by 2π and the Berry phase is π. This the topological phase.

The shape of the curve in the plane is irrelevant, what is relevant is how many times the curve encircles the origin, the so called *winding number* ν, and this is a topological invariant. In fact, the passage from $\delta t < 0$ to $\delta t > 0$ requires the curve to intersect the point of degeneracy $\mathbf{d} = 0$, where the gap closes. Both cases describe an insulator, because there is a gap $\pm|\mathbf{d}(k)|$ between the two energies, but do not describe the same phase. The trivial phase has winding number $\nu = 0$ while, on the other hand, the topological (non-trivial) phase has winding number $\nu = 1$. We can further analyze the two different phases in the fully dimerized limit $\delta t = \pm t$:

- $\delta t = t$: in this limit the Hamiltonian reduces itself to

$$H = 2t \sum_i c^\dagger_{A,i} c_{B,i} + c^\dagger_{B,i} c_{A,i} \tag{1.36}$$

  There is no inter-cell hopping, only intra-cell, and the system is a trivial insulator with constant energy $\pm 2|t|$ and gap, as we vary the momentum k.

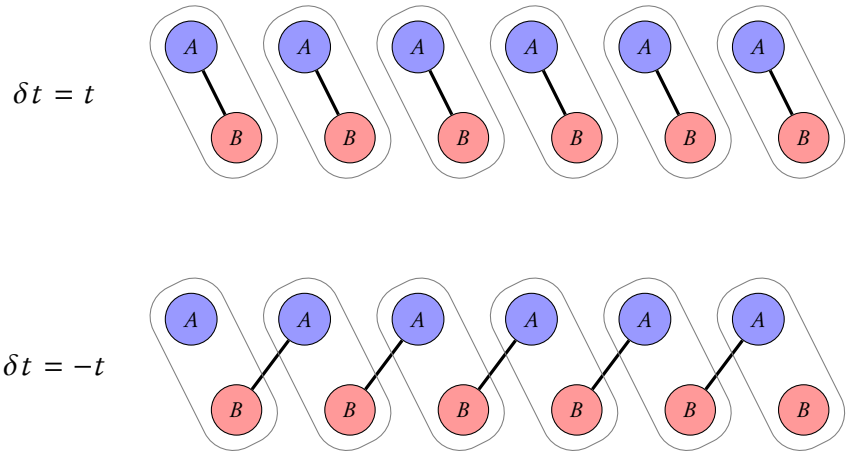

Figure 1.3: Limiting cases of the SSH Model. The trivial phase $\delta t = t$ has no hopping between cells and there is no unpaired mode. The topological phase $\delta t = -t$ has no hopping inside the cells and as a consequence we have unpaired modes at the edges.

- $\delta t = -t$: this case is more special because the Hamiltonian becomes

$$H = 2t \sum_i c^\dagger_{A,i+1} c_{B,i} + c^\dagger_{B,i} c_{A,i+1} \tag{1.37}$$

  which not only contains only inter-cell hopping but, most importantly, does not contains any term pairing the modes $c_{A,1}$ and $c_{B,N}$ with the rest of the chain. That means these modes can be excited with no cost in energy. This represents the easiest example of *edge modes* in topological insulators.

To justify our statement about the no-cost in energy of these edge modes, let us analyze the dispersion relation. It can be easily obtained, given ours is a two-band model

$$E_\pm(k) = \pm\left|\mathbf{d}(k)\right| = \pm\sqrt{2(t^2 + \delta t^2) + 2(t^2 - \delta t^2)\cos ka}. \tag{1.38}$$

In both fully dimerized cases the dispersion relation reduces to $E_\pm = \pm 2|t|$. If we are in the topological phase, this relation does not capture all the eigenstates. In fact let's consider the excited states at the edges

$$|A,1\rangle = c^\dagger_{A,1}|0\rangle, \qquad |B,N\rangle = c^\dagger_{B,N}|0\rangle \tag{1.39}$$

where $|0\rangle$ is the vacuum of the $c_{\alpha,i}$ operators, which is the state annihilated by all the annihilation operators, i.e. $c_{\alpha,i}|0\rangle = 0$ for $\alpha = A, B$ and all $i = 1, \ldots, N$. It's immediate

to show that they are annihilated by the Hamiltonian (1.37)

$$H\,|A,1\rangle = 0, \qquad H\,|B,N\rangle = 0 \tag{1.40}$$

because it does not contain any term $c_{A,1}$ or $c_{B,N}$. This proves the fact that excited states at the edges have no cost in energy, they are zero-modes. It's possible to show the wavefunctions of these zero-modes are localized at the edge and have an exponential decay, which means they don't penetrate in the bulk. This is a typical, but not general, property of edge states [3].

In the Section 1.4 we hinted at the bulk-edge correspondence and we can see that it is true in the SSH model but with some differences; the topological property of the bulk in this case is the winding number ν and the edge states are not distinguished in left-moving and right-moving but if they belong to the sublattice A or B, thus the difference we have to look at now is $N_A - N_B$. In the trivial case $\nu = 0$ and we don't have any edge state so $N_A - N_B = 0$. On the contrary in the topological phase the winding number is nonzero, $\nu = 1$, so is the number of edge states, on the left side $N_A - N_B = 1$ [3].

1.7 Topological phases of matter

What we want to discuss in this section is the classification of topological phases, supposing beforehand we are provided with spectrally gapped ground states of local Hamiltonian at zero temperature. The necessity of the spectral gap, as we have seen in Sec. 1.4, is what let us introduce the notion of adiabatic equivalence. Without the condition of the gap, every phases can be connected to every other phases and no significant classification will come out of it.

We refer to topological states as protected, or enriched, by a symmetry group G, if the Hamiltonian has a symmetry G and only G-preserving (adiabatic) interpolations are allowed [6]. Hence, the employment of symmetries makes the classification more refined.

1.7.1 Topological order

The most fundamental distinction of topological order is the one between *(intrinsic) long-range* and *short-range entangled* topological order. The characterization of a intrinsic topological order can be based on several aspects of an phase, for example:

- Ground state degeneracy

- Fractionalized excitations
- Entanglement entropy

Fractionalized excitations are low-energy excitations, which can be point-like or even line-like, that can carry fractional quantum numbers, as compared to the microscopic degrees of freedom. For example they can carry a fractional charge like in the Fractional Quantum Hall Effect [37], and they are deconfined and dynamical (i.e. free to move).

The entanglement entropy quantifies the degree of entanglement, that is the non-local correlation between the different parts of a single quantum system. Customarily, for entanglement entropy it is intended the von Neumann entropy of the reduced density matrix, i.e. $S(\rho_A) = -\mathrm{Tr}[\rho_A \ln \rho_A]$ of the operator $\rho_A = \mathrm{Tr}_A[\rho_{A+B}]$, which is the partial trace of ρ_{A+B}; the latter stands for the density operator of the global (possibly pure) state of a system, which is divided into two subsystems A and B. It is known that outside criticality, the entanglement entropy scales not with the dimension of the system but with the dimension of the boundary that divides it. This constitutes the so-called *area-law* for entanglement. Long-range entangled (LRE) states have a universal subleading correction to this scaling that is characteristic for the type of topological order.

Symmetry protected topological (SPT) phases are topological phases where the topology is protected by a symmetry. All SPT phases are short-range entangled (SRE), i.e. it they do not present intrinsic topological order or long-rang entanglement, but the converse is not necessarily true. Going further, they usually present topologically protected boundary modes (if the system is defined on a manifold with boundary), except if the boundary itself breaks the protecting symmetry. One example of SPT is the non-trivial phases of the SSH model, where the edge states are protected by the chiral symmetry.

On the other hand, phases without intrinsic topological order are not necessarily equipped with boundary modes, even if the boundary of the manifold preserves the defining symmetries of the phase. If a phase with intrinsic topological order relies on symmetries, than it is called symmetry enriched topological phase (SET).

Regarding to ground state degeneracy, in the SSH model we have already seen how the non-trivial phase present edge states which can host zero-energy excitations. This leads to a two-fold degeneracy of ground states, the one with excited edges state and the one without, distinguished by fermion parity, that is the number of fermions modulo 2.

1.7.2 Local unitary transformation and long-range entanglement

Based on the work of Chen et al.[14], we can give a more refined definition of SRE and LRE states thanks to the notion of *local unitary transformation*. Given two gapped states

$|\Psi(0)\rangle$ and $|\Psi(1)\rangle$, we say they are in the same phase if and only if they are connected by a local unitary (LU) evolution. A LU evolution is defined as an unitary operation generated by the time evolution of a local Hamiltonian for a finite time, or rather

$$|\Psi(1)\rangle \sim |\Psi(0)\rangle \quad \text{if and only if} \quad |\Psi(1)\rangle = \mathcal{T}[e^{-i\int_0^1 \tilde{H}(g)\mathrm{d}g}]\,|\Psi(0)\rangle$$

where $\mathcal{T}$ is the path-ordering operator and $\tilde{H}(g) = \sum_i O_i$ is a sum of local Hermitian operators, that is they act only on a cluster of finite size ξ which is the range of interaction of $\tilde{H}$, also $\tilde{H}(g)$ may not coincide with the Hamiltonian H of the system.

We are now in the position to give more precise definitions of SRE and LRE states: a state is SRE if and only if can be transformed into an unentangled state (i.e. a direct product state) through a LU evolution. Conversely, a state that cannot be transformed into an unentangled state through a LU evolution is a state with long-range entanglement. Thus, topological order describes the equivalence classes defined by the LU transformations.

The above definition implies that all short-range entangled states belong to the same phases and that they can be transformed into each other. This point of view ignores so far the role played by the symmetries. In fact, the local unitary transformation we just introduced is not required to preserve any symmetry. Hence, to preserve them we may define *symmetric local unitary transformation* as those who connect to the identity transformation continuously. Now, if we consider only Hamiltonians H with certain symmetries, then we define the different phases as the equivalence classes of symmetric local unitary transformations:

$$|\Psi\rangle \sim \mathcal{T}\left(e^{-i\int_0^1 \mathrm{d}g\tilde{H}(g)}\right)|\Psi\rangle$$

where $\tilde{H}(g)$ has the same symmetries of H.

Now the structure of the phases of a system with symmetries is much more detailed compared to one without symmetries. In the latter all the SRE states are in the same phase while the LRE states can have different patterns that give rise to different topological phases. On the other hand, in the former the phases structure can be much more complicated, based on which equivalence class of the symmetric LU evolution the states belong to; the different possibilities are:

- SRE states belong to different equivalence classes if they have broken symmetries.
- SRE states can belong to different equivalence classes even if they don't brake any symmetries. In this case we say these states have *symmetry protected topological order*.

- Symmetry breaking and long-range entanglement can appear together in a state.
- LRE states that do not break any symmetry can also belong to different phases, similarly to the SPT but with long-range entanglement.

1.7.3 Classification of free fermionic Hamiltonians

Previously we have stated that the SPT order in SRE states can manifest itself via the presence of gapless boundary states in open geometry. This is an exemplification of the connection between the topology of the gapped bulk and its boundary modes (the bulk-edge correspondence). The latter are protected against local perturbations on the boundary that preserve the bulk symmetry and induce no intrinsic topological order or spontaneous symmetry breaking at the boundary. The bulk-edge correspondence can be used to classify the different SPT phases. In fact if two SRE phases belong to different topological classes, then the interface must host a certain number of boundary modes, whose energy cannot be moved from the bulk gap to the bulk bands with a local perturbation [6].

In [32] Schnyder et al. used bulk-edge correspondence to classify all noninteracting fermionic Hamiltonians. The same was achieved by Kitaev [25] with the algebraic structure of Clifford algebras in various dimensions. In particular for topological phases, PHS and TRS have been considered. In fact, the different classes differ in the sign of the squares of the TR operator $\Theta^2 = \pm 1$ and PH operator $\Pi^2 = \pm 1$. Recall that from the product of the TR and PH we obtain chiral symmetry Γ. Furthermore, the mathematical structure behind this classification makes use of *homotopy groups*.

Flatband Hamiltonians and homotopy groups Every d-dimensional Bloch Hamiltonian $\mathcal{H}(\mathbf{k})$ with a gap can be adiabatically deformed into a *flatband Hamiltonian*

$$Q(\mathbf{k}) = U(\mathbf{k}) \begin{pmatrix} \mathbf{1}_m & 0 \\ 0 & -1_n \end{pmatrix} U^\dagger(\mathbf{k}) \tag{1.41}$$

which assigns $+1$ to the energy levels above the gap and -1 instead to those below the gap. The $U(\mathbf{k})$ stands for the unitary matrix that diagonalize $\mathcal{H}(\mathbf{k})$ and m and n are such that $m + n = d$, the total number of bands. This deformation preserves the eigenstates, but removes the non-universal information about the energy bands [6]. The degeneracy of the eigenspaces of $Q(\mathbf{k})$ with eigenvalues ± 1 introduces a supplementary $U(m) \times U(n)$ gauge symmetry, while $U(\mathbf{k})$ belongs to the group $U(m + n)$ for every $\mathbf{k} \in BZ$. Hence,

$Q(\mathbf{k})$ is an element of the space $C_0 = U(m+n)/[U(n)\times U(m)]$ that defines a map

$$Q : BZ \to C_0 \tag{1.42}$$

What we are interested in is the different topologically distinct classes of Q, that is the different topologically distinct Bloch Hamiltonians $\mathcal{H}$. They are given by the homotopy group

$$\pi_d(C_0)$$

for any dimension d of the BZ. The homotopy group is the group of equivalence classes of maps from the d-dimensional sphere to a target space, in this case C_0. This works even though the BZ is a d-dimensional torus because the difference between a torus and a sphere does not affect the present classification. For example for $\pi_d(C_0) = \mathbb{Z}$, which means all the topologically distinct Hamiltonians can be labelled by a integer in $\mathbb{Z}$. On the hand, if we had $\mathbb{Z}_2$ instead of $\mathbb{Z}$, that would mean there are only two topologically distinct classes and one of them would be the vacuum.

A physical example of the $\pi_2(C_0) = \mathbb{Z}$ case is the integer quantum Hall effect, discussed in Sec. 1.1. A ground state with $r \in \mathbb{N}$ filled Landau levels is topologically different from one with $r' \in \mathbb{N}$ and the interface between these two states presents $|r - r'|$ gapless edge modes running on it. This reflect the bulk-boundary correspondence of topologically phases.

The resulting classification is summarized in Tab. 1.1, which is taken from [6]. Every entry of the table it's labeled with the Cartan name of the symmetry class and they differ by the presence of TRS, PHS or chiral symmetry and the sign of the square of the relative operator, if they are present. The first two classes, A and AIII, are called *complex classes* while the remaining eight are *real classes*. The homotopy group of the complex classes present a periodicity of 2 with respect to the dimension d, while the real classes have periodicity 8 in d (Bott periodicity).

This concludes this chapter on some basic aspects of Topological Matter. This field of Condensed Matter is too rich to be exhausted in a single chapter, for this reason we redirect to the reviews by Hasan and Kane [18], and Qi and Zhang [31] and the books by Bernevig and Hughes [7], and by Shen [34] for an extensive review of the subjects.

	Θ^2	Π^2	Γ^2	d	1	2	3	4	5	6	7	8
A	∅	∅	∅		∅	$\mathbb{Z}$	∅	$\mathbb{Z}$	∅	$\mathbb{Z}$	∅	$\mathbb{Z}$
AIII	∅	∅	+		$\mathbb{Z}$	∅	$\mathbb{Z}$	∅	$\mathbb{Z}$	∅	$\mathbb{Z}$	∅
AII	−	∅	∅		∅	$\mathbb{Z}_2$	$\mathbb{Z}_2$	$\mathbb{Z}$	∅	∅	∅	$\mathbb{Z}$
DIII	−	+	+		$\mathbb{Z}_2$	$\mathbb{Z}_2$	$\mathbb{Z}$	∅	∅	∅	$\mathbb{Z}$	∅
D	∅	+	∅		$\mathbb{Z}_2$	$\mathbb{Z}$	∅	∅	∅	$\mathbb{Z}$	∅	$\mathbb{Z}_2$
BDI	+	+	+		$\mathbb{Z}$	∅	∅	∅	$\mathbb{Z}$	∅	$\mathbb{Z}_2$	$\mathbb{Z}_2$
AI	+	∅	∅		∅	∅	∅	$\mathbb{Z}$	∅	$\mathbb{Z}_2$	$\mathbb{Z}_2$	$\mathbb{Z}$
CI	+	−	+		∅	∅	$\mathbb{Z}$	∅	$\mathbb{Z}_2$	$\mathbb{Z}_2$	$\mathbb{Z}$	∅
C	∅	−	∅		∅	$\mathbb{Z}$	∅	$\mathbb{Z}_2$	$\mathbb{Z}_2$	$\mathbb{Z}$	∅	∅
CII	−	−	+		$\mathbb{Z}$	∅	$\mathbb{Z}_2$	$\mathbb{Z}_2$	$\mathbb{Z}$	∅	∅	∅

Table 1.1: Symmetry classes of noninteracting fermionic Hamiltonians, from [6], based on the works of Schnyder et al. [32] and Kitaev [25]. The first column represent the Cartan name of the symmetry class, while form the second to the forth row represent the absence (with the symbol ∅) or the sign of the squares of Θ (TRS), Π (PHS) and Γ (chiral symmetry), if they are present. The remaining columns report the homotopy groups for dimensions d from 1 to 8. As we see, the periodicity of the homotopy groups for the complex classes (A and AIII) is 2 while for the real classes is 8, with respect to d.

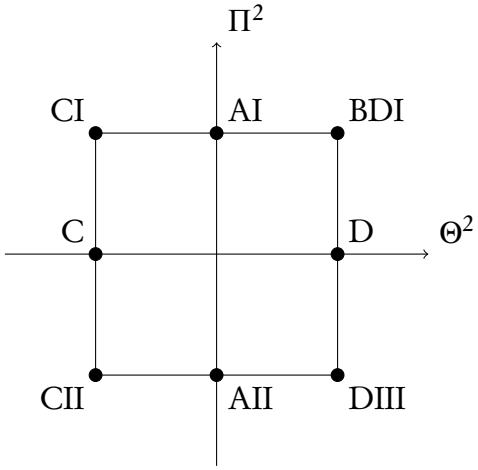

Figure 1.4: From [35]. The eight real symmetry classes that involves Θ and Π, which are distinguished by their values of $\Theta^2 = \pm 1$ and $\Pi^2 = \pm 1$, can be visualized on an eight hour "clock".

2

Toeplitz Matrices

In these chapter we are going to give a short summary about a particular class of matrices, the Toeplitz matrices, which are constants along the parallels of the diagonal, i.e. $A_{ij} = A_{i-j}$. The theory of Toeplitz matrices proved to be a useful tool for the study of 1D quantum systems, see for example [5, 15, 19] where they have been employed in a various range of subjects, from entanglement entropy of a bipartite system to the correlation functions of spin chains.

A large class of fermionic chains can be described by a Hamiltonian of the form

$$H = \sum_{i,j} \left(c_i^\dagger A_{ij} c_j + \frac{1}{2} \left(c_i^\dagger B_{ij} c_j^\dagger + c_i B_{ij} c_j \right) \right)$$

and, due to translational invariance, both A and B have to be Toeplitz matrices whereas A is symmetric while B is antisymmetric. This kind of Hamiltonian can also describe spin chains after a Jordan-Wigner transformation, which maps spin operators into Fermi operators. Furthermore, Lieb et al. [29] demonstrated that the eigenvalues Λ_k and the corresponding eigenvectors of such a Hamiltonian can be calculated through the following the equations

$$\begin{aligned} \phi_k (A - B)(A + B) &= \Lambda_k^2 \phi_k \\ \psi_k (A + B)(A - B) &= \Lambda_k^2 \psi_k \end{aligned}$$

Thus, the study of eigenvalues and singular values of a Toeplitz matrices can leads to a great deals of information about the physics of a large class one-dimensional quantum systems. The proofs of the statements made here in this chapter are not going to be reported, for the sake of clarity and brevity, but they can be found in [10–13], which are

extensive reviews of the mathematical theory of Toeplitz matrices.

2.1 Toeplitz and Hankel matrices

An *infinite* matrix T is called a *Toeplitz matrix*, or *Toeplitz operator*, if it is of the form

$$T_{ij} = \left(a_{i-j}\right)_{j,k=0}^{\infty} = \begin{pmatrix} a_0 & a_{-1} & a_{-2} & \dots \\ a_1 & a_0 & a_{-1} & \dots \\ a_2 & a_1 & a_0 & \dots \\ \vdots & \vdots & \vdots & \ddots \end{pmatrix} \tag{2.1}$$

Such a matrix is constant along the parallels of the main diagonal and it is completely determined by the sequence

$$\{a_j\}_{j=-\infty}^{\infty} = \{\dots, a_{-2}, a_{-1}, a_0, a_1, a_2, \dots\}$$

It is important to consider also the following matrices H and $\tilde{H}$, which can be built from the same sequence $\{a_j\}$

$$H_{ij} = \begin{pmatrix} a_1 & a_2 & a_3 & \dots \\ a_2 & a_3 & a_4 & \dots \\ a_3 & a_4 & a_5 & \dots \\ \vdots & \vdots & \vdots & \ddots \end{pmatrix} \quad \text{and} \quad \tilde{H}_{ij} = \begin{pmatrix} a_{-1} & a_{-2} & a_{-3} & \dots \\ a_{-2} & a_{-3} & a_{-4} & \dots \\ a_{-3} & a_{-4} & a_{-5} & \dots \\ \vdots & \vdots & \vdots & \ddots \end{pmatrix}, \tag{2.2}$$

called *Hankel matrices*.

2.1.1 Some basic properties of Toeplitz matrices

Bounded operators Given a Banach space X with norm $\|\cdot\|$, let A be an operator over X. We can define its norm as

$$\|A\| \equiv \sup_{x \neq 0} \frac{\|Ax\|}{\|x\|} \tag{2.3}$$

Bounded operators are operators with a finite norm, i.e $\|A\| < \infty$, and their set is denoted with $\mathcal{B}(X)$.

The matrices in (2.1) and (2.2) can be regarded as operators on $\ell^2(\mathbb{Z}_+) \equiv \ell^2$, that is

the space of square-summable sequences

$$\ell^2(\mathbb{Z}_+) \equiv \left\{ x = \{x_j\}_{j=0}^{\infty} : \sum_{j=0}^{\infty} |x_j|^2 < \infty \right\}.$$

An operator $A = (a_{ij})$ acts on the space ℓ^2 as

$$A : \ell^2 \to \ell^2, \; x \mapsto y = Ax \quad \text{such that} \quad y_i = \sum_j a_{ij} x_j \tag{2.4}$$

In addition, the set ℓ^2 is a Banach space where the $\|x\| = \left(\sum_{j=0}^{\infty} |x_j|^2 \right)^{1/2}$ is well defined. It is important to remark that not every Toeplitz matrix is a bounded operator over ℓ^2.

To see when a Toeplitz matrix is a bounded operator, first let $\mathbb{T}$ be the unit circle in the complex plane $\{t \in \mathbb{C} : |t| = 1\}$[1]. Next, let a be a complex-valued function of $\mathbb{T}$, i.e $a : \mathbb{T} \to \mathbb{C}$. Then, we say that $T(a)$ and $H(a)$ are respectively the Toeplitz matrix and the Hankel matrix with *symbol* a if they are build from the sequence $\{a_n\}_{n=-\infty}^{\infty}$ of the Fourier coefficients of a:

$$a_n = \frac{1}{2\pi} \int_0^{2\pi} \mathrm{d}\theta a(e^{i\theta}) e^{-in\theta}, \qquad a = \sum_{n=-\infty}^{\infty} a_n t^n = \sum_{n=-\infty}^{\infty} a_n e^{in\theta} \tag{2.5}$$

It can be showed that if [2] $a \in L^\infty$ then the Toeplitz matrix with symbol a is a bounded operator over ℓ^2. Furthermore, the norm of $a \in L^\infty$ is defined as $\|a\|_\infty = \text{ess sup}_{t \in \mathbb{T}} |a(t)|$ and it is possible to demonstrate that $\|T(a)\| = \|a\|_\infty$ [12, Th 1.9].

Hankel matrices have major role in the theory of Toeplitz operator because the product of two Toeplitz operators is not necessarily Toeplitz. In fact given $a, b \in L^\infty$ we have that

$$T(ab) = T(a)T(b) + H(a)H(\tilde{b})$$

where $\tilde{b}(t) \equiv b(1/t)$ [12, Prop. 1.12].

Clearly, a Toeplitz operator is selfadjoint, i.e. $T(a)^\dagger = T(a)$, if and only if the symbol a is a real function. In fact, $T^\dagger(a) = T(a)$ implies that $a_{-n} = \bar{a}_n$ which is equivalent to saying that $a(t) = \bar{a}(t)$.

Hardy spaces Toeplitz matrices can be regarded as canonical matrix representation of the multiplication between functions of $L^2 \equiv L^2(\mathbb{T})$, which is the Hilbert space of the

[1] Everytime we use the variable t we are going to imply $t \in \mathbb{T}$, if it is not stated otherwise.
[2] $L^\infty(\mathbb{T})$ is the of functions bounded almost everywhere on $\mathbb{T}$ and it is also a Banach space

square-summable functions. That is the set of functions $f : \mathbb{T} \to \mathbb{C}$ such that

$$\frac{1}{2\pi}\int_{\mathbb{T}} |f(t)|^2 \mathrm{d}t < \infty.$$

Furthermore, given two function $f, g \in L^2$, their inner product is defined as

$$(f, g) = \frac{1}{2\pi}\int_{\mathbb{T}} \overline{f(t)} g(t) \mathrm{d}t$$

and the norm is such that $\|f\| = \sqrt{(f, f)}$. These functions can be expressed through a Fourier series, like in (2.5), and this let us decompose L^2 into an orthogonal sum.

First, let $H^2 \equiv H^2(\mathbb{T})$ and $H^2_- \equiv H^2_-(\mathbb{T})$ be the following *Hardy spaces*

$$H^2 \equiv \{f \in L^2 : f_n = 0 \text{ for } n < 0\} \qquad H^2_- \equiv \{f \in L^2 : f_n = 0 \text{ for } n \geq 0\} \tag{2.6}$$

It is immediate to see that they decompose L^2 into the orthogonal sum $L^2 = H^2 \oplus H^2_-$.

Now, let P stand for the orthogonal projection of L^2 onto H^2. The plain waves $\exp(in\theta)/\sqrt{2\pi}$, $n = 0, 1, \ldots$, form an orthonormal basis in H^2 and it can be verified that if $a \in L^\infty$, then the matrix representation of the operator

$$H^2 \to H^2, \quad f \mapsto P(af) \tag{2.7}$$

is the Toeplitz matrix $T(a)$. The aforementioned operator is the compression $PM(a)P$ of the multiplication operator $M(a) : L^2 \to L^2$, $f \mapsto af$ to H^2 [12, Sec. 1.3]. A crucial property of H^2 is that if $f \in H^2$ then it vanishes either almost everywhere or almost nowhere on $\mathbb{T}$.

2.1.2 C^*-algebras

Banach algebra and C^*-algebra A (complex) Banach space $\mathcal{A}$ with an associative and distributive multiplication is called a *Banach algebra* if $\|ab\| \leq \|a\| \|b\|$ for $a, b \in \mathcal{A}$. If it has an unit element e such that $ae = ea = a$ for every $a \in \mathcal{A}$, then $\mathcal{A}$ is called a unital Banach algebra. Sometimes the unit element is also denoted by 1 or I and obviously we require that $\|e\| = \|1\| = \|I\| = 1$.

A conjugate-linear map $a \mapsto a^*$ of a Banach algebra into itself is called an *involution* if $a^{**} = a$ and $(ab)^* = b^* a^*$ for all $a, b \in \mathcal{A}$. Finally, a *C^*-algebra* is a Banach algebra with an involution such that $\|a^* a\| = \|a\|^2$ for all $a \in \mathcal{A}$. Similarly to Banach algebras, a unital C^*-algebra has a unit element $e = 1 = I$.

Given a unital Banach algebra $\mathcal{A}$, an element $a \in \mathcal{A}$ is said to be *invertible* (in $\mathcal{A}$) if there is an element $b \in \mathcal{A}$ such that $ab = ba = e$. If such an element exists then it is unique and will be denoted with a^{-1} and called the *inverse* of a.

A C^*-subalgebra $\mathcal{B}$ of a C^*-algebra $\mathcal{A}$ is just a subset of $\mathcal{A}$ which is by itself a C^*-algebra with the operations of $\mathcal{A}$.

If H is a Hilbert space, then $\mathcal{B}(H)$ (the set of bounded operators on H) and $\mathcal{K}(H)$ (the set of compact operators[3] on H) are C^*-algebra with point-wise algebraic operations, norm (2.3) and the passage to the adjoint operator as involution. Clearly, the unit element is the identity operator I. Another example of C^*-algebra is set of essentially bounded operators L^∞ with point-wise algebraic operations, norm $\|\cdot\|_\infty$ and complex conjugation as involution. It is a unital commutative algebra, i.e. $ab = ba$, whereas $\mathcal{B}(H)$ and $\mathcal{K}(H)$ are not commutative for $\dim H \geq 2$ and $\mathcal{K}(H)$ is unital if and only if $\dim H < \infty$, in which case $\mathcal{K}(H) = \mathcal{B}(H)$ with operations of $\mathcal{B}(H)$.

Spectrum The *spectrum* of an element a of a Banach algebra $\mathcal{A}$ is the set

$$\operatorname{sp} a \equiv \operatorname{sp}_{\mathcal{A}} a \equiv \{\lambda \in \mathbb{C} : a - \lambda e \text{ is not invertible in } \mathcal{A}\} \tag{2.8}$$

and it is known that the spectrum of an element of a unital Banach algebra is always a nonempty compact subset of the complex plane $\mathbb{C}$, which is contained into the disk $\{\lambda \in \mathbb{C} : |\lambda| \leq \|a\|\}$.

Ideals The notion of ideal is defined for an arbitrary ring G with addition and multiplication. In fact, let H be a subset of G; it is called a *left ideal* of G if H is a subgroup of G under addition and for every $g \in G$ and every $h \in H$, the product $gh \in H$. Conversely, a *right ideal* requires the condition that hg is in H instead. A *two-sided ideal* is a left ideal that is also a right ideal.

Moreover, let G be a group under addition + and H a subgroup of G. Given $g \in G$, the set $g + H = \{g + h : h \in H\}$ is the coset of H in G with respect to g. We assumed the addition to be commutative so we don't have to differentiate between left coset and right coset. Moreover, we can say that $a + H$ is an element of the quotient space G/H.

In the case of C^*-algebra, if a C^*-subalgebra $\mathcal{J}$ is an ideal of $\mathcal{A}$ then we have the following:

[3] Given an Hilbert space H, an operator $K : H \to H$ is said to be compact if the image of the unit ball under K is a compact subset in H [16, Def 5.2].

Theorem 1. *The quotient algebra $\mathcal{A}/\mathcal{J}$ is a C^*-algebra with the quotient operations*

$$\lambda(a+\mathcal{J}) \equiv \lambda a + \mathcal{J} \qquad (a+\mathcal{J})+(b+\mathcal{J}) \equiv (a+b)+\mathcal{J}$$
$$(a+\mathcal{J})(b+\mathcal{J}) \equiv ab+\mathcal{J} \qquad (a+\mathcal{J})^* \equiv a^*+\mathcal{J}$$

and the quotient norm

$$\|a+\mathcal{J}\| \equiv \inf_{j\in\mathcal{J}} \|a+j\|$$

Homomorphism and isomorphism A map $\phi : \mathcal{A} \to \mathcal{B}$ between two Banach spaces is called a *Banach algebra homomorphism* if ϕ is a bounded operator and $\phi(ab) = \phi(a)\phi(b)$ for all $a, b \in \mathcal{A}$. If ϕ is bijective then it is a Banach algebra *isomorphism*. Furthermore, ϕ is a *C^*-algebra homomorphism* (or shortly a *$*$-homomorphism*) if $\phi(a^*) = \phi(a)^*$.

For $*$-homomorphisms the following theorem is true:

Theorem 2. *Let $\mathcal{A}$ and $\mathcal{B}$ be two unital C^*-algebra and suppose that $\phi : \mathcal{A} \to \mathcal{B}$ is a $*$-homomorphism. Then the following holds*

1. *The map ϕ is contractive: $\|\phi(a)\| \leq \|a\|$ for all $a \in \mathcal{A}$.*
2. *The image $\phi(\mathcal{A})$ is a C^*-subalgebra of $\mathcal{B}$.*
3. *If ϕ is injective, the ϕ preserves spectra and norms:* $\operatorname{sp}\phi(a) = \operatorname{sp} a$ *and* $\|\phi(a)\| = \|a\|$ *for all $a \in \mathcal{A}$.*

The last point will reveal to be rather useful in the study of the spectra of operators.

2.1.3 Wiener algebra and winding number

The Wiener algebra The set of functions $a : \mathbb{T} \to \mathbb{C}$ with absolutely convergent Fourier series

$$a(t) = \sum_{n\in\mathbb{Z}} a_n t^n, \quad \sum_{n\in\mathbb{Z}} |a_n| < \infty$$

is called the *Wiener algebra* and it is denoted by $W \equiv W(\mathbb{T})$. It is a Banach algebra with point-wise operations and norm

$$\|a\|_W \equiv \sum_{n\in\mathbb{Z}} |a_n|$$

It is clear that W is contained inside $C \equiv C(\mathbb{T})$, the Banach algebra of the continuous functions on $\mathbb{T}$ with the maximum norm. For a theorem by Wiener, if $a \in W$ has no zeroes on $\mathbb{T}$, then $a^{-1} = 1/a \in W$.

It is worthwhile to mention also the set $PC \equiv PC(\mathbb{T})$ of all piecewise continuous functions. A function a is said to be piecewise continuous if for every $t = e^{i\theta} \in \mathbb{T}$ the following one-sided limits exist

$$a(t+0) \equiv \lim_{\epsilon \to 0^+} a(e^{i(\theta+\epsilon)}) \qquad a(t-0) \equiv \lim_{\epsilon \to 0^+} a(e^{i(\theta-\epsilon)}) \tag{2.9}$$

The unit circle $\mathbb{T}$ is always oriented counterclockwise. The set PC is a closed subalgebra of L^∞ and its elements have at most countably many jumps, i.e. point $t \in \mathbb{T}$ where $a(t+0) \neq a(t-0)$ [12, Example 1.7].

Winding number First of all, let $GC \equiv GC(\mathbb{T})$ be the set of all function $a \in C$ which have no zeroes on $\mathbb{T}$. For $a \in GC$, we denote by $\mathrm{wind}(a, 0)$ the *winding number* of a with respect to the origin. Every function $a \in GC$ may be written in the form $a = |a|e^{ic}$ where $c : \mathbb{T} \setminus 1 \to \mathbb{R}$ is continuous, and $\mathrm{wind}(a, 0)$ is defined as the integer

$$\frac{1}{2\pi}(c(1-0) - c(1+0)) \tag{2.10}$$

Notice that c is unique up to an additive constant $2k\pi$ ($k \in \mathbb{Z}$) and the winding number does not depend on the particular choice of c. We denote with G_0C the subset of GC with $\mathrm{wind}(a, 0) = 0$ and with GW the intersection $W \cap GC$. Moreover, if $a \in C(\mathbb{T})$ and $\lambda \in \mathbb{C} \setminus a(\mathbb{T})$, we define the winding number $\mathrm{wind}(a, \lambda)$ of a with respect to λ by $\mathrm{wind}(a, \lambda) = \mathrm{wind}(a - \lambda, 0)$. Furthermore, if $a, b \in GC$ then it can easily be seen that $\mathrm{wind}(ab, 0) = \mathrm{wind}(a, 0) + \mathrm{wind}(b, 0)$.

As an example, consider the function $\chi_n(t) = t^n$, where $n \in \mathbb{Z}$. Equivalently, $\chi_n(e^{in\theta}) = e^{in\theta}$. By the definition of winding number, $\mathrm{wind}(\chi_n, 0) = n$.

Wiener-Hopf factorization Let H^∞ and H^∞_- be the following subsets of L^∞.

$$H^\infty \equiv \{a \in L^\infty : a_n = 0 \quad \text{for} \quad n < 0\} \tag{2.11}$$

$$H^\infty_- \equiv \{a \in L^\infty : a_n = 0 \quad \text{for} \quad n > 0\} \tag{2.12}$$

These sets are closed subalgebras of the Banach algebra L^∞. Their intersection is the set of constant functions and the sum $H^\infty + H^\infty_-$ does not coincide with L^∞, unlike H^2 and H^2_- with L^2. Similarly to GC and GW, we define $GH^\infty_- = H^\infty_- \cap GC$ and

$GH^\infty = H^\infty \cap GC$, which are the subsets of H^∞_- and H^∞ of the functions with no zeros on $\mathbb{T}$, hence are invertible.

If $a \in H^\infty$, then $H(\tilde{a}) = 0$ and $T(a)$ is lower triangular. On the same note, if $a \in H^\infty_-$, then $H(a) = 0$ and $T(a)$ is upper triangular. As a consequence, if $a \in H^\infty_-$, $b \in L^\infty$, $c \in H^\infty$, then by (2.1.1) we have $T(abc) = T(a)T(b)T(c)$. This statement is the origin of the *Wiener-Hopf factorization*.

Theorem 3 (Wiener-Hopf factorization for Wiener functions)**.** *Let $a \in GW$ and let* $\operatorname{wind}(a, 0) = \omega$. *Then*

$$a = a_- \chi_\omega a_+ \tag{2.13}$$

where $a_- \in W \cap GH^\infty_-$, $a_+ \in W \cap GH^\infty$ and $\chi_\omega(t) = t^\omega$.

2.1.4 Fredholm operators

Let X be a Banach space and $A \in \mathcal{B}(X)$. The *kernel* and the image *image* (or *range*) of A are respectively defined as

$$\operatorname{Ker} A \equiv \{x \in X : Ax = 0\}, \qquad \operatorname{Im} A \equiv \{Ax : x \in X\} \tag{2.14}$$

and from these sets we also define the *cokernel* of A as the set $\operatorname{Coker} A \equiv X/\operatorname{Im} A$.

The operator A is said to be *Fredholm* if $\operatorname{Im} A$ is a closed subspace of X and $\dim \operatorname{Ker} A$ and $\dim \operatorname{Coker} A$ are finite numbers. In this case, the *index* of A is defined as the integer

$$\operatorname{Ind} A \equiv \dim \operatorname{Ker} A - \dim \operatorname{Coker} B \tag{2.15}$$

The following is an easy example of Fredholm operator

Example. *For $n \in \mathbb{Z}$, let $\chi_n : \mathbb{T} \to \mathbb{C}$, $\chi_n = t^n$. The Toeplitz matrix $T(\chi_n)$ with symbol χ_n acts on ℓ^2 by the rule*

$$T(\chi_n) : \{x_j\}_{j=0}^\infty \mapsto (\underbrace{0, \dots, 0}_{n}, x_0, x_1, \dots) \quad \text{if} \quad n \geq 0$$

$$T(\chi_n) : \{x_j\}_{j=0}^\infty \mapsto (x_{|n|}, x_{|n|+1}, \dots) \quad \text{if} \quad n < 0$$

Thus,

$$\dim \operatorname{Ker} T(\chi_n) = \begin{cases} 0 & \text{if} \quad n \geq 0 \\ |n| & \text{if} \quad n < 0 \end{cases} \qquad \dim \operatorname{Coker} T(\chi_n) = \begin{cases} n & \text{if} \quad n \geq 0 \\ 0 & \text{if} \quad n < 0 \end{cases}$$

henceforth, $\operatorname{Ind} T(\chi_n) = -n$ *for all* $n \in \mathbb{Z}$.

The next theorem shows some properties of Fredholm operators and their index:

Theorem 4. *Let* $A, B \in \mathcal{B}(H)$ *be Fredholm operators*

1. *if* $K \in \mathcal{K}(H)$, *then* $A + K$ *is Fredholm and* $\operatorname{Ind}(A + K) = \operatorname{Ind} A$.
2. *There is an* $\epsilon = \epsilon(A) > 0$ *such that* $A + C$ *is Fredholm and* $\operatorname{Ind}(A + C) = \operatorname{Ind} A$ *whenever* $C \in \mathcal{B}(H)$ *and* $\|C - A\| < \epsilon$.
3. *The product* AB *is Fredholm and* $\operatorname{Ind}(AB) = \operatorname{Ind} A + \operatorname{Ind} B$.
4. *The adjoint operator* $A^\dagger$ *is Fredholm and* $\operatorname{Ind} A^* = -\operatorname{Ind} A$.

Essential spectrum The "Fredholmness" of an operator $A \in \mathcal{B}(X)$ defines its *essential spectrum* $\operatorname{sp}_{\text{ess}} A$

$$\operatorname{sp}_{\text{ess}} A \equiv \{\lambda \in \mathbb{C} : A - \lambda I \text{ is not Fredholm on } X\} \tag{2.16}$$

The essential spectrum can be interpreted in another way. It is possible to show that $\mathcal{K}(X)$ is a closed two-sided ideal of the C^*-algebra $\mathcal{B}(X)$. Then, one can demonstrate that an operator $A \in \mathcal{B}(X)$ is Fredholm if and only if the coset $A + \mathcal{K}(X)$ is invertible in the quotient algebra $\mathcal{B}(X)/\mathcal{K}(X)$, also referred to as the Calkin algebra of X (which is also a C^*-algebra). Thus, one finds that A is Fredholm only if it is invertible modulo compact operators. Then, the essential spectrum $\operatorname{sp}_{\text{ess}} A$ of $A \in \mathcal{B}(X)$ is just the spectrum of $A + \mathcal{K}(X)$ as an element of $\mathcal{B}(X)/\mathcal{K}(X)$. Clearly, $\operatorname{sp}_{\text{ess}} A \subset \operatorname{sp} A$.

Theorem 5 (Coburn's Lemma)**.** *Let* $a \in L^\infty$ *and suppose* a *does not vanish identically. Then* $T(a)$ *has a trivial kernel on* ℓ^2 *or its image is dense in* ℓ^2. *In particular,* $T(a)$ *is invertible if and only if* $T(a)$ *is Fredholm of index zero:*

$$\operatorname{sp} T(a) = \operatorname{sp}_{ess} T(a) \cup \left\{\lambda \in \mathbb{C} \setminus \operatorname{sp}_{ess} T(a) : \operatorname{Ind}(T(a) - \lambda I) \neq 0\right\} \tag{2.17}$$

The winding number of the symbol a of a Toeplitz matrix $T(a)$ is an important quantity for the following reason [12, Th 1.17]:

Theorem 6 (Gohberg)**.** *Suppose* $a \in C$. *The operator* $T(a)$ *is Fredholm on* l^2 *if and only if* a *has no zeroes on* $\mathbb{T}$, *in which case*

$$\operatorname{Ind} T(a) = -\operatorname{wind}(a, 0) \tag{2.18}$$

Equivalently

$$\operatorname{sp}_{ess} T(a) = a(\mathbb{T}) \tag{2.19}$$

$$\operatorname{sp} T(a) = a(\mathbb{T}) \cup \{\lambda \in \mathbb{C} \setminus a(\mathbb{T}) : \operatorname{wind}(a, \lambda) \neq 0\}. \tag{2.20}$$

In particular, if $a \in W$ then $T(a)$ is invertible if and only if $a(t) \neq 0$ for all $t \in \mathbb{T}$ and $\operatorname{wind}(a, 0) = 0$ [12, Th 1.15]. In the latter case, the inverse is

$$T^{-1}(a) = T(a_+^{-1})T(a_-^{-1}) \tag{2.21}$$

2.1.5 Discontinuous symbols

We now turn our attention to Toeplitz operator with discontinuous symbols, their spectra and their relationship with Fredholm operators.

Essential range For $a \in L^\infty$, we denote by $\mathcal{R}(a)$ the spectrum of a as an element of L^∞. Equivalently, we may define $\mathcal{R}(a)$ as the spectrum of the multiplication operator $M(a) : L^2 \to L^2$, $f \mapsto af$. It is also possible to characterize $\mathcal{R}(a)$ as the following set

$$\mathcal{R}(a) = \{\lambda \in \mathbb{C} : |\{t \in \mathbb{T} : |a(t) - \lambda| < \epsilon\}| > 0 \ \forall \epsilon > 0\} \tag{2.22}$$

where $|E|$ stands for the Lebesgue measure of E. The set $\mathcal{R}(a)$ is called the *essential range* of a, which is non-empty and compact.

The following result provides a useful upper estimate of the spectrum of a Toeplitz operator [12, Th 1.18]

Theorem 7 (Brown-Halmos)**.** *If $a \in L^\infty$ then*

$$\operatorname{sp} T(a) \subset \operatorname{conv} \mathcal{R}(a)$$

where $\operatorname{conv} \mathcal{R}(a)$ *stands for the convex hull of the essential range $\mathcal{R}(a)$ of the function a.*

Sectoriality A function $a \in L^\infty$ is said to be *sectorial* if $0 \notin \operatorname{conv} \mathcal{R}(a)$. For the previous theorem, a Toeplitz operator $T(a)$ with a sectorial symbol a is invertible, because $0 \notin \operatorname{sp} T(a)$. Besides, $a \in L^\infty$ is sectorial if and only if $a \in GL^\infty$ and $\operatorname{dist}(a/|a|, \mathbf{C}) < 1$, where $\mathbf{C}$ stands for the constant functions and the distance is measured in the L^∞ norm, i.e. $\operatorname{dist}(f, \mathbf{C}) = \inf_{c \in \mathbf{C}} \|f - c\|_\infty$.

Local sectoriality Let $a \in L^\infty$ and $\tau \in \mathbb{T}$. Given a subarc U of $\mathbb{T}$, we denote by $L^\infty(U)$ the essentially bounded functions on U and we define $\mathcal{R}_U(a)$ as the essential range of the restriction $a|U$. Finally, we let $\mathcal{U}_\tau$ denote the collection of all arcs $U \subset \mathbb{T}$ containing τ, and we set

$$\mathcal{R}_\tau(a) \equiv \bigcap_{U \in \mathcal{U}_\tau} \mathcal{R}_U(a)$$

The set $\mathcal{R}_\tau(a)$ is called the *local essential range* of a at τ. The points in $\mathcal{R}_\tau(a)$ are also referred to as the essential cluster points of a at τ. For example, if $a \in PC$, then $\mathcal{R}_\tau(a) = \{a(\tau - 0), a(\tau + 0)\}$.

The function a is called *locally sectorial at* $\tau \in \mathbb{T}$ if $0 \notin \operatorname{conv} \mathcal{R}_\tau(a)$ and said to be *locally sectorial on* $\mathbb{T}$ if $0 \notin \operatorname{conv} \mathcal{R}_\tau(a)$ for every $\tau \in \mathbb{T}$. A locally sectorial function is not necessarily a (globally) sectorial function.

With locally sectorial functions we have the following [12, Th 1.21-22]

Theorem 8. *If $a \in L^\infty$ is locally sectorial on $\mathbb{T}$, then $T(a)$ is Fredholm on ℓ^2 and*

$$\operatorname{Ind} T(a) = -\operatorname{wind}(a, 0)$$

which extends Th. 6 and it can be extended even more for piecewise continuous functions.

Piecewise continuous symbols Let first $a \in PC$ be a piecewise continuous functions. We denote by $a^\#(\mathbb{T})$ the closed continuous and naturally oriented curve which results from the essential range of a by filling in the line segment $[a(t-0), a(t+0)]$ between the endpoint $a(t-0)$ and $a(t+0)$ of each jump. For $\lambda \in \mathbb{C} \setminus a^\#(\mathbb{T})$, we let $\operatorname{wind}(a^\#, \lambda)$ stand for the winding number of $a^\#(\mathbb{T})$ with respect to λ. Subsequently, the following theorem for piecewise continuous symbols is true [12, Th 1.23]

Theorem 9. *Let $a \in PC$. The operator $T(a)$ is Fredholm on ℓ^2 if and only if $0 \notin a^\#(\mathbb{T})$. In that case*

$$\operatorname{Ind} T(a) = -\operatorname{wind}(a^\#, 0) \tag{2.23}$$

Thus,

$$\operatorname{sp}_{ess} T(a) = a^\#(\mathbb{T}) \tag{2.24}$$

$$\operatorname{sp} T(a) = a^\#(\mathbb{T}) \cup \left\{\lambda \in \mathbb{C} \setminus a^\#(\mathbb{T}) : \operatorname{wind}(a^\#, \lambda) \neq 0\right\} \tag{2.25}$$

Two general results are available for functions outside PC [12, Th 1.25-26]

Theorem 10. *(Hartman-Wintner) If $a \in L^\infty$, then*

$$\mathcal{R}(a) \subset \mathrm{sp}_{ess}\, T(a) \tag{2.26}$$

This means that $\mathrm{sp}_{\mathrm{ess}}\, T(a)$ and $\mathrm{sp}\, T(a)$ are always included between $\mathcal{R}(a)$ and $\mathrm{conv}\, \mathcal{R}(a)$. Moreover

Theorem 11 (Douglas-Widom)**.** *If $a \in L^\infty$, then the two spectra $\mathrm{sp}_{ess}\, T(a)$ and $\mathrm{sp}\, T(a)$ are connected sets.*

For selfadjoint Toeplitz, which have real-valued symbols, operator we have the following [12, Th 1.27]

Theorem 12 (Hartman-Wintner)**.** *If $a \in L^\infty$ is real-valued, then*

$$\mathrm{sp}_{ess}\, T(a) = \mathrm{sp}\, T(a) = \mathrm{conv}\, \mathcal{R}(a). \tag{2.27}$$

2.2 Approximation methods

The question we want to address in this section is the following: when can we approximate an infinite system of equation like

$$Ax = y \qquad A \in \mathcal{B}(\ell^2), \quad x, y \in \ell^2$$

with a finite system like

$$A_n x^{(n)} = y^{(n)} \qquad A_n \; n \times n \text{ matrix}, \; x^{(n)}, y^{(n)} \in \ell^2$$

To answer this question we need to introduce the notion of stability of a sequence and strong convergence. Then, this problem of numerical analysis can be resolved with the application of the abstract mathematics of C^*-algebras.

Uniform and strong convergence Let X be a Banach space and $\mathcal{B}(X)$ its set of bounded operator (see (2.3)). Given a sequence $\{A_n\}_{n=1}^\infty$ in $\mathcal{B}(X)$, we say

$$\{A_n\}_{n=1}^\infty \text{ converges uniformly to } A \quad \Longleftrightarrow \quad \|A_n - A\| \underset{n\to\infty}{\longrightarrow} 0$$

and

$$\{A_n\}_{n=1}^\infty \text{ converges strongly to } A \quad \Longleftrightarrow \quad \|A_n x - Ax\| \underset{n\to\infty}{\longrightarrow} 0 \; \forall x \in X$$

Stable sequences Let $\{A_n\}_{n=1}^{\infty}$ be a sequence of $n \times n$ matrices A_n. We say that $\{A_n\}$ is a stable sequence if there is an integer n_0 such that A_n is invertible for all $n \geq n_0$ and $\sup_{n \geq n_0} \left\|A_n^{-1}\right\| < \infty$. With the convention $\left\|A^{-1}\right\| = \infty$ if A is not invertible, we can alternatively say that

$$\{A_n\}_{n=1}^{\infty} \text{ stable} \quad \Longleftrightarrow \quad \limsup_{n \to \infty} \left\|A^{-1}\right\| < \infty \tag{2.28}$$

Approximation method Let $A \in \mathcal{B}(\ell^2)$ and $\{A_n\}_{n=1}^{\infty}$ a sequence of $n \times n$ matrices A_n. Consider the system of equations $Ax = y$, which in matrix form is equivalent to

$$\begin{pmatrix} a_{11} & a_{12} & a_{13} & \dots \\ a_{21} & a_{22} & a_{23} & \dots \\ a_{31} & a_{32} & a_{33} & \dots \\ \vdots & \vdots & \vdots & \ddots \end{pmatrix} \begin{pmatrix} x_1 \\ x_2 \\ x_3 \\ \vdots \end{pmatrix} = \begin{pmatrix} y_1 \\ y_2 \\ y_3 \\ \vdots \end{pmatrix} \tag{2.29}$$

To resolve it, we can consider the finite truncation $A_n x^{(n)} = P_n y$;

$$\begin{pmatrix} a_{11} & a_{12} & \dots & a_{1n} \\ a_{21} & a_{22} & \dots & a_{2n} \\ \vdots & \vdots & \ddots & \vdots \\ a_{n1} & a_{n2} & \dots & a_{nn} \end{pmatrix} \begin{pmatrix} x_1 \\ x_2 \\ \vdots \\ x_n \end{pmatrix} = \begin{pmatrix} y_1 \\ y_2 \\ \vdots \\ y_n \end{pmatrix} \tag{2.30}$$

where P_n is the projection

$$P_n : \ell^2 \to \ell^2, \quad \Big(x_1, x_2, x_3, \dots\Big) \mapsto \Big(x_1, \dots, x_n, 0, 0, \dots\Big) \tag{2.31}$$

and $x^{(n)} \in \operatorname{Im} P_n$. The image of the projection P_n is a subspace of ℓ^2, which can be identified with the complex space $\mathbb{C}^n$. For this reason, it is possible to consider A_n as operators on ℓ^2, not just $\mathbb{C}^n$. Thus we make the identification $A_n = A_n P_n$ and, similarly, $A_n^{-1} = A_n^{-1} P_n$.

Now, suppose $A \in \mathcal{B}(\ell^2)$ is invertible. Then the solution of $Ax = y$ is just $x = A^{-1}y$. On the other hand, it is not obvious if the solutions of the finite system $A_n x^{(n)} = y^{(n)}$ converge to the solutions of A. For this reason we introduce the following notions: a sequence $\{A_n\}$ is said to be an *approximating sequence* of A if it converges strongly to it and we say that the *approximation method* $\{A_n\}$ (or just simply *method*) is *applicable* to A if

- There exist an integer n_0 such that $A_n x^{(n)} = P_n y$ is (uniquely) solved for all $y \in \ell^2$ for $n \geq n_0$
- $\left\|A_n x^{(n)} - Ax\right\| \to 0$ for $n \to \infty$. That is, the solutions $x^{(n)}$ of A_n converge strongly to the solutions x of A.

Equivalently, the method $\{A_n\}$ is applicable to A if A_n invertible for sufficiently large n and $A_n^{-1} \to A^{-1}$ strongly, i.e. $A_n^{-1} P_n y \to A^{-1} y$ for all $y \in \ell^2$. The *finite section method* consist of the sequence of $n \times n$ truncations of an operator A, which means taking $A_n = P_n A P_n|_{\operatorname{Im} P_n}$ (the restriction of $P_n A P_n$ to $\operatorname{Im} P_n$).

One of the fundamental results in functional analysis is the Banach-Steinhaus theorem, or *uniform boundedness principle*, which we can apply to the space ℓ^2

Theorem 13 (Banach-Steinhaus). *Let $\{A_n\}_{n=1}^{\infty}$ be* any *sequence of operators $A_n \in \mathcal{B}(\ell^2)$ such that $\{A_n x\}_{n=1}^{\infty}$ converges strongly in ℓ^2 for every $x \in \ell^2$. Then, $\sup_{n>0} \|A_n\| < \infty$ and the operator A is defined by*

$$Ax = \lim_{n\to\infty} A_n x \in \mathcal{B}(\ell^2)$$

and its norm is

$$\|A\| \leq \liminf_{n\to\infty} \|A_n\|$$

which implies the following [11, Prop 2.1]

Proposition 1. *Let $A \in \mathcal{B}(\ell^2)$ be invertible and $\{A_n\}$ is an approximating sequence of A. Then, the method $\{A_n\}$ is applicable to A if and only if $\{A_n\}$ is stable.*

Proof. In fact, if $A_n^{-1} \to A_n^{-1}$ strongly, then $\limsup \left\|A_n^{-1}\right\| < \infty$ due to the Banach-Steinhaus theorem, hence $\{A_n\}$ is stable. Conversely, suppose $\{A_n\}$ is stable, then for each $y \in \ell^2$,

$$\left\|A_n^{-1} P_n y - A^{-1} y\right\| \leq \left\|A_n^{-1} P_n y - P_n A^{-1} y\right\| + \left\|P_n A^{-1} y - A^{-1} y\right\|$$

Given that $P_n \to I$ strongly, the second term goes to zero. The first term on the right becomes

$$\left\|A^{-1}(P_n y - A_n P_n A^{-1} y)\right\| \leq M \left\|P_n y - A_n P_n A^{-1} y\right\| = o(1)$$

since $A_n P_n A^{-1} \to A A^{-1} = I$ strongly. □

In conclusion, we have obtained the following equivalence

$$\text{convergence} = \text{approximation} + \text{stability}$$

where *convergence* means that the method $\{A_n\}$ is applicable to A, *approximation* that A_n converges strongly to A and *stability* that $\limsup_{n\to\infty} \|A_n^{-1}\| < \infty$.

2.2.1 Perturbed Toeplitz Matrces

For $a \in L^\infty$, let $T_n(a)$ be the $n \times n$ finite Toeplitz matrix

$$T_n(a) = \begin{pmatrix} a_0 & \dots & a_{-(n-1)} \\ \vdots & \ddots & \vdots \\ a_{n-1} & \dots & a_0 \end{pmatrix}$$

We can freely identify $T_n(a)$ with the finite section $P_n T(a) P_n|_{\operatorname{Im} P_n}$, or even $P_n T(a) P_n$. Clearly $T_n(a) \to T(a)$ strongly and also $T^\dagger(a) = T_n(\bar{a}) \to T(\bar{a}) = T^\dagger(a)$ converges strongly. Hence, $\{T_n(a)\}$ is applicable to $T(a)$ only if $\{T_n(a)\}$ is stable.

We are not going to consider just the set of sequences of finite Toeplitz, but a larger class of matrix sequence $\{A_n\}$ with

$$A_n = T_n(a) + P_n K P_n + W_n L W_n + C_n \tag{2.32}$$

where $a \in L^\infty$, $K, L \in \mathcal{K}(\ell^2)$, i.e. compact operators, $\{C_n\}$ is a sequence such that $\|C_n\| \to \infty$ and W_n is the map

$$W_n : \ell^2 \to \ell^2, \ \left(x_1, x_2, \dots, \dots\right) \to \left(x_n, x_{n-1}, \dots, x_1, 0, \dots\right) \tag{2.33}$$

Clearly, $\operatorname{Im} W_n$ is a finite subset of ℓ^2 and likewise a subset of $\mathbb{C}^n$. We can think of W_n as the matrix

$$W_n = \begin{pmatrix} 0 & \dots & 0 & 1 \\ 0 & \dots & 1 & 0 \\ \vdots & \dots & \dots & \vdots \\ 1 & \dots & \dots & 0 \end{pmatrix}$$

If K and L have a finite number of non-zero entries, then $P_n K P_n$ add his entries to the upper-left corner of $T_n(a)$ while $W_n L W_n$ to the bottom right.

One of the reason why we may want to consider matrices like (2.32) is given by the following proposition by Widom [11, Prop 2.3]

Proposition 2 (Widom). *Let $a, b \in L^\infty$. Then the product of two finite Toeplitz matrices is*

not necessarily Toeplitz. In fact,

$$T_n(a)T_n(b) = T_n(ab) - P_nH(a)H(\tilde{b})P_n - W_nH(\tilde{a})H(b)W_n$$

And given that $H(a)H(\tilde{b})$ is compact [12, Th. 1.16], likewise $H(\tilde{a})H(b)$, we can say that

$$T_n(a)T_n(b) = T_n(ab) + P_nKP_n + W_nLW_n \tag{2.34}$$

for some compact operators K and L.

Another reason for why we want to consider sequences like (2.32) is because their set has a C^*-algebra structure, which will be discussed in the next subsection.

2.2.2 Algebraization of stability

Let $\mathcal{S}$ be the set of all sequences $\{A_n\}_{n=1}^{\infty}$ of $n\times n$ matrices A_n such that $\sup_{n>0}\|A_n\| < \infty$. It is a C^*-algebra with the following operations

$$\lambda\{A_n\} \equiv \{\lambda A_n\} \qquad \{A_n\} + \{B_n\} \equiv \{A_n + B_n\}$$
$$\{A_n\}\{B_n\} \equiv \{A_nB_n\} \qquad \{A_n\}^\dagger \equiv \{A^\dagger\} \quad \text{as involution}$$

and norm

$$\|\{A_n\}\| = \sup_{n>0}\|A_n\| \tag{2.35}$$

Let $\mathcal{N}$ denote the set of "null" sequences

$$\mathcal{N} \equiv \Big\{\{A_n\} \in \mathcal{S} : \lim_{n\to\infty}\|A_n\| = 0\Big\}, \tag{2.36}$$

It is a closed two-sided ideal of $\mathcal{S}$, hence the quotient space $\mathcal{S}/\mathcal{N}$ is also a C^*-algebra. For $\{A_n\} \in \mathcal{S}$, the coset $\{A_n\} + \mathcal{N}$ is an element of $\mathcal{S}/\mathcal{N}$ and from this point forward it will be indicated with $\{A_n\}^\nu$, with its norm being

$$\big\|\{A_n\}^\nu\big\| = \limsup_{n\to\infty}\|A_n\| \tag{2.37}$$

It is possible to map the problem of stability into a problem of invertibility in a C^*-algebra [11, Prop 2.4]

Theorem 14. *A sequence $\{A_n\} \in \mathcal{S}$ is stable if and only if $\{A_n\}^\nu$ is invertible in $\mathcal{S}/\mathcal{N}$.*

Proof. If $\{A_n\}$ is stable, there is a sequence $\{B\} \in \mathcal{S}$ such that

$$B_n A_n = P_n + C'_n, \quad A_n B_n = P_n + C''_n$$

where $C'_n = C''_n = 0$ for all $n > n_0$.

This implies that $\{B_n\}^\nu$ is the inverse of $\{A_n\}^\nu$. On the other hand, if $\{A_n\}^\nu$ has the inverse $\{B_n\}^\nu$ in $\mathcal{S}/\mathcal{N}$, then the previous equation holds with certain $\{C'_n\} \in \mathcal{N}$ and $\{C''_n\} \in \mathcal{N}$. Clearly, $\|C'_n\| < 1/2$ for all sufficiently large n. For these n, the matrix $(P_n + C'_n)|\operatorname{Im} P_n = I + C'_n$ is invertible, whence

$$\|A_n^{-1}\| = \|(I + C'_n)^{-1} B_n\| \leq 2\|B_n\|$$

which shows that $\{A_n\}$ is stable. □

The algebra $\mathcal{S}/\mathcal{N}$ is far too big for our purpose. We shall restrict our attention to a subset of $\mathcal{S}$ which contains Toeplitz matrices with continuous symbols. This is the subset $\mathcal{S}(C)$, whose elements are the sequences $\{A_n\}$, where

$$A_n = T_n(a) + P_n K P_n + W_n L W_n + C_n \tag{2.38}$$

with $a \in L^\infty$, K and L compact operator and $\{C_n\} \in \mathcal{N}$. The reason why we picked the set $\mathcal{S}(C)$ and not just the set of the sequences $\{T_n(a)\}$ is because the sets $\mathcal{S}(C)$ and $\mathcal{S}(C)/\mathcal{N}$ are both C^*-subalgebra of $\mathcal{S}$ and $\mathcal{S}/\mathcal{N}$ respectively [11, Th. 2.6]. If fact, while the closure under addition and product with a scalar is obvious, the closure under multiplication is guaranteed by Prop. 2. Hence, by Th. 14, a sequence in $\mathcal{S}(C)$ is stable if and only if the corresponding coset is invertible in $\mathcal{S}(C)/\mathcal{N}$.

Proposition 3. *Suppose* $\{A_n\} \in \mathcal{S}(C)$ *as in* (2.38). *Then*

$$A_n \longrightarrow A \equiv T(a) + K \quad \textit{strongly} \tag{2.39}$$

$$W_n A_n W_n \longrightarrow \tilde{A} \equiv T(\tilde{a}) + L \quad \textit{strongly} \tag{2.40}$$

This can be derived from the fact that $P_n \to I$ strongly and from the identities $W_n^2 = P_n$ and $W_n P_n = P_n W_n = W_n$. Consider now the two maps

$$\psi_0 : \mathcal{S}(C)/\mathcal{N} \to \mathcal{B}(\ell^2), \quad \{A_n\}^\nu \mapsto A \tag{2.41}$$

$$\psi_1 : \mathcal{S}(C)/\mathcal{N} \to \mathcal{B}(\ell^2), \quad \{A_n\}^\nu \mapsto \tilde{A}, \tag{2.42}$$

they are well-defined $*$-homomorphism. Now we can prove this important theorem about stability using C^*-algebra techniques.

Theorem 15 (Silbermann)**.** *A sequence $\{A_n\}$ in the algebra $\mathcal{S}(C)$ is stable if and only if A and $\tilde{A}$ are invertible.*

Proof. Consider the $*$-homomorphism

$$\psi = \psi_0 \oplus \psi_1 : \mathcal{S}(C)/\mathcal{N} \to \mathcal{B}(\ell^2) \oplus \mathcal{B}(\ell^2), \quad \{A_n\}^\nu \mapsto (A, \tilde{A}) \tag{2.43}$$

where obviously $\mathcal{B}(\ell^2) \oplus \mathcal{B}(\ell^2)$ is the C^*-algebra of the ordered pairs (A, B) with norm $\|(A, B)\| = \max(\|A\|, \|B\|)$.

We claim that ϕ is injective, which means that $\phi(\{A_n\}^\nu) = 0$ only if $\{A_n\}^\nu = 0$. Indeed, if

$$A = T(a) + K = 0, \qquad \tilde{A} = T(\tilde{a}) + L = 0$$

then $a = 0$, because $T(a)$ (and likewise $T(\tilde{a})$) has to be equal to a compact operator and the only compact Toeplitz operator is the zero operator [11, Prop. 1.2]. Hence, also $K = L = 0$ which implies $\{A_n\}^\nu = 0$.

The map ψ is an injective $*$-homomorphism, thus by Th. 2 it must preserve the spectra: $\{A_n\}^\nu$ is invertible if and only if A and $\tilde{A}$ are invertible. The invertibility of $\{A_n\}^\nu$ is equivalent to the stability of $\{A_n\}$, by Th. 14, hence we arrive at the assertion. □

By applying this theorem to Toeplitz matrices, we immediately obtain the following

Proposition 4. *Let $a \in C$. The sequence $\{T_n(a)\}$ is stable if and only if $T(a)$ is invertible.*

Proof. Just consider that $\tilde{A} = T(\tilde{a})$ is the transpose of $A = T(a)$, so it is invertible is only if $T(a)$ is invertible. □

Which direct us to the conclusion of this subsection

Proposition 5. *The finite section method is applicable to every invertible Toeplitz operator with a continuous symbol.*

Proof. The sequence of truncations $T_n(a) = P_n T(a) P_n|\operatorname{Im} P_n$ converges strongly to $T(a)$, so it is applicable only if $\{T_n(a)\}$ is stable and we have just proved that it is equivalent to the condition of invertibility of $T(a)$. □

2.2.3 Asymptotic inverses and norms

The following is a theorem that reveals the structure of the asymptotic inverses of an elements of $\mathcal{S}(C)$

Theorem 16. *Let $\{A_n\} \in \mathcal{S}(C)$ as in (2.38) and suppose $T(a) + K$ and $T(a) + L$ are invertible. Then for sufficiently large n,*

$$A_n^{-1} = T_n(a^{-1}) + P_n X P_n + W_n Y W_n + D_n \tag{2.44}$$

where

$$X = (T(a) + K)^{-1} - T(a^{-1}), \qquad Y = (T(\tilde{a}) + L)^{-1} - T(\tilde{a}^{-1})$$

For reference see [11, Th. 2.11].

Now, we want to get an estimate of the norms. First of all, what is the limit of $\|A_n\|$? Recall that the map ψ from (2.43), which is an injective $*$-homomorphism, henceforth it conserves the norms, see Th. 2. Thus

$$\left\|\{A_n\}^\nu\right\| = \left\|\psi(\{A_n\}^\nu)\right\| = \max(\|A\|, \|\tilde{A}\|)$$

with $\left\|\{A_n\}^\nu\right\| = \limsup_{n>0} \|A_n\|$. On the other hand, A is the limit of $A_n = T_n +$ compact operators, which means that $\|A\| = \liminf_{n>0} \|A_n\|$. Hence,

$$\|A\| = \lim_{n\to\infty} \|A_n\|.$$

From this reasoning we arrive at an estimate of the norms of the inverses

Theorem 17. *If $\{A_n\} \in \mathcal{S}(C)$, then*

$$\lim_{n\to\infty} \left\|A_n^{-1}\right\| = \max\left(\left\|A^{-1}\right\|, \|\tilde{A}^{-1}\|\right)$$

which can be applied to Toeplitz matrices:

Proposition 6. *If $a \in C$, then*

$$\lim_{n\to\infty} \left\|T_n^{-1}(a)\right\| = \left\|T^{-1}(a)\right\|$$

2.2.4 Eigenvalues

Limiting sets Let $\{E_n\}_{n=1}^{\infty}$ be a sequence of sets $E_n \subset \mathbb{C}$. The *uniforming limiting set*

$$\liminf_{n\to\infty} E_n$$

is defined as the set of all numbers $\lambda \in \mathbb{C}$ for which there is a sequence $\{\lambda_n\}_{n=1}^{\infty}$ such that $\lambda_n \in E_n$ and $\lambda_n \to \lambda$ for $n \to \infty$. Conversely, the *partial limiting set*

$$\limsup_{n\to\infty} E_n$$

is the set of all numbers $\lambda \in \mathbb{C}$ which are the partial limits of sequences $\{\lambda_n\}_{n=1}^{\infty}$ such that $\lambda_n \subset E_n$. Clearly

$$\liminf_{n\to\infty} E_n \subset \limsup_{n\to\infty} E_n$$

For example, if $E_n = \{0\}$ for odd n and $E_n = \{1\}$ for even n, then $\liminf E_n = \emptyset$ and $\limsup E_n = \{0, 1\}$.

Limiting set of the spectrum Returning to the algebra $\mathcal{S}(C)$, we have the following [11, Th. 2.17]: if $\{A_n\} \in \mathcal{S}(C)$, then

$$\liminf_{n\to\infty} \operatorname{sp} A_n \subset \limsup_{n\to\infty} \operatorname{sp} A_n \subset \operatorname{sp} A \cup \operatorname{sp} \tilde{A} \tag{2.45}$$

and if $\{A_n\}$ is a sequence of *Hermitian matrices* then

$$\liminf_{n\to\infty} \operatorname{sp} A_n = \limsup_{n\to\infty} \operatorname{sp} A_n = \operatorname{sp} A \cup \operatorname{sp} \tilde{A} \tag{2.46}$$

By applying this statement to Toeplitz matrices, we obtain that if $a \in C$ then

$$\liminf_{n\to\infty} \operatorname{sp} T_n(a) \subset \limsup_{n\to\infty} \operatorname{sp} T_n(a) \subset \operatorname{sp} T_n(a) \tag{2.47}$$

and if $a \in C$ is real-valued then

$$\liminf_{n\to\infty} \operatorname{sp} T_n(a) = \limsup_{n\to\infty} \operatorname{sp} T_n(a) = \operatorname{sp} T_n(a) = [\min a, \max a] \tag{2.48}$$

2.3 Circulant matrices

Consider now a finite $n \times n$ Toeplitz matrix $T_n(a)_{ij} = a_{i-j}$. If the coefficients a_j are periodic with modulo n, then we have a *circulant matrix*

$$C_{ij} = \left(a_{i-j \bmod n}\right) = \begin{pmatrix} a_0 & a_{n-1} & a_{n-2} & \dots & a_1 \\ a_1 & a_0 & a_{n-1} & \dots & a_2 \\ a_2 & a_1 & a_0 & & \vdots \\ \vdots & \vdots & & \ddots & \vdots \\ a_{n-1} & a_{n-2} & \dots & \dots & a_0 \end{pmatrix} \tag{2.49}$$

These matrices are rather easy to deal with, as their eigenvalues and eigenvector are immediate to calculate.

Eigenvalues and eigenvectors Given a $n \times n$ matrix C, its eigenvectors ψ_k of eigenvalue λ_k, with $k = 1, \dots, n$, satisfy the equation $C\psi_k = \lambda_k \psi_k$. Consider now the circulant matrix in (2.49). Let F_n be the following matrix

$$(F_n)_{jl} = \frac{e^{i2\pi jl/n}}{\sqrt{n}} \tag{2.50}$$

called the *Fourier matrix*. It can be readily verified that (2.50) diagonalize the circulant matrix C in (2.49) [10, 17]

$$F_n^\dagger C F_n = \operatorname{diag}(\lambda_1, \lambda_2, \dots, \lambda_n) \tag{2.51}$$

with eigenvalues

$$\lambda_k = \sum_j a_j e^{-i2\pi kj/n} \tag{2.52}$$

and eigenvectors

$$\psi_k = \frac{1}{\sqrt{n}} \left(1, e^{-i2\pi k/n}, e^{-i2\pi 2k/n}, \dots, e^{-i2\pi(n-1)k/n}\right)^T \tag{2.53}$$

with $k = 0, \dots, n-1$. This is true for every $n \times n$ circulant matrix. In fact, the following is true [17]

Theorem 18. *Every circulant matrix C has eigenvectors (2.53) and corresponding eigenvalues (2.52) and can be expressed in the form $C = F_n \operatorname{diag}(\lambda_i) F_n^\dagger$. In particular, all circulant*

matrices share the same eigenvectors, the same matrix F_n works for all circulant matrices, and any matrix of the form $C = F_n \operatorname{diag}(\lambda_k) F_n^\dagger$ is circulant.

Moreover, let $C = \{c_{k-j}\}$ and $B = \{b_{k-j}\}$ be two circulant $n \times n$ matrices with eigenvalues λ_m and μ_m respectively. Then

1. C and B commute and $CB = BC = F_n \operatorname{diag}(\lambda_m \mu_m) F_n^\dagger$, and CB is also a circulant matrix
2. $C + B$ is a circulant matrix and $C + B = F_n \operatorname{diag}(\lambda_m + \mu_m) F_n^\dagger$
3. If $\lambda_m \neq 0$ for $m = 0, \ldots, n-1$, then C is non-singular and $C^{-1} = F_n \operatorname{diag}(\lambda_m^{-1}) F_n^\dagger$

In the next chapter we will see how circulant matrices can used to calculates the bulk energies and correlation function of a fermionic chain.

2.4 Singular values

Let H be a Hilbert space and $A \in \mathcal{B}(H)$. Then $\operatorname{sp} A^\dagger A \subset [0, \infty)$ and the non-negative square roots of the numbers in $\operatorname{sp} A^\dagger A$ are called the *singular values* of A [11, 12]. We are going to denote the set of all the singular values of A with $\Sigma(A)$

$$\Sigma(A) = \left\{ s \in [0, \infty) : s^2 \in \operatorname{sp} A^\dagger A \right\} \tag{2.54}$$

If we are dealing with a $n \times n$ matrix A_n, then $A^\dagger A$ admits n eigenvalues $\lambda_j(A^\dagger A)$ and we going to suppose they are always ordered in an increasing order

$$0 \leq \lambda_1(A_n^\dagger A_n) \leq \lambda_2(A_n^\dagger A_n) \leq \cdots \leq \lambda_n(A_n^\dagger A_n) = \|A_n\|^2$$

Thus, also the set of the n singular values $s_j(A_n) \equiv (\lambda_j(A_n^\dagger A_n))^{1/2}$ is ordered

$$0 \leq s_1(A_n) \leq s_2(A_n) \leq \ldots s_n \leq (A_n) = \|A_n\|^2$$

and for convenience we set $s_0(A_n) = 0$.

Singular values decomposition Every $n \times n$ matrix can be factorized as a product of a diagonal matrix, with the singular values along the diagonal, and two unitary matrix, as the following the theorem shows [11, 12]:

Theorem 19 (Singular Value Decomposition)**.** *For every $n \times n$ matrix A_n, there exist unitary matrices U_n and V_n such that*

$$A_n = U_n S_n V_n \tag{2.55}$$

where $S_n = \mathrm{diag}(s_1(A_n), ..., s_n(A_n))$.

Approximation numbers The numbers $s_j(A_n)$ can also be thought as *approximation numbers* in the following sense: for $j = 0, \ldots, n$, let $\mathcal{F}_j^{(n)}$ be the set of the $n \times n$ matrices of rank at most j; the j-th approximation number n $a_j(A_n)$ of $n \times n$ matrix A_n is defined as the distance between A_n and the set $\mathcal{F}_j^{(n)}$

$$a_j(A_n) \equiv \mathrm{dist}\left(A_n, \mathcal{F}_j^{(n)}\right) \equiv \min\left\{\|A_n - F_n\| : F_n \in \mathcal{F}_j^{(n)}\right\} \tag{2.56}$$

The set of the approximation numbers is clearly ordered: $0 = a_n(A_n) \leq a_{n-1}(A_n) \leq \cdots \leq a_0(A_n) = \|A_n\|$. Then, the following is true

Theorem 20. *If A is an $n \times n$ matrix, then $s_j(A_n) = a_{n-j}(A_n)$ for every $j = 0, \ldots, n$.*

2.4.1 The lowest singular value

Since the norm of a diagonal matrix is the maximum of the moduli of the diagonal entries, we obtain from the Singular Value Decomposition theorem that if $A_n \in \mathcal{B}(\mathbb{C}^n)$, then

$$s_1(A_n) = \begin{cases} 1/\left\|A_n^{-1}\right\| & \text{if} \quad A_n \quad \text{is invertible} \\ 0 & \text{if} \quad A_n \quad \text{is not invertible} \end{cases}$$

Thus, given a sequence $\{A_n\}_{n=1}^{\infty}$, we have

$$s_1(A_n) \to 0 \qquad \Longleftrightarrow \qquad \left\|A_n^{-1}\right\| \to \infty$$

This immediately shows that whether the lowest singular value $s_1(A_n)$ converges to zero is closely connected with the stability of the sequence $\{A_n\}$:

$$\liminf_{n\to\infty} s_1(A_n) > 0 \qquad \Longleftrightarrow \qquad \{A_n\} \quad \text{is stable}$$

In the case of Toeplitz matrices $\{T_n(a)\}$, we can reuse some previous results

Theorem 21. *Suppose $a \in L^\infty$ is locally sectorial on $\mathbb{T}$ or $a \in PC$. Then the following are*

equivalent

1. $s_1(T_n(a)) \to 0$
2. $\liminf_{n\to\infty} s_1(T_n(a)) = 0$
3. $\{T_n(a)\}$ *is not stable*
4. $T(a)$ *is not invertible*

If $a \in L^\infty$ *is locally sectorial on* $\mathbb{T}$*, then*

$$\lim_{n\to\infty} s_1(T_n(a)) = \frac{1}{\left\|T^{-1}(a)\right\|}$$

the limit being zero if $T(a)$ *is not invertible.*

2.4.2 The splitting phenomenon

An interesting result is known about the singular values of a sequence of truncated Toeplitz matrices $\{T_n(a)\}_{n=1}^{\infty}$ of a Toeplitz operator $T(a)$. It is called the *splitting phenomenon*. First of all, we say that the singular values of a sequence $\{A_n\}_{n\in\mathbb{N}}$ of $n \times n$ matrices A_n have the *splitting property* if there are $c_n \to 0$ and $d > 0$ such that

$$\Sigma(A_n) \subset [0, c_n] \cup [d, \infty] \quad \text{for all} \quad n \geq 1 \tag{2.57}$$

Furthermore, we say $\Sigma(A)$ enjoy the *k-splitting property* if exactly k singular values of A_n lie in $[0, c_n]$, for all sufficiently large n, while the remaining $n - k$ belong to $[d, \infty)$. Equivalently, we can say that the sequence $\{A_n\}$ has the k-splitting property if and only if

$$\lim_{n\to\infty} s_k(A_n) = 0 \quad \text{and} \quad \liminf_{n\to\infty} s_{k+1}(A_n) > 0 \tag{2.58}$$

Theorem 22 (The splitting phenomenon)**.** *Let* $a : \mathbb{T} \to \mathbb{C}$ *be a piecewise continuous function. If* $T(a)$ *is Fredholm of index* $k \in \mathbb{Z}$*, then the singular values of* $\{T_n(a)\}$ *have the* $|k|$*-splitting property, i.e.*

$$\lim_{n\to\infty} s_{|k|}(T_n(a)) = 0 \quad \textit{and} \quad \liminf_{n\to\infty} s_{|k|+1}(T_n(a)) > 0 \tag{2.59}$$

if $T(a)$ *is not Fredholm, then*

$$\lim_{n\to\infty} s_k(T_n(a)) = 0 \quad \textit{for each} \quad k \geq 1 \tag{2.60}$$

For the proof of this theorem see [12, Sec 4.3], which is rather laborious. In the case $T(a)$ is Fredholm of index k, the first k singular values go to zero with an exponential speed, i.e. $s_{|k|}(T_n(a)) = O(e^{-\delta n})$ for some $\delta > 0$, if the symbol a is a rational function [11, Th. 5.4]. Otherwise, if it is not Fredholm then $\sigma_k(T_n(b)) = O(1/n^{\alpha})$ for each k and some α [10, Th. 9.8].

2.4.3 Limiting sets of singular values

As we said earlier, the singular values of a matrix A are the square roots of the eigenvalues of $A^{\dagger}A$. The last matrix is clearly a hermitian matrix. This mean we can apply the results of Sub. 2.2.4 to study the limiting sets of singular values. We immediately have that for $\{A_n\} \in \mathcal{S}(C)$

$$\liminf_{n\to\infty} \Sigma(A_n) = \limsup_{n\to\infty} \Sigma(A_n) = \Sigma(A) \cup \Sigma(\tilde{A})$$

Hence

$$\liminf_{n\to\infty} \Sigma(T_n(a)) = \limsup_{n\to\infty} \Sigma(T_n(a)) = \Sigma(T(a))) \cup \Sigma(T(\tilde{a}))$$

Furthermore

$$[\min|a|, \max|a|] \subset \Sigma(T(a)) \subset [0, \max|a|]$$

and if $T_n(a)$ is not Fredholm

$$\Sigma(T(a)) \cup \Sigma(T(\tilde{a}))) = [0, \max|a|]$$

2.5 Final remarks

In conclusion, we can summarize the most important results of this chapter with the following diagram

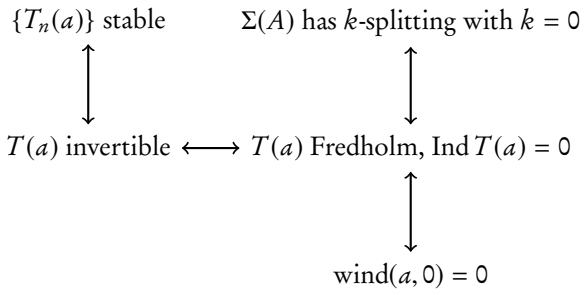

Our main purpose is the study of the band structure of a fermionic chain. In particular we are interested in any energy levels outside the bulk bands which can signal the

presence of edge states. Obviously, the edge states should disappear in the thermodynamic limits.

From the point of view of Toeplitz matrices, the bulk bands constitute set of the singular values $\Sigma(T(a))$, but the information about the edge states is encoded in the finite sections $T_n(a)$. We have seen that a non invertible $T(a)$, means that the limit of the sequence $\{T_n(a)\}$ does not converge in any meaningful way to $T(a)$. This can suggest that the physics in the thermodynamic limit does not faithfully represent what happens in a finite system. The could the "missing physics" possibly be the edge state physics? For now, we don't have any definitive answer but it seems so. The splitting phenomenon appear to have a deep connection with the zero modes (or massless modes) of a topological phase, as the winding number $\mathrm{wind}(a, 0)$ seems connected to the Berry phase of a 1d system, as will be shown later.

3

The Kitaev Model

In this chapter we are going to discuss a particular model, the *Kitaev model*, and a generalization of it with the introduction of a long-range pairing. Before proceeding though, it is useful to introduce the subject of superconductors, and the Bogoliubov-de Gennes formalism, along side with the notion of Majorana fermions, essential to the study of edge modes in topological superconductor.

3.1 Majorana fermions

Basically, a Majorana fermion can be thought as half a fermion. To elaborate on that, suppose we have N (Dirac) fermionic operators $c_1, \dots, c_N$. They satisfy the following anticommutation relationships

$$\{c_i, c_j\} = \{c_i^\dagger, c_j^\dagger\} = 0 \qquad\qquad \{c_i^\dagger, c_j\} = \delta_{ij} \tag{3.1}$$

which entail the Pauli Exclusion Principle, i.e. two fermions cannot occupy the same state.

A Majorana fermion is a fermionic particle which is the antiparticle of itself. We can construct operators to represent such particles from our set of N Dirac fermions $\{c_i\}$ by separating the real and the imaginary part:

$$m_{2j+1} = \left(c_j + c_j^\dagger\right) \qquad\qquad m_{2j} = -i\left(c_j - c_j^\dagger\right) \tag{3.2}$$

They are $2N$ self-conjugate operators, i.e. $m_j^\dagger = m_j$, with the following inverse relations

$$c_i = \frac{1}{2}\left(m_{2j+1} + i m_{2j}\right) \qquad\qquad c_i^\dagger = \frac{1}{2}\left(m_{2j+1} - i m_{2j}\right) \tag{3.3}$$

and the number operator $c_j^\dagger c_j$ becomes $(1 - im_{2j}m_{2j+1})$.

Subsequently, one finds that their commutation relationships are

$$\{m_j, m_k\} = 2\delta_{jk} \tag{3.4}$$

which are rather important because, even if they are reminiscent of the Dirac fermions ones, their consequences are substantially different. We immediately see that $(m_j)^2 = (m_j^\dagger)^2 = 1$, which means that there is no Pauli Exclusion principal for Majorana fermions. Acting twice with m_j gives as back the same state. In fact, it is not even possible to speak about the occupancy number of a Majorana mode, because if we are to construct a number operator for it then it is just $m_j^\dagger m_j = (m_j)^2 = 1$. The same for $m_j m_j^\dagger = 1$. Thus, the Majorana mode is in a sense always empty and always filled and counting does not make any sense [27].

3.2 A brief introduction to superconductors

Roughly speaking, superconductivity is a quantum phenomenon where the resistivity in certain materials vanishes below a critical temperature. Other than zero resistance, it is also characterized by the Meissner effect (perfect diamagnetism) and flux quantization. Discovered in the 1911 by Onnes [21], superconductivity was explained by the BCS-theory, developed by Bardeen et al. [4], and recognized as a purely quantum phase. The idea behind BCS-theory is the formation of bound pairs of electrons with opposite momenta and spin, and energy near the Fermi level, favoured by the electron-phonon interaction in the metal. These bounded pairs of fermions behave like bosons thus, at very low temperature, they can form a Bose-Einstein condensate, which is the responsible for the superconductivity.

An effective Hamiltonian for the quasiparticles in BCS-theory in momentum space can be written as [33, 34]

$$H_{\text{eff}} = \sum_{\mathbf{k}} \left[h(\mathbf{k}) c_{\mathbf{k}}^\dagger c_{\mathbf{k}} + \frac{1}{2}\left(\Delta(\mathbf{k}) c_{-\mathbf{k}} c_{\mathbf{k}} + \Delta^*(\mathbf{k}) c_{\mathbf{k}}^\dagger c_{-\mathbf{k}}^\dagger \right) \right] \tag{3.5}$$

if we are dealing with spinless fermions (this an is example of a p-wave pairing). The function $h(\mathbf{k})$ is the kinetic term, plus the chemical potential if present, while $\Delta(\mathbf{k})$ is the *superconductive gap*. These functions are to be taken even and odd, respectively. The Hamiltonian (3.5) derives from a mean-field theory approach, where the electron-phonon interaction gives rise to an electron-electron interaction, represented by the last

two terms of the Hamiltonian. Thus, the $\Delta^*(\mathbf{k})c_{\mathbf{k}}^\dagger c_{-\mathbf{k}}^\dagger$ is the Cooper pair creation term while $\Delta(\mathbf{k})c_{\mathbf{k}}c_{-\mathbf{k}}$ is the annihilation term. Furthermore, it is evident that these two terms do not conserve the fermion number but only the fermion parity (i.e the number of fermions modulo 2).

In the Bogoliubov-de Gennes (BdG) formalism, the Hamiltonian in (3.5) can be written in the same form as a single-particle free Hamiltonian, by defining the spinor $\Psi_{\mathbf{k}}^\dagger = (c_{\mathbf{k}}^\dagger \;\; c_{-\mathbf{k}})$ [7]

$$H_{\text{eff}} = \frac{1}{2}\sum_{\mathbf{k}} \Psi_{\mathbf{k}}^\dagger H_{\text{BdG}}(\mathbf{k})\Psi_{\mathbf{k}} = \frac{1}{2}\sum_{\mathbf{k}} \begin{pmatrix} c_{\mathbf{k}}^\dagger & c_{-\mathbf{k}} \end{pmatrix} \begin{pmatrix} h(\mathbf{k}) & \Delta^*(\mathbf{k}) \\ \Delta(\mathbf{k}) & -h(\mathbf{k}) \end{pmatrix} \begin{pmatrix} c_{\mathbf{k}} \\ c_{-\mathbf{k}}^\dagger \end{pmatrix} \tag{3.6}$$

where, as we can see, H_{BdG} contains both the kinetic term and the superconducting gap. This is possible because, given the commutation relationship of the fermionic operators (3.1), the kinetic term can be "doubled" as

$$\{c_{\mathbf{k}}^\dagger, c_{\mathbf{p}}\} = \delta_{\mathbf{kp}} \longrightarrow c_{\mathbf{k}}^\dagger c_{\mathbf{k}} = \frac{1}{2}\left(c_{\mathbf{k}}^\dagger c_{\mathbf{k}} - c_{\mathbf{k}} c_{\mathbf{k}}^\dagger\right) + \frac{1}{2} \tag{3.7}$$

where the constant term can be discarded, as it is just a shift of the energy. Then, we can rename the index $\mathbf{k}$ into $-\mathbf{k}$ in the second term, because it appears in a sum over all $\mathbf{k}$ and the function $h(\mathbf{k})$ is even. Using Pauli matrices, H_{BdG} can be expressed as

$$H_{\text{BdG}}(\mathbf{k}) = h(\mathbf{k})\sigma_z + \text{Re}\,\Delta(\mathbf{k})\sigma_x + \text{Im}\,\Delta(\mathbf{k})\sigma_y \equiv \mathbf{d}(\mathbf{k})\cdot\boldsymbol{\sigma} \tag{3.8}$$

consequently, it resembles a two-band insulator system.

Moreover, an important property of the BdG Hamiltonian is that it has intrinsic PHS (see Sec. 1.3)

$$\Pi H_{\text{BdG}}(\mathbf{k})\Pi^{-1} = -H_{\text{BdG}}(-\mathbf{k}) \tag{3.9}$$

which can be readily verified by mapping $c_{\mathbf{k}} \mapsto c_{\mathbf{k}}^\dagger$, i.e. mapping particles into antiparticles and vice versa. The relation (3.9) implies the existence of a partner eigenstate $\Pi\,|u_{-E}\rangle$ with energy $-E$ for every eigenstate $|u_E\rangle$ with energy E. This is an effect of the redundancy within the BdG formalism [7], which is useful for solving the model.

Now, the single-particle spectrum of the superconducting model can be resolved easily, as it is just the spectrum of the single non-interacting particles Ψ. Hence, the energies are just the eigenvalues of H_{BdG}, which are

$$E(\mathbf{k})^2 = h(\mathbf{k})^2 + \left|\Delta(\mathbf{k})\right|^2 \quad \longrightarrow \quad E_\pm(\mathbf{k}) = \pm\sqrt{h(\mathbf{k})^2 + \left|\Delta(\mathbf{k})\right|^2} \tag{3.10}$$

and, as anticipated, due to the PHS we have two symmetric energy bands, one above and one below the zero-energy, $E_- = -E_+$. We take $E \equiv E_+$.

3.2.1 Bogoliubov transformation

Meanwhile, the eigenvectors can be found through a Bogoliubov transformation (firstly introduced in [9, 38])

$$\Psi'_{\mathbf{k}} \equiv \begin{pmatrix} \eta_{\mathbf{k}} \\ \eta^\dagger_{-\mathbf{k}} \end{pmatrix} \equiv U(\mathbf{k})\Psi_k \equiv \begin{pmatrix} u_{\mathbf{k}} & -v_{\mathbf{k}} \\ -v^*_{-\mathbf{k}} & u^*_{-k} \end{pmatrix} \begin{pmatrix} c_{\mathbf{k}} \\ c^\dagger_{-\mathbf{k}} \end{pmatrix}, \qquad |u_{\mathbf{k}}|^2 + |v_{\mathbf{k}}|^2 = 1 \tag{3.11}$$

The new modes η_k, $\eta^\dagger_k$ have to be such that the new Hamiltonian is diagonal

$$U(\mathbf{k})H_{\mathrm{BdG}}U(\mathbf{k})^\dagger = \begin{pmatrix} E(\mathbf{k}) & 0 \\ 0 & -E(\mathbf{k}) \end{pmatrix} \tag{3.12}$$

Furthermore, in the one dimensional case we can parametrize u_k and v_k as $\cos\theta_k$ and $-i\sin\theta_k$ respectively, then the matrix equation corresponding to (3.12)

$$\begin{pmatrix} \cos\theta_k & i\sin\theta_k \\ i\sin\theta_k & \cos\theta_k \end{pmatrix} \begin{pmatrix} h(k) & \Delta(k) \\ \Delta^*(k) & -h(k) \end{pmatrix} \begin{pmatrix} \cos\theta_k & -i\sin\theta_k \\ -i\sin\theta_k & \cos\theta_k \end{pmatrix} = 0 \tag{3.13}$$

leads to

$$\Delta \sin^2\theta_k + \Delta^* \cos^2\theta_k = ih(k)\sin 2\theta_k \tag{3.14}$$

which completely determine the coefficients u_k and v_k for a 1D system.

Now that the Hamiltonian (3.5) has been diagonalized, we can express the ground state $|\mathrm{GS}\rangle$ of the system, which corresponds to the vacuum of the operators $\eta_{\mathbf{k}}$, that is $\eta_{\mathbf{k}}|\mathrm{GS}\rangle = 0$ for every $\mathbf{k}$. It is possible to demonstrate that the normalized ground state is [33]

$$|\mathrm{GS}\rangle = \prod_{\mathbf{k}} \left(u_{\mathbf{k}} + v_{\mathbf{k}} c^\dagger_{\mathbf{k}} c^\dagger_{-\mathbf{k}}\right)|0\rangle, \tag{3.15}$$

where $|0\rangle$ is the vacuum of the particles $c_{\mathbf{k}}$, i.e. $c_{\mathbf{k}}|0\rangle = 0$ for every $\mathbf{k}$, and we can see that this is a superposition of Cooper pairs, to be more precise it is a coherent state of Cooper pairs.

3.2.2 Lieb-Schultz-Mattis method

The BCS Hamiltonian (3.5) has been resolved with the help of the Bogoliubov transformation and this worked because the problem was defined in momentum space. Suppose now we start with a generic quadratic Hamiltonian in lattice space

$$H = \sum_{i,j} \left(c_i^\dagger A_{ij} c_j + \frac{1}{2} \left(c_i^\dagger B_{ij} c_j^\dagger + \text{ h.c.} \right) \right) \tag{3.16}$$

where A is symmetric while B is antisymmetric and the indexes i and j run over all the N sites of the chain. To diagonalize such a Hamiltonian, one can think to apply a Fourier transform, like in (1.33), to pass to the momentum space and then follow the method used to resolve (3.5). To do so, one has to impose periodic boundary conditions on a finite system, because it is necessary to preserve the translational invariance, which is a requirement for the Fourier transform.

This method is useful for studying the bulk properties but loses information about the dynamics on the boundary. In the case of 1D fermionic systems, Lieb et al. (LSM) in their paper [29] proposed a method of diagonalization of quadratic fermionic models that does not require a Fourier transform nor a Bogoliubov transform. Thus, it can capture energy levels that live outside the bulk bands and can be used to investigate possible edge modes.

To present the LSM method, we start from the Hamiltonian (3.16). Then, we search for a linear transformation of the operators c_i in the form

$$\eta_k = \sum_k \left(g_{ki} c_i + h_{ki} c_i^\dagger \right) \qquad\qquad \eta_k^\dagger = \sum_k \left(g_{ki} c_i^\dagger + h_{ki} c_i \right) \tag{3.17}$$

with real coefficients g_{ki} and h_{ki}, such that the resulting Hamiltonian is diagonal

$$H = \sum_k \Lambda_k \eta_k^\dagger \eta_k + \text{constant} \tag{3.18}$$

Such a transformation has to be canonical, in the sense that the new operators η_k and $\eta_k^\dagger$ have to be Fermi operators. For this purpose, we consider the following equation for the eigenvalues and eigenvectors

$$[\eta_k, H] - \Lambda_k \eta_k = 0 \tag{3.19}$$

which derive directly from (3.18). Next, by substituting (3.17) into (3.19) one obtains[1] a set of equations for g_{ki} and h_{ki}

$$\begin{aligned}\sum_j \Big(g_{kj}A_{ji} - h_{kj}B_{ji}\Big) &= \Lambda_k g_{ki} \\ \sum_j \Big(g_{kj}B_{ji} - h_{kj}A_{ji}\Big) &= \Lambda_k h_{ki}\end{aligned} \tag{3.20}$$

which are valid only if *A and B are real matrices*. These equations can be further simplified by the linear combinations

$$\phi_{ki} = g_{ki} + h_{ki} \qquad\qquad \psi_{ki} = g_{ki} - h_{ki} \tag{3.21}$$

into the following ($\boldsymbol{\phi}_k \equiv (\phi_{ki})$ and $\boldsymbol{\psi}_k \equiv (\psi_{ki})$)

$$\boldsymbol{\phi}_k(A - B) = \Lambda\boldsymbol{\psi}_k \qquad\qquad \boldsymbol{\psi}_k(A + B) = \Lambda\boldsymbol{\phi}_k \tag{3.22}$$

Moreover, these equations can be easily decoupled into

$$\boldsymbol{\phi}_k(A - B)(A + B) = \Lambda^2\boldsymbol{\phi}_k \tag{3.23}$$

$$\boldsymbol{\psi}_k(A + B)(A - B) = \Lambda^2\boldsymbol{\psi}_k \tag{3.24}$$

The equations (3.23) and (3.24) are the essence of the LSM method. By solving them, one finds the solutions $\boldsymbol{\phi}_k$ and $\boldsymbol{\psi}_k$ from which is possible to reconstruct the modes η_k and $\eta_k^\dagger$ that diagonalize the Hamiltonian (3.16).

Now, because A is symmetric while B is antisymmetric, we have $(A+B)^T = (A-B)$. Then, it follows that Λ_k^2 are eigenvalues of a real symmetric semi-definite positive matrix, which means they are real and positive. Furthermore, the $\boldsymbol{\phi}_k$'s and $\boldsymbol{\psi}_k$ can be chosen real and orthonormal. The orthonormality of the eigenvectors $\boldsymbol{\phi}_k$ and $\boldsymbol{\psi}_k$ is equivalent

[1] One has to recall the commutation relations of Fermi operators (3.1) and the rule

$$[A, BC] = \{A, B\}C - B\{A, C\}$$

to the constraints

$$\begin{aligned}\sum_i (g_{ki}g_{li} + h_{ki}h_{li}) &= \delta_{kl} \\ \sum_i (g_{ki}h_{li} + h_{ki}g_{li}) &= 0\end{aligned} \tag{3.25}$$

which are necessary and sufficient conditions to impose if we want the transformation (3.17) to be canonical. In fact, it can be readily verified that

$$\begin{aligned}\left\{\eta_k^\dagger, \eta_l\right\} &= \sum_{ij} \left\{g_{ki}c_i^\dagger + h_{ki}c_i\ ,\ g_{lj}c_j + h_{lj}c_j^\dagger\right\} \\ &= \sum_{ij} \left(g_{ki}g_{lj}\left\{c_i^\dagger, c_j\right\} + h_{ki}h_{lj}\left\{c_i, c_j^\dagger\right\}\right) \\ &= \sum_i \left(g_{ki}g_{li} + h_{ki}h_{li}\right) = \delta_{kl}\end{aligned} \tag{3.26}$$

In similar manner, we can also prove the second set of constraints from $\{\eta_k, \eta_l\} = 0$.

We move on to calculate the constant term (3.18). If the trace of (3.16) is taken, one finds

$$\operatorname{tr} H = 2^{N-1} \sum_i A_{ii} \tag{3.27}$$

while from (3.18) one finds

$$\operatorname{tr} H = 2^{N-1} \sum_i \Lambda_i + 2^N \times \text{constant} \tag{3.28}$$

which means the constant is $\frac{1}{2}(\sum_i A_{ii} - \sum_i \Lambda_i)$, thus

$$H = \sum_k \Lambda_k \eta_k^\dagger \eta_k + \frac{1}{2}\left(\sum_i A_{ii} - \sum_i \Lambda_i\right) \tag{3.29}$$

3.2.3 1D correlation functions

The essential tools for capturing the physics of a quantum system are the correlation functions. Here, we are going to give some general expression for a 1D p-wave Hamiltonian like

$$H = \frac{1}{2}\sum_k \begin{pmatrix} c_k^\dagger & c_{-k} \end{pmatrix} \begin{pmatrix} h(k) & \Delta^*(k) \\ \Delta(k) & -h(k) \end{pmatrix} \begin{pmatrix} c_k \\ c_{-k}^\dagger \end{pmatrix} \tag{3.30}$$

in momentum space

One-body correlation functions To start, we call the expectation value $g_1(i-j) \equiv \langle \mathrm{GS}|c_i^\dagger c_j|\mathrm{GS}\rangle \equiv \langle c_i^\dagger c_j\rangle$ the *one-body correlation function* and $g_1^a(i-j) \equiv \langle \mathrm{GS}|c_i^\dagger c_j^\dagger|\mathrm{GS}\rangle$ the *anomalous correlation function*, where c_i and $c_i^\dagger$ are defined in the lattice space. Given the fact that they are evaluated on the ground state (3.15) of the Bogoliubov quasi-particles (3.11), it is convenient to express $c_i^\dagger$ and c_i in terms of η_k and $\eta_k^\dagger$.

First, we start from the Fourier transform [2]

$$c_m = \frac{1}{\sqrt{N}}\sum_k e^{ikm}\tilde{c}_m \qquad\qquad c_m^\dagger = \frac{1}{\sqrt{N}}\sum_k e^{-ikm}\tilde{c}_m^\dagger \tag{3.31}$$

Then, we rewrite $\tilde{c}_k$ and $\tilde{c}_k^\dagger$ using the inverse of (3.11) in the 1D case

$$\begin{pmatrix} c_k \\ c_{-k}^\dagger \end{pmatrix} = \begin{pmatrix} \cos\theta_k & -i\sin\theta_k \\ -i\sin\theta_k & \cos\theta_k \end{pmatrix}\begin{pmatrix} \eta_k \\ \eta_{-k}^\dagger \end{pmatrix} \tag{3.32}$$

The final expressions for c_m and $c_m^\dagger$ are then

$$\begin{aligned} c_m &= \frac{1}{\sqrt{N}}\sum_k e^{ikm}\left(\cos\theta_k\eta_k - i\sin\theta_k\eta_{-k}^\dagger\right) \\ c_m^\dagger &= \frac{1}{\sqrt{N}}\sum_k e^{-ikm}\left(\cos\theta_k\eta_k^\dagger + i\sin\theta_k\eta_{-k}\right) \end{aligned} \tag{3.33}$$

Afterward, we substitute these into the definitions of $g_1(i-j)$ and $g_1^a(i-j)$ and, since $\langle\eta_k\eta_p^\dagger\rangle = \delta_{kp}$ while the other combinations vanish, we obtain

$$g_1(m-n) = \langle c_m^\dagger c_n\rangle = \frac{1}{N}\sum_k e^{ik(m-n)}\sin^2\theta_k \tag{3.34}$$

$$g_1^a(m-n) = \langle c_m^\dagger c_n^\dagger\rangle = \frac{i}{N}\sum_k e^{ik(m-n)}\sin\theta_k\cos\theta_k \tag{3.35}$$

[2] By employing the Fourier transform, we are assuming periodic boundary conditions. This does not pose any problem, because we are interested in the correlation functions in the bulk and in the thermodynamic limit.

In the thermodynamic limit the functions g_1 and g_1^a becomes

$$g_1(R) = \frac{1}{2\pi}\int_0^{2\pi} e^{ikR}\sin^2\theta_k \tag{3.36}$$

$$g_1^a(R) = \frac{1}{2\pi}\int_0^{2\pi} e^{ikR}\sin\theta_k\cos\theta_k \tag{3.37}$$

$$\tag{3.38}$$

Two-body correlation functions The main two-body function we are interested in is the *density-density correlation function*

$$g_2(i-j) = \langle n_i n_j\rangle - \langle n_i\rangle\,\langle n_j\rangle \tag{3.39}$$

where $n_i = c_i^\dagger c_j$ is the number operator of the i-th site. The function g_2 which can be broken down to product of one-body CRs, thanks to Wick's theorem[3]

$$\begin{aligned} g_2(i-j) &= \langle c_i^\dagger c_i c_j^\dagger c_j\rangle - \langle c_i^\dagger c_i\rangle\,\langle c_j^\dagger c_j\rangle \\ &= \langle c_i^\dagger c_i\rangle\,\langle c_j^\dagger c_j^\dagger\rangle - \langle c_i^\dagger c_j^\dagger\rangle\,\langle c_i c_j\rangle + \langle c_i^\dagger c_j\rangle\,\langle c_i c_j^\dagger\rangle - \langle c_i^\dagger c_i\rangle\,\langle c_j^\dagger c_j\rangle \\ &= \left|g_1^a(i-j)\right|^2 - \left|g_1(i-j)\right|^2 \end{aligned} \tag{3.40}$$

3.3 Correlation functions and circulant matrices

Now we show how to obtain the correlation functions from the LSM method by making use of the circulant matrices described in Sec. 2.3. This method was for the first time introduced by Keating and Mezzadri [23] and also used by Its et al. [20] in the context of entanglement entropy of quantum spin chains.

Majorana operators First of all we define the Majorana operators m_j from the Fermi operators c_j and $c_j^\dagger$

$$m_{2j+1} = c_j + c_j^\dagger \qquad\qquad m_{2j} = i(c_j - c_j^\dagger) \tag{3.41}$$

[3] For example the product $\langle c_i c_j c_l c_m\rangle$ can be expressed as

$$\langle c_i c_j c_l c_m\rangle = \langle c_i c_j\rangle\,\langle c_l c_m\rangle - \langle c_i c_l\rangle\,\langle c_j c_m\rangle + \langle c_i c_m\rangle\,\langle c_j c_l\rangle$$

because is the sum of all possible contractions in pairs of the quadruple product. Plus, there is minus sign every time the permutation is odd. The Wick Theorem is valid only when the theory is free, i.e. quadratic.

The inverse relations are just

$$c_j^\dagger = \frac{1}{2}\Big(m_{2j+1} + i m_{2j}\Big) \qquad\qquad c_j = \frac{1}{2}\Big(m_{2j+1} - i m_{2j}\Big) \tag{3.42}$$

We now want to express the Majorana modes in terms of the modes η_k and $\eta_k^\dagger$ in (3.18). Starting from the LSM method in Sub. 3.2.2, one finds that

$$\begin{aligned}
\eta_k &= \sum_j \Big(g_{kj} c_j + h_{kj} c_j^\dagger\Big) \\
&= \sum_j \left(\frac{\phi_{kj} + \psi_{kj}}{2} c_j + \frac{\phi_{kj} - \psi_{kj}}{2} c_j^\dagger\right) \\
&= \sum_j \left(\phi_{kj} \frac{c_j + c_j^\dagger}{2} + \psi_{kj} \frac{c_j - c_j^\dagger}{2}\right)
\end{aligned}$$

and by using (3.41), it leads to

$$\begin{aligned}
\eta_k &= \frac{1}{2} \sum_j \Big(\phi_{kj} m_{2j+1} - i \psi_{kj} m_{2j}\Big) \\
\eta_k^\dagger &= \frac{1}{2} \sum_j \Big(\phi_{kj} m_{2j+1} + i \psi_{kj} m_{2j}\Big).
\end{aligned} \tag{3.43}$$

Then, by exploiting the orthonormality of the eigenvectors ϕ_k and ψ_k, we can invert (3.43) and arrive at the following expressions:

$$m_{2j} = i \sum_k \psi_{kj} \Big(\eta_k - \eta_k^\dagger\Big) \qquad\qquad m_{2j+1} = \sum_k \phi_{kj} \Big(\eta_k + \eta_k^\dagger\Big). \tag{3.44}$$

This form of the Majorana operators m_j is useful for the evaluation of their expectation values on the vacuum.

Expectation values Let $|\mathrm{GS}\rangle$ be the ground state of the η_k particles, i.e. $\eta_k |\mathrm{GS}\rangle = 0$ for all k. We want to prove that the expectation values of a pair of the operators m_i can be written in the form

$$\langle \mathrm{GS} | m_i m_j | \mathrm{GS} \rangle \equiv \big\langle m_i m_j \big\rangle = \delta_{ij} + i (C_L)_{ij} \tag{3.45}$$

where C_L is a $2L \times 2L$ block matrix. Its components are $(C_L)_{ij} = (C_{ij})_{i,j=1\ldots L}$, where

$$C_{ij} = \begin{pmatrix} 0 & (T_L)_{ij} \\ -(T_L)_{ji} & 0 \end{pmatrix}, \qquad (T_L)_{ij} = \sum_k \psi_{ki}\phi_{kj} \tag{3.46}$$

We first evaluate $\langle m_{2i} m_{2j} \rangle$:

$$\begin{aligned} \langle m_{2i} m_{2j} \rangle &= i^2 \sum_{kl} \psi_{ki}\psi_{lj} \left\langle (\eta_k - \eta_k^\dagger)(\eta_l - \eta_l^\dagger) \right\rangle \\ &= \sum_{kl} \psi_{ki}\psi_{lj} \left\langle \eta_k \eta_l^\dagger \right\rangle \\ &= \sum_k \psi_{ki}\psi_{kj} = \delta_{ij}, \end{aligned}$$

thanks to the orthonormality of the vectors ψ_k. Analogously, $\langle m_{2i+1} m_{2j+1} \rangle$ becomes

$$\begin{aligned} \langle m_{2i+1} m_{2j+1} \rangle &= \sum_{kl} \phi_{ki}\phi_{lj} \left\langle (\eta_k + \eta_k^\dagger)(\eta_l + \eta_l^\dagger) \right\rangle \\ &= \sum_{kl} \phi_{ki}\phi_{lj} \left\langle \eta_k \eta_l^\dagger \right\rangle \\ &= \sum_k \phi_{ki}\phi_{kj} = \delta_{ij}, \end{aligned}$$

for the orthonormality of ϕ_k instead. On the other hand, the expectation values $\langle m_{2i} m_{2j+1} \rangle$ and $\langle m_{2i+1} m_{2j} \rangle$ are non-trivial. In fact,

$$\begin{aligned} \langle m_{2i} m_{2j+1} \rangle &= i \sum_{kl} \phi_{lj}\psi_{ki} \langle (\eta_k - \eta_k^\dagger)(\eta_l + \eta_l^\dagger) \rangle \\ &= i \sum_{kl} \phi_{lj}\psi_{ki} \langle \eta_k \eta_l^\dagger \rangle \\ &= i \sum_k \psi_{ki}\phi_{kj} \equiv i(T_L)_{ij} \end{aligned}$$

and likewise

$$\langle m_{2i+1} m_{2j} \rangle = -i \sum_k \phi_{ki}\psi_{kj} = -i(T_L)_{ji} \tag{3.47}$$

All of this can be summarized as

$$\left\langle \begin{pmatrix} m_{2i}m_{2j} & m_{2i}m_{2j+1} \\ m_{2i+1}m_{2j} & m_{2i+1}m_{2j} \end{pmatrix} \right\rangle = \delta_{ij} + i \begin{pmatrix} 0 & (T_L)_{ij} \\ -(T_L)_{ji} & 0 \end{pmatrix} = \delta_{ij} + i(C_L)_{ij} \tag{3.48}$$

3.3.1 Solution of the eigenvalue equation

The class of translationally invariant Hamiltonians we are interested in are in the form

$$H = -t \sum_{j,k=1}^{L} c_j^\dagger A_{jk} c_k - \mu \sum_{j=1}^{L} \left(c_j^\dagger c_j - \frac{1}{2} \right) - \frac{\Delta}{2} \sum_{j,k=1}^{L} \left(c_j B_{jk} c_k - c_j^\dagger B_{jk} c_k^\dagger \right) \tag{3.49}$$

where L is the number of sites and A and B are real matrices. Also, the kinetic term, the chemical potential and the superconductive pairing have been explicated. Because of the *translational invariance*, the matrices A and B have to be *Toeplitz matrices*, in the sense that $A_{ij} = A_{i-j}$ and $B_{ij} = B_{i-j}$. Furthermore, we are interested in the properties of the bulk, i.e. the correlation functions, which means we can impose *periodic boundary conditions*. This elevates A and B to *circulant matrices*, that is $A_{ij} = A_{i-j \mod L}$ and likewise $B_{ij} = B_{i-j \mod L}$.

Let $a, b : \mathbb{Z}/L\mathbb{Z} \to \mathbb{R}$ be two periodic real-valued functions, with period L, defined as

$$a(i-j) \equiv \bar{A}_{ij} \equiv -tA_{ij} - \mu\delta_{ij} \qquad b(i-j) \equiv \bar{B}_{ij} \equiv \Delta B_{ij} \tag{3.50}$$

which are respectively even and odd functions

$$a(-j) = a(j) \qquad b(-j) = -b(j)$$

They encapsulate the coefficients of the circulant matrices $\bar{A}$ and $\bar{B}$, which makes a and b respectively their symbols. With the matrices $\bar{A}$ and $\bar{B}$, we establish a direct connection with the Hamiltonian (3.18), studied by Lieb et al. in [29].

First of all, we readily obtain that also the matrices $(\bar{A}+\bar{B})$ and $(\bar{A}-\bar{B})$ are by themself circulant matrices, see Sec. 2.3, with symbols

$$\begin{aligned} (\bar{A} + \bar{B}_{jk}) &= a(j-k) + b(j-k) \\ (\bar{A} - \bar{B}_{jk}) &= a(j-k) - b(j-k) \end{aligned} \tag{3.51}$$

hence, also the products $(\bar{A}+\bar{B})(\bar{A}-\bar{B})$ and $(\bar{A}-\bar{B})(\bar{A}+\bar{B})$ are circulant. Thanks to the Th. 18 about the eigenvalues and eigenvectors of a circulant matrix, we can immediately

solve the fundamental equations of the LSM method (3.23) and (3.24).

Before proceeding, we can make some harmless simplification. As it have been said already in Sec. 3.2.2, the eigenvalues Λ_k^2 are real and positive. Thus, we can take Λ_k^2 to be the modulo squared of complex number, i.e. $\Lambda_k^2 = |\Lambda_k|^2$. This assumption slightly transform the LSM equations into

$$\begin{aligned} \phi_k(\bar{A}-\bar{B})(\bar{A}+\bar{B}) &= |\Lambda_k|^2\phi_k & \qquad \phi_k(\bar{A}-\bar{B}) &= |\Lambda_k|\psi_k \\ \psi_k(\bar{A}+\bar{B})(\bar{A}-\bar{B}) &= |\Lambda_k|^2\phi_k & \qquad \psi_k(\bar{A}+\bar{B}) &= |\Lambda_k|\phi_k \end{aligned}$$

Furthermore, we want the eigenvectors ϕ_k and ψ_k to be multiplied from the left, not from the right. To achieve this, it is sufficient to transpose all the equation, which flips all the signs.

$$(\bar{A}+\bar{B})(\bar{A}-\bar{B})\phi_k = |\Lambda|^2\phi_k \qquad (\bar{A}+\bar{B})\phi_k = |\Lambda_k|\psi_k \tag{3.52}$$

$$(\bar{A}-\bar{B})(\bar{A}+\bar{B})\psi_k = |\Lambda_k|^2\phi_k \qquad (\bar{A}-\bar{B})\psi_k = |\Lambda_k|\phi_k \tag{3.53}$$

Now, we can work on (3.52) and (3.53). Based on Th. 18, we take as a basis of eigenvectors the plain waves

$$\phi_{kj} = \frac{\exp(i2\pi jk)}{\sqrt{L}}$$

which diagonalize both $(\bar{A}-\bar{B})$ and $(\bar{A}+\bar{B})(\bar{A}-\bar{B})$. From (3.53) we get

$$(\bar{A}-\bar{B})\psi_k = \Lambda'_k\psi_k = |\Lambda_k|\phi_k \tag{3.54}$$

where Λ'_k is the eigenvalue of ψ_k with respect to the matrix $(\bar{A}-\bar{B})$. Thus, one finds that $\phi_k = \Lambda'_k\psi_k/|\Lambda_k|$ and, given the fact that both ϕ_k and ψ_k are normalized to one, the number $\Lambda'_k/|\Lambda_k|$ must have modulo one (it is just a phase), hence we can put $\Lambda'_k = \Lambda_k$ [20, 23].

The eigenvalues can be calculated with the aid of the formula (2.52), which in our case yields

$$\Lambda_k = \sum_{k=-(L-1)/2}^{(L-1)/2} \big(a(j)-b(j)\big)e^{ikj} \qquad \text{if } L \text{ even} \tag{3.55}$$

$$\Lambda_k = \sum_{k=-(L-1)/2}^{(L-1)/2} \big(a(j)-b(j)\big)e^{ikj} + (-1)^l a(L/2) \qquad \text{if } L \text{ odd} \tag{3.56}$$

where k is the wave-number $k = 2\pi l/L$, with $l = 0, \ldots, L-1$. Thus, the dispersion relation can be found just by taking the modulus $|\Lambda_k|$.

Even though the eigenvectors ϕ_k and ψ_k we have found are complex, opposed to what Lieb et al. have suggested, this is not of great concern. They are connected to the real eigenvectors with just a unitary transformation [20, 23]. This means the expression (3.46) for T_L is not much different, it sufficient to substitute ψ_{ki} with $\bar{\psi}_{ki}$. One finds that

$$(T_L)_{jl} = \sum_{n=0}^{L-1} \bar{\psi}_{nj}\phi_{nl} = \frac{1}{2\pi} \sum_{k=0}^{2\pi(1-1/L)} \frac{\Lambda_k}{|\Lambda_k|} e^{-ik(j-l)} \tag{3.57}$$

which, in the thermodynamic limit, becomes

$$(T_L)_{jl} = \frac{1}{2\pi} \int_0^{2\pi} \mathrm{d}k \frac{\Lambda_k}{|\Lambda_k|} e^{-ik(j-l)} \tag{3.58}$$

This result is valid for every Hamiltonian of the form (3.49). Moreover, it shows that the correlation matrix T_L is in fact a Toeplitz matrix, $(T_L)_{jl} = (T_L)_{j-l}$, with symbol $\Lambda_k/|\Lambda_k|$, which can be directly deduced from Hamiltonian.

It is worthwhile to mention that with just a simple application of circulant matrices, we have single-handedly obtained the spectra $|\Lambda_k|^2$, the eigenvectors ψ_k and ϕ_k and an analytic formula for correlation matrix T_L without the employment of Fourier transformation or Bogoliubov transformation, which can be tedious sometimes to calculate.

One-body correlation functions The last step is to derive the correlation functions for the Fermi operators, which can be done easily. Recalling the inverse relations (3.42), one finds that

$$\begin{aligned}
\langle c_i^\dagger c_j \rangle &= \frac{1}{4} \langle (m_{2i+1} + i m_{2i})(m_{2j+1} - i m_{2j}) \rangle \\
&= \frac{1}{4} \Big(\langle m_{2i+1} m_{2j+1} \rangle - i \langle m_{2i+1} m_{2j} \rangle + i \langle m_{2i} m_{2j+1} \rangle + \langle m_{2i} m_{2j} \rangle \Big) \\
&= \frac{1}{4} (2\delta_{ij} - (T_L)_{ji} - (T_L)_{ij})
\end{aligned}$$

which, with $i \neq j$, means that

$$\langle c_i^\dagger c_j \rangle = g_1(i-j) = -\frac{1}{4} \Big((T_L)_{ij} + (T_L)_{ji} \Big) = -\frac{1}{4\pi} \int_0^{2\pi} \mathrm{d}k \frac{\Lambda_k}{|\Lambda_k|} \cos\big(k(i-j)\big) \tag{3.59}$$

in the thermodynamic limit. Analogously, the anomalous correlation function becomes

$$\langle c_i^\dagger c_j^\dagger \rangle = g_1^a(i-j) = \frac{1}{4}\Big((T_L)_{ji} - (T_L)_{ij}\Big) = \frac{i}{4\pi}\int_0^{2\pi} \mathrm{d}k \frac{\Lambda_k}{|\Lambda_k|}\sin\big(k(i-j)\big) \tag{3.60}$$

3.4 The Kitaev model

Kitaev [24], while investigating the possibility of fault-tolerant quantum computation, proposed a model of a quantum wire, i.e. a 1D quantum system, which should act as *quantum memory*. The reason behind this model is to go around some of the errors that can happen with quantum computation with qubits. These errors can be of two kind; a *classical error*, usually represented by an operator σ_j^x, that flips a qubit from $|0\rangle$ to $|1\rangle$, or phase error, represented by σ_j^z, which modifies the relative phase between the $|1\rangle$ and $|0\rangle$ states. We can protect a system from classical errors by using electrons' occupation state as a qubit. Then, such an error would require a violation of charge conservation but it will not protect against phase errors, which are described by $c_j^\dagger c_j$.

If we want to do so, one way is to employ Majorana fermions. Suppose we construct a Dirac fermion from a couple of Majorana fermions c_{2j+1}, c_{2j} belonging to different sites, then a phase error $a_j^\dagger a_j = \frac{1}{2}(1 - im_{2j}m_{2j+1})$ becomes rather unlikely because it would require an interaction between different, possibly distant, sites, which is avoidable. Furthermore, a single isolated Majorana mode cannot appear in a Hamiltonian, as it violates fermionic parity, thus unpaired Majorana fermions are protected from any kind of error [24].

The goal is then to construct a Hamiltonian that gives rise to such fermions and it can be achieved in superconducting quantum wires. Indeed, Kitaev proposed the following model

$$H = \sum_j \left(-t\left(c_j^\dagger c_{j+1} + c_{j+1}^\dagger c_j\right) - \mu\left(c_j^\dagger c_j - \frac{1}{2}\right) + \Delta c_j c_{j+1} + \Delta^* c_{j+1}^\dagger c_j^\dagger\right) \tag{3.61}$$

where $j = 1, \dots, N$ is an index that runs over all sites, t is the hopping amplitude, $\Delta = |\Delta|e^{i\theta}$ the superconducting gap and μ the chemical potential. The phase in Δ can be reabsorbed in the fermion operator with a gauge transformation, i.e. $c_j \mapsto e^{-i\theta/2}c_j$, then $\Delta = |\Delta|$.

Spectrum of the Kitaev model We now proceed to solve the Hamiltonian by finding its spectrum. To do so, we pass to momentum space with a Fourier transform

$$c_j = \frac{1}{\sqrt{N}} \sum_k e^{ikj} c_k \qquad\qquad c_j^\dagger = \frac{1}{\sqrt{N}} \sum_k e^{-ikj} c_k^\dagger \tag{3.62}$$

where $k = 2\pi l/N$, $l = 0 \dots N-1$, is the momentum, then

$$H = \sum_k \left[-(t\cos k + \mu) c_k^\dagger c_k - i\Delta \sin k \left(c_{-k} c_k + c_k^\dagger c_{-k}^\dagger \right) \right] \tag{3.63}$$

which can be rewritten in the BdG-formalism (see Section 3.2) as

$$H = \frac{1}{2} \sum_k \begin{pmatrix} c_k^\dagger & c_{-k} \end{pmatrix} \begin{pmatrix} -2t\cos k - \mu & i2\Delta \sin k \\ -i2\Delta \sin k & 2t\cos k + \mu \end{pmatrix} \begin{pmatrix} c_k \\ c_{-k}^\dagger \end{pmatrix} \tag{3.64}$$

From this, we can obtain the spectrum

$$E(k) = \pm\sqrt{(2t\cos k + \mu)^2 + (2\Delta \sin k)^2} \tag{3.65}$$

which is gapped for $2|t| \neq |\mu|$, otherwise the gap closes at $k = \pm\pi$ for $2|t| = |\mu|$. This means we may have a phase transition at $2|t| = |\mu|$ and in fact there is.

3.4.1 Phases of the Kitaev chain

Majorana fermions in the Kitaev model To further analyze the different phases of the Kitaev chain, first we need to rewrite the Hamiltonian (3.61) in terms of the Majorana fermions

$$m_{2j-1} = c_j + c_j^\dagger \qquad\qquad m_{2j} = -i(c_j - c_j^\dagger) \tag{3.66}$$

$$c_j = \frac{1}{2}\left(m_{2j-1} + i m_{2j} \right) \qquad\qquad c_j^\dagger = \frac{1}{2}\left(m_{2j-1} - i m_{2j} \right) \tag{3.67}$$

the labeling is a bit different from what has been done in Section 3.1, but this is not a problem because such a labeling is arbitrary. By substitution, the kinetic terms becomes

$$c_j^\dagger c_{j+1} + c_{j+1}^\dagger c_j = \frac{i}{2}\left(m_{2j-1} m_{2j+2} - m_{2j} m_{2j+1} \right) \tag{3.68}$$

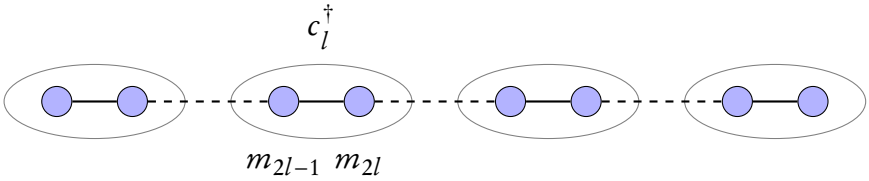

Figure 3.1: Example of a Kitaev chain where we show the splitting of each Dirac fermion into two Majorana fermion.

while the chemical potential transforms as

$$c_j^\dagger c_j - \frac{1}{2} = \frac{i}{2} m_{2j-1} m_{2j} \tag{3.69}$$

and the superconductive pairing is mapped to

$$c_j c_{j+1} + c_{j+1}^\dagger c_j^\dagger = \frac{i}{2}\left(m_{2j-1} m_{2j+2} + m_{2j} m_{2j+1}\right) \tag{3.70}$$

These calculations can be simplified by recognizing that a product of two Majorana fermions is purely imaginary, in fact $(m_i m_j)^\dagger = m_j m_i = -m_i m_j$, so only terms in the form $i m_j m_i$ can appear in a Hermitian Hamiltonian. Lastly, we can finally express (3.61) in terms of Majorana fermions

$$H = \frac{i}{2} \sum_j \left(-\mu m_{2j-1} m_{2j} + (\Delta - t) m_{2j-1} m_{2j+1} + (\Delta + t) m_{2j} m_{2j+1}\right) \tag{3.71}$$

Trivial and topological phases To further characterize these phases ($2|t| < |\mu|$ and $2|t| > |\mu|$) we now consider two special cases, with open boundaries:

1. $\Delta = t = 0,\ \mu < 0$. It is the trivial phase where the pairing is between Majorana fermions of the same site

$$H = -\frac{i\mu}{2} \sum_j m_{2j-1} m_{2j}$$

2. $\Delta = t > 0,\ \mu = 0$. It is the *non-trivial* phase where the pairing is between Majorana fermions of *different* sites

$$H = it \sum_j m_{2j} m_{2j+1}$$

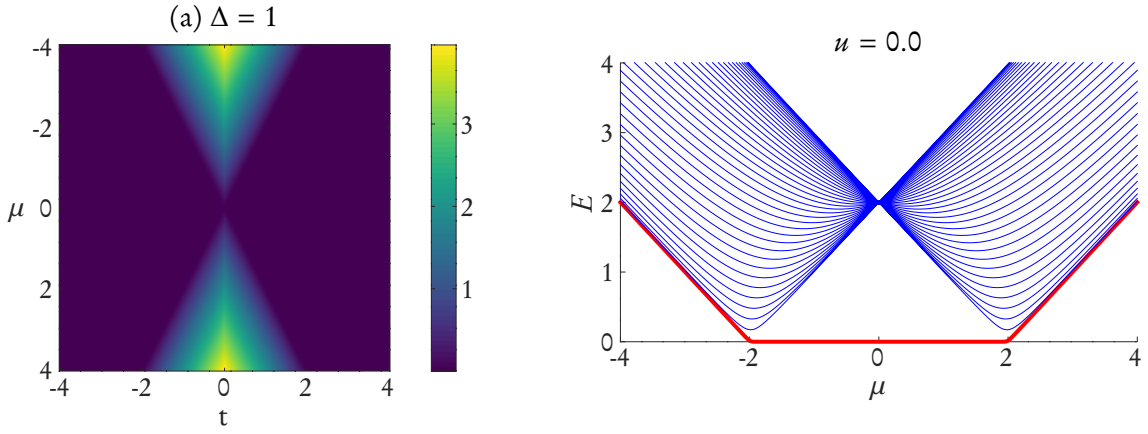

Figure 3.2: **(a)** The graph shows the lowest energy of the Kitaev chain as a function of the chemical potential μ and the hopping parameter t. We clearly see the distinction between the region $|\mu| > 2t$ and $|\mu| < 2t$. The former region is gapped and no zero mode can be found, in fact the lowest energy is above the zero. The second region is the topological sector of the phase diagram and, as we can see, the lowest energy solution is a zero energy mode. **(b)** The graph shows the various energy level as a function of the chemical potential μ, with fixed $\Delta = 1$ and $t = 1$, for $N = 200$ sites. We see that zero-energy mode for $\mu < 2$ acquires a mass (i.e. it becomes gapped) for $\mu > 2$ and the same time it enters the energy band.

In the non-trivial case 2) it's immediate to see that there are two *unpaired* Majorana fermions, to be specific m_1 and m_{2L}. Moreover, we can define some new Dirac fermions as $\tilde{c}_j = (m_{2j} + i m_{2j+1})/2$, thus $H = 2t \sum_j (\tilde{c}_j^\dagger \tilde{c}_j - 1/2)$. Then, the ground state $|\Omega\rangle$ is annihilated by the $\tilde{c}$ operators, so $\tilde{c}_j |\Omega\rangle = 0$. But it is not unique, in fact there are two orthogonal ground states $|\Omega_0\rangle$ and $|\Omega_1\rangle$ and the difference between them lies in the *parity*.

Parity of the ground state A parity operator measures if the number of occupied states, in this case the number of electrons, is even or odd. It is usually defined as

$$P = \prod_j (-i m_{2j-1} m_{2j}) = \prod_j (1 - 2 c_j^\dagger c_j), \tag{3.72}$$

given the fact that the only eigenvalues of $c_j^\dagger c_j$ are 0 (empty j-th state) or 1 (occupied j-th state), we conclude that

$$P = \begin{cases} 1 & \text{even number of fermions} \\ -1 & \text{odd number of fermions} \end{cases}$$

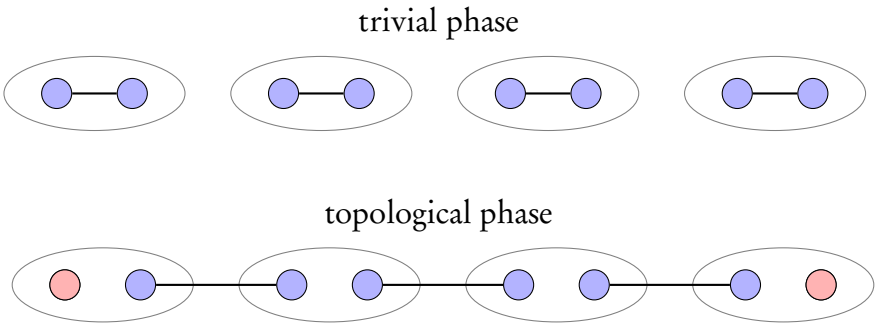

Figure 3.3: A picture of the two different phases. We clearly see that in the topological phase there are unpaired Majorana fermions at the boundary. The situation is similar to the one we had in the SSH model

Returning to the non-trivial case, the ground states contain no particle $\tilde{c}_j$ but on the other hand the Majorana modes m_1 and m_{2N} can still host excitations. They would be *zero-energy excitations*, because they don't appear in the Hamiltonian, but would still affect the parity. To this purpose, we define the *non-local fermion* $\Psi = \frac{1}{2}(m_{2N} + im_1)$. Then, the number operator of this particular fermion is $\Psi^\dagger\Psi = \frac{1}{2}(1 + im_1m_{2N})$. Furthermore, valued on the ground state of the case 2), the parity operator reduces to $P = 1 - 2\Psi^\dagger\Psi = -im_1m_{2L}$, such that two orthogonal ground states $|\Omega_0\rangle$ and $|\Omega_1\rangle$ can be found, which are distinguished by their parity

$$-im_1m_{2N}\,|\Omega_0\rangle = |\Omega_0\rangle \qquad\qquad -im_1m_{2N}\,|\Omega_1\rangle = -\,|\Omega_1\rangle$$

In conclusion, $|\Omega_0\rangle$ has a even parity whereas $|\Omega_1\rangle$ is odd. In particular, $|\Omega_0\rangle$ does not host the excitation of the Ψ particle while $|\Omega_1\rangle$ does. *This degeneracy of the ground state is a sign of the presence of edge modes and of a topological phase.*

3.4.2 Edge states in the Kitaev model

What we want to achieve here is the calculation of the wavefunction of the edge states for any μ and verify that they are indeed exponentially localized at the edges in the topological phase $|\mu| < 2|t|$. For this goal we are going to use the same method used in [39].

We have seen that for $\mu = 0$ we have two unpaired Majorana fermions, m_1 on the left end and m_{2N} on the right end (see Fig. 3.3). For $\mu \neq 0$ the two are no longer unpaired, because the chemical potential introduces the interaction terms m_1m_2 and $m_{2N-1}m_{2N}$, but we can still verify that for $|\mu| < 2|t|$ we can still have Majorana zero modes localized

at the edges.

It is better to distinguish the two types of Majorana fermions that constitute a single Dirac fermions. For this reason we let

$$m_{L,j} = m_{2j-1} \quad \text{and} \quad m_{R,j} = m_{2j}$$

In this way we see that the Hamiltonian (3.71) mixes the "left" Majorana fermions $m_{L,j}$ and the "right" Majorana fermions $m_{R,j}$. For simplicity we also put $\Delta = t = 1$.

In the limit $\mu = 0$, the Hamiltonian reduces to

$$H = i \sum_{j=1}^{N-1} m_{R,j} m_{L,j+1}$$

and is it clear that the left unpaired Majorana fermion is $\Psi_L = m_{L,1}$ while the right one is $\Psi_R = m_{R,N}$. For $\mu \neq 0$ we take as an Ansatz for Ψ_L a superposition of all left Majorana fermions

$$\Psi_L = \sum_{j=1}^{N} \alpha_j m_{L,j} \tag{3.73}$$

and we require that $\Psi_L(\mu \to 0) = m_{L,1}$. The Hamiltonian for $\mu \neq 0$ is just

$$H = -\frac{i\mu}{2} \sum_{j=1}^{N} m_{L,j} m_{R,j} + i \sum_{j=1}^{N-1} m_{R,j} m_{L,j+1} \tag{3.74}$$

If Ψ_L has to be a Majorana zero mode, then it must satisfy the eigenvalue equation (3.19) for $\Lambda = 0$:

$$[H, \Psi_L] = 0.$$

By direct substitution, one obtains that $[H, \Psi_L]$ has two different terms

$$-\frac{i\mu}{2} \sum_{j=1}^{N} \sum_{k=1}^{N} \alpha_k \left[m_{L,j} m_{R,j}, m_{L,k} \right] = \frac{i\mu}{2} \sum_{j} \alpha_j m_{R,j}$$

$$i \sum_{j=1}^{N-1} \sum_{k=1}^{N} \alpha_k \left[m_{R,j} m_{L,j+1}, m_{L,k} \right] = i \sum_{j=1}^{N-1} \alpha_{j+1} m_{R,j}$$

and by putting them together one arrives at

$$\sum_{j=1}^{N-1}\left(\frac{\mu}{2}\alpha_j+\alpha_{j+1}\right)m_{R,j}+\frac{\mu}{2}\alpha_N m_{R,N}=0.$$

Thus, the coefficients that multiplies the different $m_{R,j}$, for $j=1\dots N-1$ must be zero and α_N is completely determined by the equations for α_j, $j\neq N$:

$$\frac{\mu}{2}\alpha_j+\alpha_{j+1}=0 \qquad j=1,\dots,N-1 \tag{3.75}$$

For continuity with $\Psi_L(\mu=0)=m_{L,1}$, one must have $\alpha_1=1$, up to a overall normalization of the wavefunction. Thus, the recursive equation (3.75) can be easily solved:

$$\alpha_j=\left(-\frac{\mu}{2}\right)^{j-1} \tag{3.76}$$

In this way, the complete wavefunction for Ψ_L turns out to be

$$\Psi_L=\sum_{j=1}^{N}\left(-\frac{\mu}{2}\right)^{j-1}m_{L,j} \tag{3.77}$$

which is localized at the left edge when $\mu<2$.

The same reasoning can be applied to the right Majorana fermion Ψ_R. In a similar fashion, we take as Ansatz for Ψ_R

$$\Psi_R=\sum_{j=1}^{N}\beta_j m_{R,j}$$

and then by substituting Ψ_R into $[H,\Psi_R]=0$ one finds

$$[H,\Psi_R]=-\frac{i\mu}{2}\beta_1 m_{L,1}-i\sum_{j=2}^{N}\left(\frac{\mu}{2}\beta_j+\beta_{j-1}\right)m_{L,j}, \tag{3.78}$$

which means that the coefficients β_j, for $j=2,\dots,N$ must satisfy

$$\frac{\mu}{2}\beta_j+\beta_{j-1}=0 \qquad j=2,\dots,N \tag{3.79}$$

with the condition that $\beta_N=1$. The number β_1 is completely determined by the

previous recursive equation. This time the coefficients turn out to be $\beta_j = (-\mu/2)^{N-j}$, which implies

$$\Psi_R = \sum_{j=1}^{N} \left(-\frac{\mu}{2}\right)^{N-j} m_{R,j} \tag{3.80}$$

Hence, while Ψ_L is localized on the left edge, Ψ_R is localized on the opposite side for $|\mu| < 2$ but both do not commute exactly with the Hamiltonian for a finite number N of sites. They become effective Majorana zero modes in the limit $N \to \infty$.

$$[H, \Psi_L] = i\frac{\mu}{2}\left(-\frac{\mu}{2}\right)^{N-1} m_{R,N}, \qquad [H, \Psi_R] = -i\frac{\mu}{2}\left(-\frac{\mu}{2}\right)^{N-1} m_{L,1} \tag{3.81}$$

Both Ψ_L and Ψ_R can be combined in a single non-local Dirac fermion $\Psi = \frac{1}{2}(\Psi_L + i\Psi_R)$, which does not commute with the Hamiltonian

$$[H, \Psi] = \frac{\mu}{2}\left(-\frac{\mu}{2}\right)^{N-1}\left(\frac{m_{L,1} + i m_{R,N}}{2}\right) \tag{3.82}$$

but the coefficient is exponentially small for $|\mu| < 2$. This means that in the thermodynamic limit the fermionic mode Ψ becomes a zero mode and the Majorana modes Ψ_L and Ψ_R become unpaired.

3.4.3 Winding number and topological phases

In these paragraph, for *winding number* we don't refer to the topological invariant defined by the Berry phase, but to the number of windings around the origin of a function $\mathbb{T} \to \mathbb{C}$, the same kind used in the theory of Toeplitz matrices. The Hamiltonian of the Kitaev model (3.61), with open boundaries, can be put in the form (3.49) by defining the matrices

$$A_{ij} = \begin{cases} 1 & i - j = \pm 1 \\ 0 & \text{otherwise} \end{cases} \qquad B_{ij} = \begin{cases} 1 & i - j = 1 \\ -1 & i - j = -1 \\ 0 & \text{otherwise} \end{cases} \tag{3.83}$$

By following (3.53) and (3.52), the energy levels can be found by either studying the singular values of $\bar{A} + \bar{B}$ or $\bar{A} - \bar{B}$. In this case we choose $\bar{A} - \bar{B}$, without loss of generality. With open boundary conditions, this matrix is no longer a circulant matrix but only a

Toeplitz matrix; in fact

$$\bar{A} - \bar{B} \equiv T_N(g) = \begin{pmatrix} -\mu & -t-\Delta & 0 & \dots & 0 \\ -t+\Delta & -\mu & -t-\Delta & \dots & 0 \\ 0 & -t+\Delta & -\mu & & \vdots \\ \vdots & \vdots & & \ddots & -t-\Delta \\ 0 & 0 & \dots & -t+\Delta & -\mu \end{pmatrix} \tag{3.84}$$

where the symbol $g : \mathbb{T} \to \mathbb{C}$ of $T_N(g)$ is

$$g(e^{ik}) = -2t\cos k - \mu - 2i\Delta \sin k \tag{3.85}$$

We now recall the *splitting phenomenon* discussed in Sec. 2.4.2. It states that if $T(g)$ is a Fredholm operator of index k, then there are $|k|$ singular values, i.e. energy levels, that go exponentially to zero. Furthermore, for a large class of symbols (see Th. 6 and Sec. 2.1.5) we have that $\operatorname{Ind} T(g) = -\operatorname{wind}(g, 0)$. Thus, one can think to use the winding number $\operatorname{wind}(g, 0)$ as a tool for predicting if there are any phases with zero modes.

This kind of connection between the *winding number* of a symbol and the number of *zero modes* seems to point towards the *bulk-edge correspondence*. The symbol g of the matrix $T_N(g)$ contains all the information about the local coupling that the system is subject to. Hence, in a certain sense, it contains all information about the bulk. Moreover, the winding number of g resembles another kind of winding number; it seem to be connected to the winding number ν of the vector $\mathbf{d}(k)$ we used, for example, in Sec. 1.6 and, by the bulk-edge correspondence, $\nu \neq 0$ is a signal for a topological phase.

The winding number $\operatorname{wind}(g, 0)$ is a valid topological indicator, at least for the symmetry class BDI, which is the one the Kitaev model belongs to. In fact, based on the 10-fold classification in Tab. 1.1, the phases of a class BDI system in one dimension are classified through an integer $\mathbb{Z}$, which is exactly what the winding number $\operatorname{wind}(g, 0)$ describes. It is also necessary to point out that ν and $\operatorname{wind}(g, 0)$ have two quite different origins: the former comes from the Berry phase when we go across the whole BZ, while $\operatorname{wind}(g, 0)$ comes from the number of windings around the origin of the complex plane of the image of the function g. Thus, even if $\operatorname{wind}(g, 0)$ and ν are not exactly the same, they at least give the same amount of information.

Returning to the Kitaev model, by simply graphing the image of g in (3.85), as we did in Fig. 3.4, is possible to distinguish three different cases:

- $|\mu| < 2|t|$, the curve $g(\mathbb{T})$ encircles the origin only one time, thus $\operatorname{wind}(g, 0) = 1$.

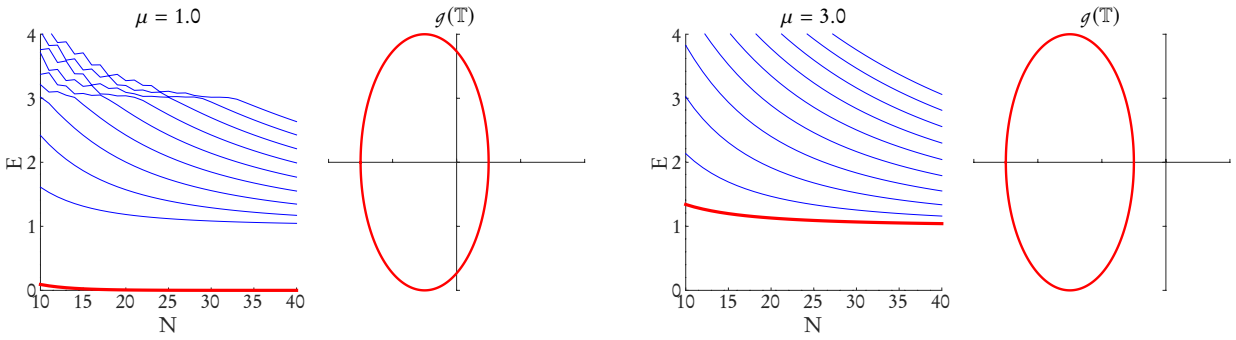

Figure 3.4: These pairs of pictures show the plot of the first ten singular values of $T_N(g)$ for different value of the chemical potential, at fixed $t = 1$ and $\Delta = 2$, as a function of the total number of sites N, and the respective curve $g(\mathbb{T})$. The lowest singular values is drawn in red. The topological phase is on the left, where $\mu = 1$. The curve $g(\mathbb{T})$ wraps around the origin only one time and we have a practically vanishing singular value. On the other hand, on the right side, where $\mu = 3$, $g(\mathbb{T})$ does not encircle th origin and all the singular values are separated from the zero.

- $|\mu| > 2|t|$, the winding number is exactly zero, $\mathrm{wind}(g, 0) = 0$.
- $|\mu| = 2|t|$, the curve $g(\mathbb{T})$ contains the origin.

The first two cases correspond exactly to the topological phase and to the trivial phase, respectively. The last case correspond to the critical phase, where the gap closes. In this particular instance, we have that $0 \in g(\mathbb{T}) = \mathrm{sp}_{\mathrm{ess}}\, T(g)$, which means that $T(g)$ is not Fredholm. From Th. 22, it follows that all the energy levels are distributed around the zero, with no gap, which is exactly what happens in a critical (gapless) phase.

3.4.4 Relationship with the XY Model

The spin-$\frac{1}{2}$ XY model is a generalization of the quantum Ising model with anisotropy in the $x - y$ plane and magnetic field along the z-direction. Its Hamiltonian is

$$H_{\mathrm{XY}} = \frac{J}{2} \sum_j \left((1+\gamma)\sigma_j^x \sigma_{j+1}^x + (1-\gamma)\sigma_j^y \sigma_{j+1}^y \right) - \frac{h}{2} \sum_j \sigma_j^z \tag{3.86}$$

where j runs of the sites of the chain and σ_j^i are just the Pauli matrices σ^i, $i = x, y, z$, acting on the internal space of the j-th sites. Also, J is the coupling between the nearest spins, γ the anisotropy parameter and h the external magnetic field.

A spin chain can be mapped into a fermionic chain, and vice versa, through a *Jordan-Wigner transformation*, which will be readily introduced. In the case of the XY model, this will turn out to be exactly the Kitaev model.

Jordan-Wigner transformation Before proceeding, we recall the properties of the Pauli matrices:

$$(\sigma^i)^\dagger = \sigma^i \qquad \left\{\sigma^i, \sigma^j\right\} = 2\delta^{ij} \qquad \left[\sigma^i, \sigma^j\right] = 2i\epsilon^{ijk}\sigma^k \tag{3.87}$$

where ϵ^{ijk} is the Levi-Civita symbol. Going further, the spin-$\frac{1}{2}$ is a two-state system, so one can imagine to have a pair of Fermi creation and annihilation operators and in fact it is possible to build such a pair by defining

$$\sigma^+ = \sigma^x + i\sigma^y, \qquad \sigma^- = \sigma^x - i\sigma^y \tag{3.88}$$

and this pair satisfies the relation $\{\sigma^+, \sigma^-\} = 2$. It is important to remember that the Pauli matrices of different sites commute with each other. It is natural to suppose that the Fermi operators $c_j^\dagger$ and c_j are going to be related to σ_j^+ and σ_j^-, but such a direct substitution is not doable, because it will generate operators which are bosonic on different sites but fermionic on the same site. To solve this, we will see that is necessary to introduce a sort of "tail" into the definition of c_j and $c_j^\dagger$, which will make them into non-local fermions.

First of all, we define the Majorana operators m_{2j} and m_{2j+1} from which we are going to build the Fermi operators:

$$m_{2l+1} = \left(\prod_{j=0}^{l-1} \sigma_j^z\right)\sigma_l^x, \qquad m_{2l} = \left(\prod_{j=0}^{l-1} \sigma_j^z\right)\sigma_l^y \tag{3.89}$$

and they satisfy

$$\left\{m_l, m_p\right\} = \delta_{lp}, \qquad m_l^\dagger = m_l.$$

For completeness, we also write the inverse relations:

$$\begin{aligned} \sigma_l^z &= i m_{2l} m_{2l+1} \\ \sigma_l^x &= \left(\prod_{j=0}^{l-1} i m_{2j} m_{2j+1}\right) m_{2l+1} \\ \sigma_l^y &= \left(\prod_{j=0}^{l-1} i m_{2j} m_{2j+1}\right) m_{2l} \end{aligned} \tag{3.90}$$

Now, the Fermi operators can be introduced

$$m_{2l+1} + i m_{2l} \equiv c_l^\dagger, \qquad m_{2l+1} - i m_{2l} \equiv c_l$$

and one finds that $\sigma_l^z = im_{2l}m_{2l+1} = 2c_l^\dagger c_l$, which let us express σ_l^+ and σ_l^- in terms of $c_l^\dagger$ and c_l:

$$\begin{aligned}\sigma_l^+ &= \sigma_l^x + i\sigma_l^y = \left(\prod_{j=0}^{l-1}(2c_j^\dagger c_j - 1)\right) c_l^\dagger \\ \sigma_l^- &= \sigma_l^x - i\sigma_l^y = \left(\prod_{j=0}^{l-1}(2c_j^\dagger c_j - 1)\right) c_l\end{aligned} \tag{3.91}$$

Then, one is left with the task of expressing H_{XY} in terms of σ^+ and σ^- and translating them in the language of the Fermi operators (3.91). The kinetic term of H_{XY} becomes

$$(1-\gamma)\sigma_j^x\sigma_{j+1}^x + (1+\gamma)\sigma_j^y\sigma_{j+1}^y = \frac{1}{2}\left(\sigma_j^+\sigma_{j+1}^- + \sigma_j^-\sigma_{j+1}^+\right) + \frac{\gamma}{2}\left(\sigma_j^+\sigma_{j+1}^+ + \sigma_j^-\sigma_{j+1}^-\right)$$

while the interaction along the z-axis remains unmodified. The latter will become the chemical potential term, because $\sigma^z = 2c_l^\dagger c_l - 1$. Then, thanks to the fact that different operators σ^+ and σ^- on different sites commute, one finds that

$$\begin{aligned}\sigma_l^+\sigma_{l+1}^+ &= -c_l^\dagger c_{l+1}^\dagger & \sigma_l^-\sigma_{l+1}^- &= c_l c_{l+1} \\ \sigma_l^+\sigma_{l+1}^- &= -c_l^\dagger c_{l+1} & \sigma_l^-\sigma_{l+1}^+ &= c_l^- c_{l+1}^\dagger\end{aligned}$$

Hence,

$$H = -\frac{J}{2}\sum_l\left(c_l^\dagger c_l + c_{l+1}^\dagger c_l\right) - h\sum_l\left(c_l^\dagger c_l - \frac{1}{2}\right) + \frac{J\gamma}{2}\sum_l\left(c_l c_{l+1} - c_l^\dagger c_l^\dagger\right)$$

which is exactly the Kitaev Hamiltonian, if we identify $J = t$, $\gamma = \Delta$ and $h = \mu$.

3.5 The Long-Range Kitaev Model

Now we are going to introduce the Kitaev model with long-range superconductive pairing (LRK), which is a particular extension of the Kitaev model that have been already analyzed in detail by Vodola et al. in [40–42]. For this model we are going to consider the following Hamiltonian

$$H = \sum_{j=1}^{L}\left[-t\left(c_j^\dagger c_{j+1} + c_{j+1}^\dagger c_j\right) - \mu\left(c_j^\dagger c_j - \frac{1}{2}\right) + \frac{\Delta}{2}\sum_{l=1}^{L-1}\frac{1}{d_l^\alpha}\left(c_j c_{j+l} + c_{j+l}^\dagger c_j^\dagger\right)\right] \tag{3.92}$$

where L is the number of sites, t is the hopping parameter, μ the chemical potential, Δ the superconductive gap and d_l is distance function defined as

$$d_l = \begin{cases} \begin{cases} l & l < L/2 \\ L-l & l > L/2 \end{cases} & \text{for closed chain} \\ \\ l & \text{for open chain and discard every } c_{j>L} \end{cases} \tag{3.93}$$

The long-range interaction decays as a power-law $l^{-\alpha}$, governed by the exponent α. Our interest is towards the new physics that arises with the introduction of such an interaction, especially the correlation functions, because the tuning of α greatly modifies their behaviour.

3.5.1 Diagonalization with Lieb-Schultz-Mattis

To explicitly solve the Hamiltonian (3.92) it is useful to express it in the form (3.49), hence we have to build the matrices A and B in such a way that they are circulant. The first one is immediate, as it is just

$$A = \begin{pmatrix} 0 & 1 & \dots & 0 & 1 \\ 1 & 0 & \dots & \dots & 0 \\ \vdots & \vdots & \ddots & & \vdots \\ 0 & \vdots & & 0 & 1 \\ 1 & 0 & \dots & 1 & 0 \end{pmatrix} \quad \Longrightarrow \quad a(j) = \begin{cases} -\mu & j = 0 \\ -t & j = \pm 1 \\ 0 & \text{otherwise} \end{cases} \tag{3.94}$$

The second one is less trivial. First we have to make a little adjustment to the function $1/d_l^\alpha$ in order to obtain an explicitly antisymmetric matrix. For $l \geq 0$ let $1/d_l^\alpha$ be

$$\frac{1}{d_l^\alpha} = \begin{cases} 0 & l = 0 \\ l^{-\alpha} & j < L/2 \\ -|L-l|^{-\alpha} & j > L/2 \end{cases} \quad \Longrightarrow \quad b(j) = \frac{1}{d_j^\alpha} \quad \text{and} \quad b(-j) = -b(j)$$

in this way the matrix B is antisymmetric and circulant. In fact, if for example we set

$L = 5$ and $\alpha = 1$ we have

$$B = \begin{pmatrix} 0 & 1 & \frac{1}{2} & -\frac{1}{2} & -1 \\ -1 & 0 & 1 & \frac{1}{2} & -\frac{1}{2} \\ -\frac{1}{2} & -1 & 0 & 1 & \frac{1}{2} \\ \frac{1}{2} & -\frac{1}{2} & -1 & 0 & 1 \\ 1 & \frac{1}{2} & -\frac{1}{2} & -1 & 0 \end{pmatrix}$$

which confirms what we have said.

The eigenvalues can be calculated with formula

$$\Lambda_k = \sum_{j=-(L-1)/2}^{(L-1)/2} \big(a(j) - \Delta b(j)\big) e^{ikj} \tag{3.95}$$

which in this case is valid for both L even or odd, as $a(L/2)$ vanishes for $L > 2$ and k is the wave-number $2\pi l/L$, with $l = 0, \ldots, L-1$. The first part gives

$$\sum_j a(j) e^{ikj} = \sum_{j=-1,0,1} a(j) e^{ikj} = -t(e^{ik} + e^{-ik}) - \mu = -2t \cos k - \mu$$

while the second term is a bit more laborious

$$\begin{aligned} \sum_{j=-(L-1)/2}^{(L-1)/2} b(j) e^{ikj} &= \left(\sum_{j=-(L-1)/2}^{-1} + \sum_{j=1}^{(L-1)/2} \right) b(j) e^{ikj} \\ &= \sum_{j=-(L-1)/2}^{-1} \left(-\frac{e^{ikj}}{|L-j|^\alpha} \right) + \sum_{j=1}^{(L-1)/2} \frac{e^{ikj}}{j^\alpha} \\ &= -\sum_{j=1}^{(L-1)/2} \frac{e^{-ikj}}{j^\alpha} + \sum_{j=1}^{(L-1)/2} \frac{e^{ikj}}{j^\alpha} \\ &= 2i \sum_{j=1}^{-(L-1)/2} \frac{\sin kj}{j^\alpha} \end{aligned}$$

thus,

$$\Lambda_k = -2t \cos k - \mu - 2i\Delta \sum_{j=1}^{(L-1)/2} \frac{\sin kj}{j^\alpha} \tag{3.96}$$

In the thermodynamic limit we obtain the following dispersion relationship $|\Lambda_k|$:

$$\Lambda_k = -(2t\cos k + \mu) - i\big(\Delta f_\alpha(k)\big) \tag{3.97}$$

$$|\Lambda_k| = \sqrt{(2t\cos k + \mu)^2 + (\Delta f_\alpha(k))^2} \tag{3.98}$$

where we have defined the function

$$\begin{aligned} f_\alpha(k) &= 2\sum_{j=1}^{\infty} j^{-\alpha}\sin kj = \frac{1}{i}\sum_{j=1}^{\infty} j^{-\alpha}e^{ikj} - \frac{1}{i}\sum_{j=1}^{\infty} j^{-\alpha}e^{ikj} \\ &= \frac{1}{i}\Big(\mathrm{Li}_\alpha(e^{ik}) - \mathrm{Li}_\alpha(e^{-ik})\Big) \end{aligned} \tag{3.99}$$

and $\mathrm{Li}_s(z) = \sum_{j=1}^{\infty} j^{-s}z^j$ is the *polylogarithm* function. Some of its properties will be listed in App. A.

The difference with the (short-range) Kitaev model is in the second term of the dispersion relation, as the function $2\Delta\sin k$ has been substituted with the much intricate $\Delta f_\alpha(k) = -i\Delta(\mathrm{Li}_\alpha(e^{ik}) - \mathrm{Li}_\alpha(e^{-ik}))$. We can recover the short-range model in the limit $\alpha \to \infty$, where only the first term in the sum (3.99) survives.

3.5.2 Correlation functions

Now we pass to the evaluation of the correlation functions. For a general Hamiltonian (3.49), we have already found the expressions (3.59) and (3.60). From (3.98), we see that the symbol that generates the Toeplitz correlation matrix T_L is

$$\frac{\Lambda_\alpha(k)}{|\Lambda_\alpha(k)|} = -\frac{2t\cos k + \mu + i\Delta f_\alpha(k)}{\sqrt{(2t\cos k + \mu)^2 + (\Delta f_\alpha(k))^2}} \tag{3.100}$$

where we have slightly modified the notation to make it explicit the dependence on the exponent α of the power-law decay and the fact the k is now a continuous variable. By substituting the previous equation into (3.59) and (3.60), one finds that the one-body correlation functions $g_1(R)$ and $g_1^a(R)$ of the LRK model are

$$g_1(R) = \frac{1}{4\pi}\int_0^{2\pi} \mathrm{d}k\, \frac{2t\cos k + \mu + i\Delta f_\alpha(k)}{\sqrt{(2t\cos k + \mu)^2 + (\Delta f_\alpha(k))^2}}\cos(kR) \tag{3.101}$$

$$g_1^a(R) = \frac{-i}{4\pi}\int_0^{2\pi} \mathrm{d}k\, \frac{2t\cos k + \mu + i\Delta f_\alpha(k)}{\sqrt{(2t\cos k + \mu)^2 + (\Delta f_\alpha(k))^2}}\sin(kR) \tag{3.102}$$

Subsequently, these integral can be simplified by a parity argument of the integrand around the $k = \pi$ axis. In fact, we put $A(k) = 2t\cos k + \mu$ and $B(k) = \Delta f_\alpha(k)$. The product $B(k)\cos(kR)$ is odd around the $k = \pi$ in the interval $[0, 2\pi]$, because it is a sum of term like $\sin(kj)\cos(Rk)$, hence it vanishes

$$g_1(R) = \frac{1}{2\pi}\int_0^{2\pi} \mathrm{d}k \frac{2t\cos k + \mu}{2|\Lambda_\alpha(k)|}\cos kR. \tag{3.103}$$

In a similar manner, the product $A(k)\sin kR$ is odd while $B(k)\sin Rk$ is even and

$$g_1^a(R) = \frac{1}{2\pi}\int_0^{2\pi} \mathrm{d}k \frac{\Delta f_a(k)}{2|\Lambda_\alpha(k)|}\sin kR \tag{3.104}$$

Furthermore, it is convenient to use complex exponentials instead of trigonometric functions. On that note, thanks to the same parity arguments made before, we can substitute $\cos kR$ and $\sin kR$ in (3.103) and (3.104), respectively, with e^{ikR}:

$$g_1(R) = \frac{1}{2\pi}\int_0^{2\pi} \mathrm{d}k \frac{2t\cos k + \mu}{2|\Lambda_\alpha(k)|}e^{ikR}. \tag{3.105}$$

$$g_1^a(R) = -\frac{i}{2\pi}\int_0^{2\pi} \mathrm{d}k \frac{\Delta f_a(k)}{2|\Lambda_\alpha(k)|}e^{ikR} \tag{3.106}$$

These results reflects the correlation functions found in [40] by Vodola et al., up to a (irrelevant) numerical factor. In Ref. [40–42], extensive analytical study of these correlation function has been conducted and we are going to report the main results.

3.5.3 Asymptotic behaviour of the correlation functions

The long-range extension of the Kitaev model is characterized by the parameter α, which is the exponent in the power-law interaction $l^{-\alpha}$, and we expect that for large values of $\alpha \gg 1$ to restore the short-range behaviour. Meanwhile, interesting phenomenon happens for low $\alpha \sim 1$, that is the correlation functions acquire an hybrid behaviour, that is part algebraic and part exponential, in the gapped phases. This is in contrast with what we expect in short-range models, where the correlators decays exponentially in the gapped phase while it is algebraic in the gapless (critical) phases. In particular, the $k \to 0$ part is responsible for the power-law behaviour at long distance while the $k \to \infty$ part is responsible for the exponential behaviour at short distance. This overall behaviour can be analyzed semi-analytically.

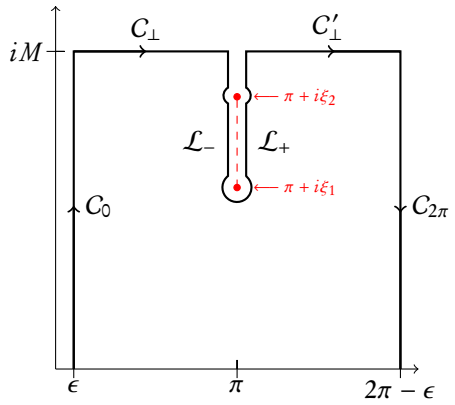

Figure 3.5: Integration contour for evaluating the integral in (3.107), as $M \to \infty$. The red dashed line indicated the branch cut for $|\Lambda_\alpha(k)|$

To achieve this, following [41, 42], we consider the integration contour in Fig. 3.5, for $M \to \infty$, for the correlation function $g_1(R)$ in (3.105):

$$g_1(R) = \frac{1}{2\pi} \lim_{M\to\infty} \left(\int_{C_0} + \int_{\mathcal{L}_-} + \int_{\mathcal{L}_+} + \int_{C_{2\pi}} \right) \mathrm{d}z e^{izR} \mathcal{G}_\alpha(z) \tag{3.107}$$

where

$$\mathcal{G}_a(z) = \frac{2t\cos z + \mu}{2|\Lambda_\alpha(k)|} \quad \text{and} \quad z = k + iy.$$

We ignored the contribution of the segments $C_\perp$ and $C'_\perp$, as they vanish for $M \to \infty$. The contours $\mathcal{L}_\pm$ have been chosen since the denominator in $\mathcal{G}_\alpha(z)$, once extended to the complex plane, on the line $\pi + iy$ changes its sign, since it vanishes for two values $\xi_1 < \xi_2$ which are the solutions of

$$(\mu - 2t\cosh\xi_{1,2})^2 + \Delta^2 f_\alpha(\pi + i\xi_{1,2})^2 = 0$$

The presence of these roots leads to a branch cut for $|\Lambda_\alpha(k)|$ on the line $\pi + iy$ in the complex plane. These cuts have been chosen in the following way

$$|\Lambda_\alpha(k)| = \begin{cases} \sqrt{(2t\cosh y - \mu)^2 + \Delta^2 f_\alpha(\pi + iy)^2} & \text{if} \quad z = \pi + iy, \quad y < \xi_1 \ \text{ or } \ y > \xi_2 \\ i\sqrt{-(2t\cosh y - \mu)^2 - \Delta^2 f_\alpha(\pi + iy)^2} & \text{if} \quad z = \pi^+ + iy, \quad \xi_1 < y < \xi_2 \\ -i\sqrt{-(2t\cosh y - \mu)^2 - \Delta^2 f_\alpha(\pi + iy)^2} & \text{if} \quad z = \pi^- + iy, \quad \xi_1 < y < \xi_2 \end{cases} \tag{3.108}$$

Exponential part First of all, we set $2t = \Delta = 1$ for convenience. Then, on $\mathcal{L}_-$, where $z = \pi^- + iy$, we have

$$\begin{aligned} I_{\mathcal{L}_-} = &- \frac{ie^{i\pi R}}{2\pi} \int_{\infty}^{\xi_2} \frac{e^{-yR}(\mu - \cosh y)}{\sqrt{(\mu - \cosh y)^2 + f_\alpha^2(\pi + iy)}} \mathrm{d}y \\ &- \frac{ie^{i\pi R}}{2\pi} \int_{\xi_2}^{\xi_1} \frac{e^{-yR}(\mu - \cosh y)}{-i\sqrt{-(\mu - \cosh y)^2 + f_\alpha^2(\pi + iy)}} \mathrm{d}y \end{aligned} \tag{3.109}$$

by choosing the right expression for $\left|\Lambda_\alpha(k)\right|$, based on (3.108). Likewise, on $\mathcal{L}_+$ we have

$$I_{\mathcal{L}_+} = \frac{ie^{i\pi R}}{2\pi} \int_{\xi_2}^{\infty} e^{-yR} \mathcal{G}_\alpha(\pi^+ + iy)\mathrm{d}y + \frac{ie^{i\pi R}}{2\pi} \int_{\xi_1}^{\xi_2} e^{-yR} \mathcal{G}_\alpha(\pi^+ + iy)\mathrm{d}y \tag{3.110}$$

and by summing $I_{\mathcal{L}_-}$ and $I_{\mathcal{L}_+}$ one obtains

$$\begin{aligned} I_{\mathcal{L}_-} + I_{\mathcal{L}_+} &= \frac{ie^{i\pi R}}{\pi} \int_{\xi_1}^{\xi_2} \mathrm{d}y e^{-yR} {}_-\alpha(\pi^+ + iy) \\ &= \frac{ie^{i\pi R}}{\pi} e^{-\xi_1 R} \int_0^{\xi_2} \mathrm{d}y e^{-yR} \mathcal{G}_\alpha(\pi + i(y + \xi_1)). \end{aligned} \tag{3.111}$$

The exponential decay is the result of $\left|\Lambda_a(\pi^\pm + iy)\right|$ when $z = \pi^\pm + iy$ from (3.108). The inverse correlation length is given by ξ_1, which is one of the zero of $|\Lambda_\alpha|$ on the line $\pi + iy$, once it is extended on the complex plane.

By recognizing that the previous integral is a Laplace-type integral, in the sense that it is the Laplace transform of some function, one considers [42]

$$\mathcal{G}_\alpha(\pi^+ + i(y + \xi_1)) \sim \frac{A_\alpha(\mu)}{i\sqrt{y}} \quad \text{if} \quad y \to 0 \tag{3.112}$$

with

$$A_\alpha(\mu) = \frac{\mu - \cosh \xi_1}{2\sqrt{2}\left(\mathrm{Li}_{\alpha-1}(-e^{\xi_1}) + \mathrm{Li}_{\alpha-1}(-e^{-\xi_1})\right)^{1/2}\left(\mathrm{Li}_\alpha(-e^{\xi_1}) - \mathrm{Li}_\alpha(-e^{-\xi_1})\right)^{1/2}} \tag{3.113}$$

because the leading term of $I_{\mathcal{L}_-} + I_{\mathcal{L}_+}$ can be found by first replacing ξ_2 with ∞, as the integrand is exponentially decaying, and then by integrating the $y \to \infty$ part of

$-_\alpha(\pi^+ + i(y+\xi_1))$. Thus, one has

$$I_{\mathcal{L}_-} + I_{\mathcal{L}_+} = A_\alpha(\mu)\frac{e^{i\pi R}e^{-\xi_1 R}}{\sqrt{\pi R}}, \tag{3.114}$$

which shows the exponential decay

Power-law part For the power-law part we consider the path C_0 and $C_{2\pi}$ on which $z = \epsilon + iy$ and $z = 2\pi - \epsilon + iy$ respectively. One obtains

$$\begin{aligned} I_{C_0} &= \frac{1}{2\pi}\int_{C_0} e^{izR}\mathcal{G}_\alpha(z)\mathrm{d}z = \frac{i}{2\pi}\int_0^\infty e^{-yR}\mathcal{G}_\alpha(\epsilon+iy)\mathrm{d}y \\ I_{C_{2\pi}} &= \frac{1}{2\pi}\int_{C_{2\pi}} e^{izR}\mathcal{G}_\alpha(z)\mathrm{d}z = -\frac{i}{2\pi}\int_0^\infty e^{-yR}\mathcal{G}_\alpha(2\pi-\epsilon+iy)\mathrm{d}y. \end{aligned} \tag{3.115}$$

As $\mathcal{G}_\alpha(2\pi - \epsilon + iy) = \overline{\mathcal{G}}_\alpha(\epsilon + iy)$, this leads to

$$I_{C_0} + I_{C_{2\pi}} = \frac{1}{\pi}\int_0^\infty \mathrm{d}y e^{-yR}\,\mathrm{Im}\,\mathcal{G}_\alpha(\epsilon+iy) = \frac{1}{\pi}\int_0^\infty \mathrm{d}y e^{-yR}\,\mathrm{Im}\,\mathcal{G}_\alpha(iy) \tag{3.116}$$

where we have let $\epsilon \to 0$.

For the same reason as before, given the fact the $I_{C_0} + I_{C_{2\pi}}$ is a Laplace-type integral, we compute the $y \to 0$ part of $\mathcal{G}_\alpha(iy)$ and then we integrate. We consider the cases $\alpha \neq 1, 2, \ldots$, where the series expansion (A.2) for the polylogarithm can be used, for $z = e^{\pm y}$. Hence, one finds

$$\mathrm{Li}_\alpha(e^y) - \mathrm{Li}_\alpha(e^y) = -\Gamma(1-\alpha)(e^{i\pi\alpha}+1)y^{\alpha-1} + 2\sum_{j=0}^{\infty}\frac{\zeta(\alpha-(2j+1))}{(2j+1)!}y^{2j+1}$$

which means that the main contribution to the imaginary part is

$$\mathcal{G}_\alpha(iy) \sim \frac{\mu+1}{2\sqrt{(\mu+1)^2 - \Gamma^2(1-\alpha)(e^{i\pi\alpha}+1)^2 y^{2\alpha-2} + 4\Gamma(1-\alpha)(e^{i\pi\alpha}+1)\zeta(\alpha-1)y^\alpha}} \tag{3.117}$$

Now to continue this analysis we must distinguish three cases: $\alpha > 2$, $1 < \alpha < 2$ and $\alpha < 1$

Case $\alpha > 2$ If we perform a Taylor expansion and then take the imaginary part, we obtain

$$\operatorname{Im} \mathcal{G}_\alpha(iy) \sim -\frac{\Gamma(1-\alpha)\sin(\pi\alpha)\zeta(\alpha-1)y^\alpha}{\operatorname{sgn}(\mu+1)(\mu+1)^2}$$

because the leading term is y^α. This expression have to be integrated from 0 to ∞ with respect to y. The only dependence in $\operatorname{Im} \mathcal{G}_\alpha(iy)$ is the term y^α, thus the integral of $e^{-yR}y^\alpha$ gives

$$\int_0^\infty \mathrm{d}y e^{-yR}y^\alpha = \frac{\Gamma(\alpha+1)}{R^{\alpha+1}}$$

Furthermore, by using the Euler's reflection formula $\Gamma(a)\Gamma(1-\alpha) = \pi/\sin(\pi\alpha)$ we finally arrive at

$$I_{C_0} + I_{C_{2\pi}} \sim -\frac{\alpha\zeta(\alpha-1)}{\operatorname{sgn}(\mu+1)(1+\mu)^2}\frac{1}{R^{\alpha+1}} \tag{3.118}$$

Case $1 < \alpha < 2$ In this case, the leading term of the Taylor expansion of (3.117) is $y^{2\alpha-2}$, thus if we take the imaginary part we obtain

$$\operatorname{Im} \mathcal{G}_\alpha(iy) \sim \frac{\Gamma(1-\alpha)^2\sin(\pi\alpha)\cos^2(\pi\alpha/2)y^{2\alpha-2}}{\operatorname{sgn}(\mu+1)(\mu+1)^2}$$

Thus, by

$$\int_0^\infty \mathrm{d}y e^{-yR}y^{2\alpha-2} = \frac{\Gamma(2\alpha-1)}{R^{2\alpha-1}}$$

we finally end up with

$$I_{C_0} + I_{C_{2\pi}} \sim \frac{\Gamma(1-\alpha)^2\sin(\pi\alpha)\cos^2(\pi\alpha/2)\Gamma(2\alpha-1)}{\pi\operatorname{sgn}(\mu+1)(\mu+1)^2}\frac{1}{R^{2\alpha-1}} \tag{3.119}$$

Case $\alpha < 1$ By multiplying both the denominator and the numerator of $\mathcal{G}_\alpha(iy)$ in (3.117) by $y^{1-\alpha}$ and then by Taylor expansion we have

$$\operatorname{Im} \mathcal{G}_\alpha(iy) \sim \frac{\mu+1}{4\Gamma(1-\alpha)}y^{1-\alpha}$$

which, by following the same type of arguments made before, leads to

$$I_{C_0} + I_{C_{2\pi}} = \frac{(\mu+1)(1-\alpha)}{4\pi}\frac{1}{R^{2-\alpha}} \tag{3.120}$$

It is finally possible to gather all the information and obtain the asymptotic behaviour

of $g_1(R)$ for large R:

$$g_1(R) \sim \begin{cases} \dfrac{1}{R^{\alpha+1}} & \text{if } \alpha > 2 \\ \dfrac{1}{R^{2\alpha-1}} & \text{if } 1 < \alpha < 2 \\ \dfrac{1}{R^{2-\alpha}} & \text{if } \alpha < 1 \end{cases} \quad \text{for} \quad R \gg 1 \tag{3.121}$$

Anomalous correlator Until now we only focused on the one-body correlation function $g_1(R)$ but we can execute the same kind of analysis for the anomalous one-body correlator $g_1^a(R)$

$$g_1^a(R) = \frac{1}{2\pi}\int_0^{2\pi} e^{ikR}\mathcal{F}_\alpha(k), \qquad \mathcal{F}_\alpha = i\frac{\Delta f_\alpha(k)}{2|\Lambda_\alpha(k)|} \tag{3.122}$$

By reusing the integration contour in Fig 3.5 we have

$$g_1^a(R) = \frac{e^{i\pi R}e^{-\xi_1 R}}{\pi}\int_0^\infty \mathrm{d}y e^{-yR}\mathcal{F}_\alpha(\pi^+ + i(y+\xi_1)) - \frac{1}{\pi}\int_0^\infty \mathrm{d}y e^{-yR}\,\mathrm{Im}\,\mathcal{F}_\alpha(iy) \tag{3.123}$$

which shows both the exponential and power-law parts. The number ξ_1 is still the smallest solution of the equation

$$\left(\mu - \cosh\xi_{1,2}\right)^2 - \left(\mathrm{Li}_\alpha(-e^{-\xi_{1,2}}) - \mathrm{Li}_\alpha(-e^{\xi_{1,2}})^2\right) = 0 \tag{3.124}$$

Continuing on the same path, we have now two different cases this time: $\alpha < 1$ and $\alpha > 1$

Case $\alpha > 1$ Here

$$\mathrm{Im}\,\mathcal{F}_\alpha(iy) \sim \frac{\Gamma(1-\alpha)\sin\pi\alpha}{2|\mu+1|} \tag{3.125}$$

which leads to

$$g_1^a(R) = \frac{B_\alpha(\mu)e^{i\pi R}e^{-\xi_1 R}}{\sqrt{\pi R}} - \frac{1}{2|\mu+1|}\frac{1}{R^\alpha} \tag{3.126}$$

where

$$B_\alpha(\mu) = \frac{\left(\mathrm{Li}_\alpha(-e^{\xi_1}) - \mathrm{Li}_\alpha(-e^{-\xi_1})\right)^{1/2}}{2\sqrt{2}\left(\mathrm{Li}_{\alpha-1}(-e^{\xi_1}) - \mathrm{Li}_{\alpha-1}(-e^{-\xi_1})\right)^{1/2}} \tag{3.127}$$

Case $\alpha > 1$ In this case, we have simply

$$\operatorname{Im} \mathcal{F}_\alpha(iy) \sim \frac{1}{2} \tag{3.128}$$

which means that

$$g_1^a(R) = \frac{B_\alpha(\mu) e^{i\pi R} e^{-\xi_1 R}}{\sqrt{\pi R}} - \frac{1}{2\pi}\frac{1}{R} \tag{3.129}$$

Hence, we can summarize the asymptotic behaviour of the anomalous correlator as

$$g_1^a(R) \sim \begin{cases} \dfrac{1}{R^\alpha} & \text{if} \quad \alpha > 1 \\ \dfrac{1}{R} & \text{if} \quad \alpha < 1 \end{cases} \tag{3.130}$$

Two-body correlation function The most important two-body correlation function is the density-density correlation $g_2(R) = \left|g_1^a(R)\right|^2 - \left|g_1(R)\right|^2$, which we already talked about in Sec. 3.2.3. It also has an hybrid behaviour, it is exponentially decaying for short distances but follows a power law for large distances. In particular, at a large distance

$$g_2(R) = \begin{cases} \dfrac{1}{R^{2\alpha}} & \text{if} \quad \alpha > 1 \\ \dfrac{1}{R^2} & \text{if} \quad \alpha < 1 \end{cases} \tag{3.131}$$

3.5.4 Massive edge states in LRK

The LRK model presents some novel topological edge states, which have been analyzed in [39–41]. In short, for $\alpha < 1$ the model is subject to a substantial qualitative change, where the Majorana zero modes disappear and are replaced by *Dirac modes*, which are *non-local massive edge states*. For *massive* edge state we mean that its energy is non-zero but still located inside the gap, separated from the bulk band, but its wavefunction is localized at the edges.

Viyuela et al. in [39] have analyzed the phase diagram of the LRK chain through the *winding vector* $\boldsymbol{n}_k$, which for $t = \Delta = 1$ is

$$\boldsymbol{n}_k = -\frac{1}{E_k}(0, \quad f_\alpha(k), \quad \mu + 2\cos k), \tag{3.132}$$

where the dispersion relation E_k is

$$E_k = \sqrt{(\mu + 2\cos k)^2 + f_\alpha(k)^2} \tag{3.133}$$

and $f_\alpha(k)$ is the same function defined in (3.99). The winding vector $\boldsymbol{n}_k$ is defined from the Bloch Hamiltonian, similarly to the vector $\mathbf{d}(\mathbf{k})$ in (1.35) of the SSH model which has basically the same role. The LRK model belongs to the class BDI of the 10-fold classification, reported in Tab. 1.1, because it possesses particle-hole, time-reversal and also chiral symmetry, like the (short-range) Kitaev model. Their presence restrict the movement of $\boldsymbol{n}_k$ to just S^1, not S^2, similarly to what happened in the SSH model (see the discussion in Sec. 1.6). Thus, in the spirit of the 10-fold classification, presented in Sec. 1.7.3, the map from the BZ $\equiv S^1$ to the sphere S^1 can be characterized by a $\mathbb{Z}$ topological invariant; that is the *winding number* ω, which is the angle swept by $\boldsymbol{n}_k$ when the crystal momentum k is varied across the whole BZ

$$\omega = \frac{1}{2\pi}\oint \mathrm{d}\theta = \frac{1}{2\pi}\oint \left(\frac{\partial_k n_k^z}{n_k^y}\right)\mathrm{d}k \tag{3.134}$$

where $\theta = \arctan n_k^z/n_k^y$. Due to the singular behaviour of the function $f_\alpha(k)$ near $k = 0$, where it diverges for $\alpha < 1$ (see App.A), the dispersion relation E_k, together with the group velocity, diverges. Nevertheless, the winding number ω is still integrable. The divergence in $f_\alpha(k)$ cannot be removed with a gauge transformation and, therefore, the point $k = 0$ constitute a *topological singularity*.

According to [39], three different topological sectors can be identified, depending on the value of the exponent α:

$\alpha > \frac{3}{2}$	massless Majorana sector
$\alpha < 1$	massive Dirac sector
$1 < \alpha < \frac{3}{2}$	crossover sector

The Majorana sector is topologically equivalent to the short-range Kitaev chain. In here, the function $f_\alpha(k)$ has a regular behaviour and the winding number ω can be calculated without much trouble. For[4] $|\mu| > 2$ we have a trivial phase ($\omega = 0$) with no edge states, whereas for $|\mu| < 2$ ($\omega = 1$) Majorana zero modes are always present.

The Dirac sector is much trickier. For sufficiently slow decaying pairing, an unconventional topological phase appears. For $\mu > 2$, the system is in a trivial phase with no

[4] Δ and t have been fixed to 1.

edge states. On the other hand, for $\mu < 2$ the chain presents massive Dirac fermion at the edges, as the two Majorana fermions at the two distant ends have paired up into a single Dirac fermion. This fermion is highly non-local and its appearance is deeply related to the long-range character of the pairing. Like the Majorana mode in the short-range Kitaev chain, this topological quasi-particle is protected by fermion parity. Viyuela et al. have found that the Dirac sector is characterized by a half-integer winding number; for the trivial phase $\mu > 2$ we have $\omega = -1/2$, while in the topological phase $\mu < 2$, $\omega = +1/2$. This half-integer character is a consequence of the divergence at $k = 0$ of $f_\alpha(k)$. Nonetheless, the jump of the topological number between these two different phases is still an integer, $\Delta\omega = \omega_{\text{top}} - \omega_{\text{trivial}} = 1$. Furthermore, the gap closes at $\mu = 2$, where the phase transition happens. Therefore, it is still possible to establish a bulk-edge correspondence in the Dirac sector.

Lastly, the crossover sector, $1 < \alpha < 3/2$, as the name says, is a crossover region between the Majorana sector and the Dirac sector. There are Majorana edge states for $-2 < \mu < 2$ but for $\mu < -2$ they are instead massive, while for $\mu > 2$ is trivial. A pictorial view of the classification of the phases of the LRK model is presented in Fig. 3.6.

It is important to remark that, both in the crossover and in the Majorana sector, the gap closes for $\mu = \pm 2$, while in the Dirac sector it only closes for $\mu = +1$. This make it theoretically possible to go from a topological phase with $\alpha > 3/2$ and $|\mu| < 2$ to a trivial phase $\alpha > 3/2$ $\mu < -2$, without closing the gap, that is *without going through a phase transition*. It sufficient to build a path that crosses the line $0 < \alpha < 1$ and $\mu = -2$, where the gap is still open.

This rather unconventional behaviour has also been noticed by Vodola et al. in [41]; On that note, the authors observed that where the mass gap is finite and non-zero, the ground state has to be unique. This indicates that the $\mathbb{Z}_2$ symmetry of the model, which is broken in the topological phase $\alpha > 1$ and $|\mu| < 2$, is restored for $\alpha < 1$. Thus, the two regions must be separated by a quantum phase transition, even if no closure of the gap arises in the bulk.

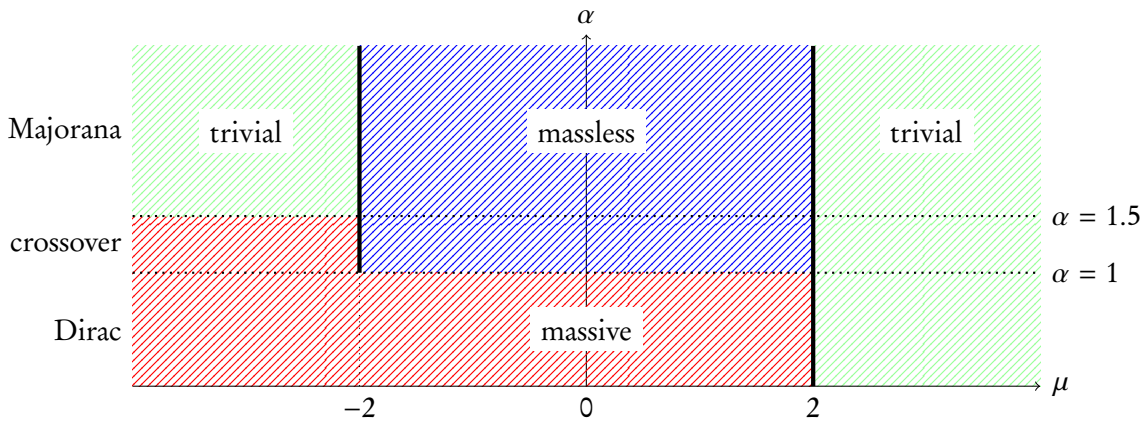

Figure 3.6: Phase diagram for the long-range Kitaev model, based on [39]. The think black lines represents the critical lines, where the gap closes. The *massless* region is where the edge states are Majorana zero modes, while in the *massive* region are Dirac modes. In the *trivial* regions there are no edge states. From the picture it is clear that potentially there is a path that connects the massless sector with the trivial sector, that does not cross any critical line.

4

On some extensions of the Kitaev model

In this chapter we are going to present some qualitative analysis of some extensions of the Kitaev model, mainly the long-range superconductive pairing. In preparation to that, we first analyze the case where we put a coupling term at the boundaries of the chain. Effectively this can be seen as a long-range coupling between just the first site of the chain and the last. In fact, the simple addition of this coupling give rise to massive edge states, like in the LRK in Sec. 3.5. We will conclude the chapter with a conjecture about the emergence of massive edge states, that will let us explain an unconventional phase transition in the LRK chain.

4.1 Coupling at the boundaries

The subject of this section is a qualitative study of the Kitaev chain with a coupling term only at the end of the chain:

$$H = -t\sum_{i=1}^{N-1}\left(c_i^\dagger c_{i+1} + c_{i+1}^\dagger c_i\right) - \mu\sum_{i=1}^{N}\left(c_i^\dagger c_i - \frac{1}{2}\right) + \frac{\Delta}{2}\sum_{i=1}^{N-1}\left(c_i c_{i+1} + c_{i+1}^\dagger c_i^\dagger\right) + u\left(c_N^\dagger c_1 + c_1^\dagger c_N\right) \quad (4.1)$$

This coupling is governed by a real[1] constant u. We notice that as u varies from zero to $-t$, we interpolate between open boundaries and periodic hopping.

Using the formalism of the LSM method, which has been exposed in the Sec. 3.2.2,

[1] The LSM method works only for real matrices A and B

we find that the matrices A and B that describe the spectrum are

$$A = \begin{pmatrix} -\mu & -t & \dots & 0 & u \\ -t & -\mu & \dots & \dots & 0 \\ \vdots & \vdots & \ddots & & \vdots \\ 0 & \vdots & & \ddots & -t \\ u & 0 & \dots & -t & -\mu \end{pmatrix} \quad \text{and} \quad B = \begin{pmatrix} 0 & \Delta & \dots & \dots & 0 \\ -\Delta & 0 & \dots & \dots & 0 \\ \vdots & \vdots & \ddots & & \vdots \\ \vdots & \vdots & & \ddots & \Delta \\ 0 & 0 & \dots & -\Delta & 0 \end{pmatrix} \tag{4.2}$$

Thus, the energies of the system can be found by inspecting the singular values of the following matrix:

$$A + B \equiv T_N^u = \begin{pmatrix} -\mu & -t+\Delta & \dots & 0 & u \\ -t-\Delta & -\mu & \dots & \dots & 0 \\ \vdots & \vdots & \ddots & & \vdots \\ 0 & \vdots & & \ddots & -t+\Delta \\ u & 0 & \dots & -t-\Delta & -\mu \end{pmatrix} \tag{4.3}$$

If the system has N sites, then T_N^u is bound to be an $N \times N$ real matrix. Even though T_N^u and A appear to be finite Toeplitz matrices, one has to careful to consider them as such. A finite $n \times n$ Toeplitz matrix $T_n(a)$, with symbol a, is usually thought as the finite truncation of an infinite Toeplitz matrix $T(a)$ with the same symbol a.

In our case, the finite matrix T_N^u has the symbol

$$a(e^{ik}) = -2t\cos k - \mu + i2\Delta \sin k + 2u \cos kN$$

which *depends on the number of sites*. This means that for different N the matrix T_N^u has a different symbol a and cannot be viewed as the finite truncation of a single infinite-dimensional Toeplitz operator. This raises the question of *what is the limit for* $N \to \infty$ *of* T_N^u? It has to be noted that it is not granted whether or not the sequence T_N^u converges to some operator in $\mathcal{B}(\ell^2)$.

We investigate that by first separating T_N^u into two parts

$$T_N^u = T_N(a) + C_N \tag{4.4}$$

where $T_N(a)$ is the proper $N \times N$ truncation of the infinite Toeplitz matrix $T(a)$ with symbol $a(e^{ik}) = -2t\cos k - \mu + i2\Delta \sin k$, while C_N represents the coupling at the

borders

$$C_N = \begin{pmatrix} 0 & \dots & u \\ \vdots & \ddots & \vdots \\ u & \dots & 0 \end{pmatrix}. \tag{4.5}$$

The matrices $T_N^u(a)$ are thought as elements $\mathcal{B}(\ell^2)$. The question we want to answer now is: does the sequence $\{T_N^u\}$ converge in $\mathcal{B}(\ell^2)$? Given the fact $\mathcal{B}(\ell^2)$ is a Banach space, which is a *complete* normed vector space, the sequence $\{T_N^u\}$ converges if only if is a Cauchy sequence, thus

$$\{T_N^u\} \text{ converges} \qquad \Longleftrightarrow \qquad \left\|T_{N+1}^u - T_N^u\right\| \to 0 \quad \text{for} \quad N \to \infty$$

Clearly, we have that

$$\left\|T_{N+1}^u - T_N^u\right\| = \left\|T_{N+1}(a) + C_{N+1} - T_N^u - C_N\right\| \leq \|T_{N+1}(a) - T_N(a)\| + \|C_{N+1} - C_N\|$$

for the triangle inequality. As we have said in Sec. 2.2, the sequence of finite truncations $\{T_N(a)\}$ converges strongly onto $T(a)$, hence $\|T_{N+1}(a) - T_N(a)\| \to 0$ for $N \to \infty$. Thus, we are left with the task of evaluating $\|C_{N+1} - C_N\|$.

The $(N+1) \times (N+1)$ section[2] of the matrix $C_{N+1} - C_N$ reads as

$$C_{N+1} - C_N = \begin{pmatrix} 0 & \dots & 0 & -u & u \\ \vdots & \ddots & & 0 & 0 \\ 0 & & \ddots & \vdots & \vdots \\ -u & 0 & \dots & 0 & 0 \\ u & 0 & \dots & 0 & 0 \end{pmatrix}. \tag{4.6}$$

Consider now the canonical base $\{\mathbf{e}_i\}_{i=1}^{\infty}$ for ℓ^2

$$\mathbf{e}_i = (0, \dots, 0, 1, 0, \dots, 0)$$

where the only non-zero term is in the i-th position. From (4.6), the action of $C_{N+1} - C_N$

[2] Keep in mind we are considering them as elements of $\mathcal{B}(\ell^2)$

of the canonical base is

$$(C_{N+1} - C_N)\mathbf{e}_j = \begin{cases} -u\mathbf{e}_N + u\mathbf{e}_{N+1} & j = 1 \\ -u\mathbf{e}_1 & j = N \\ u\mathbf{e}_1 & j = N+1 \\ 0 & \text{otherwise} \end{cases} \tag{4.7}$$

Furthermore, $C_{N+1} - C_N$ is a real symmetric matrix, so it can always be put in a diagonal form, with its eigenvalues on the diagonal. Then, the norm $\|C_{N+1} - C_N\|$ will correspond to eigenvalue with the highest modulus. It is evident from (4.7), the eigenvectors of the non-zero eigenvalues of $C_{N+1} - C_N$ will belong to the subspace V_{N+1} generated by the vectors $\{\mathbf{e}_1, \mathbf{e}_N, \mathbf{e}_{N+1}\}$. The matrix elements of $C_{N+1} - C_N$, restricted to the space V_{N+1}, read as

$$(C_{N+1} - C_N)|_{V_{N+1}} = \begin{pmatrix} 0 & -u & u \\ -u & 0 & 0 \\ u & 0 & 0 \end{pmatrix} \tag{4.8}$$

and its eigenvalues can be easily calculated.

In fact, from the characteristic equation $\det\big((C_{N+1} - C_N)|_{V_{N+1}} - \lambda I\big) = 0$, one finds that the non-zero eigenvalues are

$$\lambda_\pm = \pm\sqrt{2}|u|$$

which are also the non-zero eigenvalues of the whole $C_{N+1} - C_N$. Hence

$$\|C_{N+1} - C_N\| = \sqrt{2}|u|$$

for every N. Subsequently, from (4.1) and from the fact that $T_N(a) \to T(a)$ strongly, we get

$$\left\|T^u_{N+1} - T^u_N\right\| \longrightarrow \sqrt{2}|u| \quad \text{for} \quad N \to \infty$$

which means that $\{T^u_N\}$ is not a Cauchy sequence, thus it *does not converge uniformly* in $\mathcal{B}(\ell^2)$. This, however, does not exclude the possibility that it may converge in a dense subset of $\mathcal{B}(\ell^2)$. Also, it does not even exclude the possibility that it converges in some other norm. On that note, if we set $\Delta = 0$ and $u = t$ in our model, we obtain that T^u_N has to be a circulant matrix.

In general, if we take a circulant matrix $C_n(b)$ (not to be confused with C_N) and a Toeplitz matrix $T_n(b)$, both built from the same symbol b, then it is known that $T_n(b)$

and $C_n(b)$ are *asymptotically equivalent for* $n \to \infty$ [17, Lem. 4.2], in the following sense: both matrices are bounded in the strong norm, that is the operatorial norm $\|\cdot\|$ we have used until now for the space $\mathcal{B}(\ell^2)$; furthermore, their difference tends to zero *in the Hilbert-Schmidt norm*, or *weak norm*, i.e

$$\lim_{n\to\infty} \left\| T_n(b) - C_n(b) \right\|_{HS} = 0 \tag{4.9}$$

where, given a matrix $A = (a_{ij})_{i,j=0}^{n}$, the Hilbert-Schimdt norm $\|\cdot\|_{HS}$ is defined as [17, Sec. 2.2]

$$\|A\|_{HS} = \left(\frac{1}{n} \sum_{k,j=0}^{n-1} |a_{jk}|^2 \right)^{1/2} = \left(\frac{1}{n} \operatorname{Tr}\left[A^\dagger A\right] \right)^{1/2} = \left(\frac{1}{n} \sum_{k=0}^{n-1} s_k(A) \right)^{1/2} \tag{4.10}$$

where $s_k(A)$ are the singular values of A. Now, let $\tau_{n,k}$ be the eigenvalues of $T_n(b)$ and $\psi_{n,k}$ the eigenvalues of $C_n(b)$. From [17, Th. 2.2], we have that for every integer s the following is true

$$\lim_{n\to\infty} \frac{1}{n} \sum_{k=0}^{n-1} \tau_{n,k}^s = \lim_{n\to\infty} \frac{1}{n} \sum_{k=0}^{n-1} \psi_{n,k}^s \tag{4.11}$$

This implies that the eigenvalue distribution of $T_n(b)$ can be well approximated by the one of $C_n(b)$, in the sense that $\{\tau_{n,k}\}$ and $\{\psi_{n,k}\}$ are *asymptotically equally distributed* [17, Th. 2.4].

The same reasoning can be applied to our problem. It is possible to prove that T_N^u and $T_N(a)$ are asymptotically equivalent sequences of matrices. Indeed, $\left\| T_N^u - T_N(a) \right\|_{HS}$ yields

$$\left\| T_N^u - T_N(a) \right\|_{HS} = \|C_N\|_{HS} = \frac{2|u|}{N} \tag{4.12}$$

which goes to zero for $N \to \infty$. Therefore, because of (4.11), the eigenvalues distribution of T_N^u and $T_N(a)$ are asymptotically equivalent. From a physical point of view, that would mean that the spectra of the system, in the thermodynamic limit, *is insensitive to the boundary conditions*. Intuitively, this is exactly what we expect from a system brought to the thermodynamic limit.

This physical consideration suggests another idea; that it is possible to define the thermodynamic limit T^u of the matrix T_N^u. In fact, it is always a bounded operator, because $T_N(a)$ and C_N are bounded for every N, and we can *conjecture* that T^u is well defined on a dense subset $\mathcal{D}$ of ℓ^2. Furthermore, we conjecture that such a dense subset is the set of eigenvectors of T^u, because they are well defined for every N. The novelty here

is supposing that the set of eigenvectors $\mathcal{D}$ is dense in ℓ^2 and that is possible to extend the operator T^u from $\mathcal{D}$ to the whole space ℓ^2. If such a extension is possible, then we hope to make T^u accessible through the various properties of bounded operators.

4.1.1 Numerical analysis

The presence of the u-coupling affects the spectrum of the system, especially at the lower levels. The spectrum of (4.1) can be calculated with a singular valued decomposition of the matrix T_N^u in (4.3), which can been done numerically[3]. The results are presented in Fig. from 4.2 to 4.6. If there are any zero modes, we expect to find the lowest singular value near zero and separated from the others that constitute the bulk band, see the discussion in Sec. 3.4.2. On the other hand, if there are no zero mode but only massive edge states, then the lowest singular value of (4.3) should be above zero but still separated from the bulk band. For this reason, we have plotted different color maps of the lowest singular value E_1 and the difference $E_2 - E_1$, from Fig. 4.2 to 4.4.

First thing we notice in Fig. 4.2-4.3 is that the critical lines $\mu = \pm 2t$ survives, even if we add coupling at the borders. On such a critical line we expect the gap to close, i.e. $E_1 \sim 0$, and the bulk band to vary continuously, i.e. $E_2 - E_1 \sim 0$.

Another property that emerges is that even for $u \neq 0$ the edges states in the region $|\mu| < 2|t|$ still survive. This is verified by the graph of the lowest energy solution ϕ_1 and ψ_1 of the LSM equations (3.23) and (3.24) in Fig. 4.6 for $\mu = 1$. For $u \neq 0$ and $\mu < 2t$, E_1 becomes separated from the zero as well as $E_1 - E_2$ does. This signals that the non-zero energy E_1 is located inside the bulk gap, which is a characteristic of massive edge states.

From Fig. 4.5 we can see that the coupling at the border does not affect the bulk bands and only modifies the lowest energy level. We also notice that for $u \gtrsim 2$ there are two additional points where E_1 vanishes. As a matter of fact, this phenomenon can also be observed in Fig. 4.4; for $|\mu| = \pm|u|$, only E_1 appears to vanish while the bulk band remains gapped. More importantly, in Fig. 4.4 we can see that there is a region where $E_1 > 0$ but also $E_2 - E_1 > 0$, which is an indicator of the presence of massive edge state. This fact is corroborated by the plot of the wavefunctions in Fig. 4.6 for $\mu = 3$. In particular, by increasing the coupling u we go through from a phase with no edge states to one with, and again to one without.

It important to note that on the line $\mu = 3$, there no critical line where both E_1 and

[3]The numerical analysis has been possible thanks to the tools and subroutines provided by the software package GNU Octave.

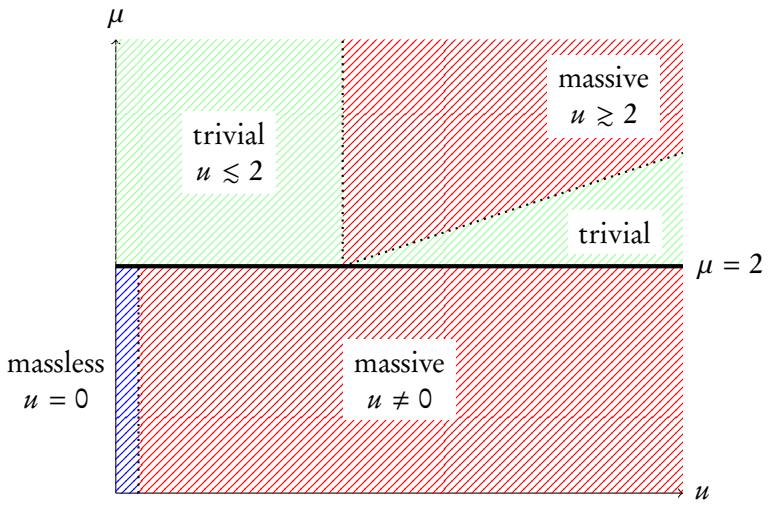

Figure 4.1: Approximative view of the phase diagram of the Kitaev chain with u-coupling. The heavy black line indicates the critical phase, where the gap closes. The red area stand for the topological phase with massive edge modes, while the blue one, which is restricted to the $u = 0$ line, is the topological phase with massless edge states, i.e. zero modes. For last, the green represent the trivial phase, with no edge states whatsoever.

$E_2 - E_1$ go to zero. What happens instead is the separation of E_1 from the bulk band in a particular interval of u. It seems that is in fact this separation that brings localization for the massive states. Sadly, at the time of this writing, it was not possible to obtain any analytic estimate on this interval.

For positive μ and u, the phase diagram of the Kitaev chain with u-coupling is summarized. The overall μ-u is symmetric with respect to the lines $\mu = 0$ and $u = 0$.

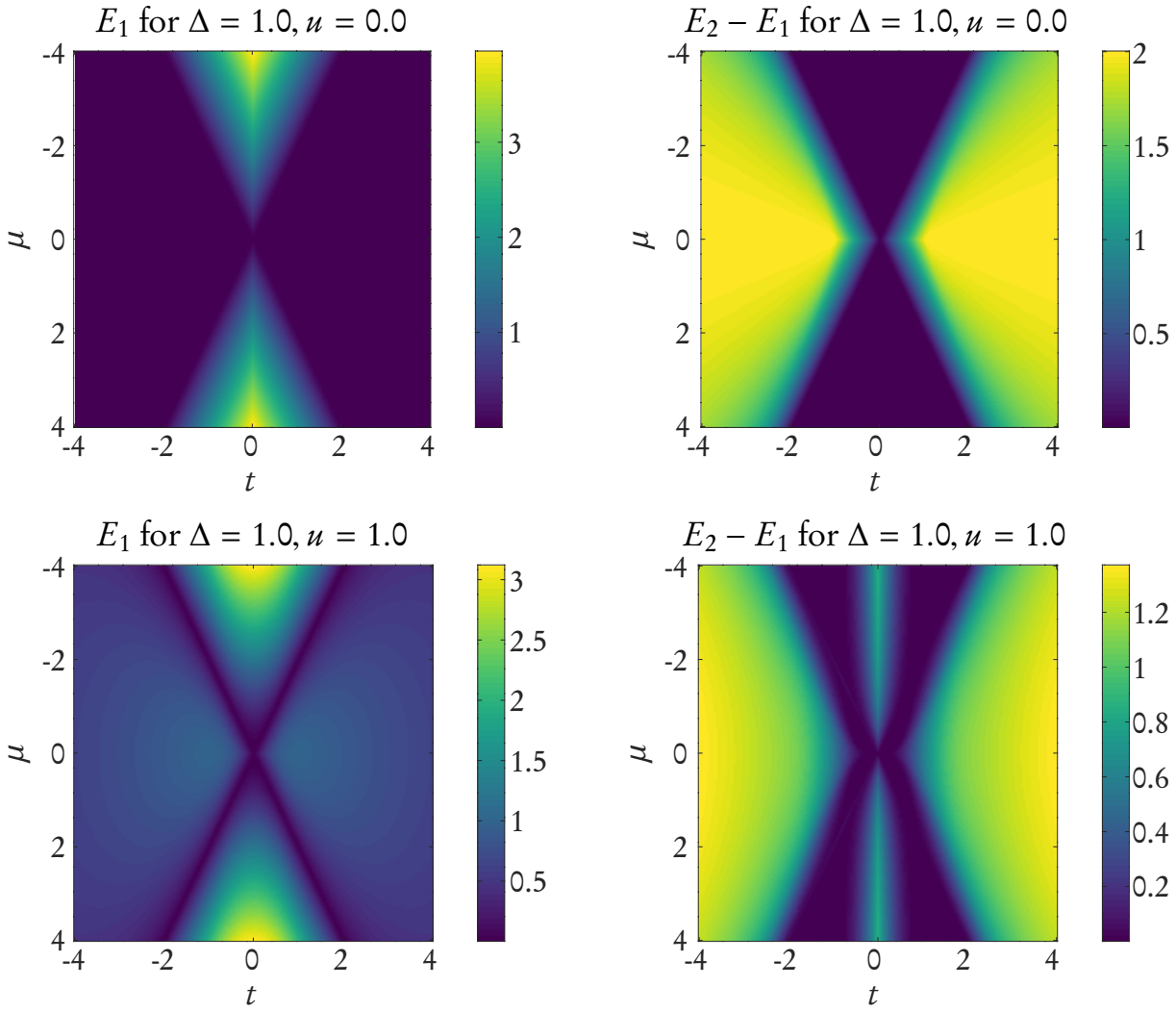

Figure 4.2: Here we have different plots of the μ-t plane for both the lowest energy E_1 (left column) and for the difference $E_2 - E_1$ (right column), for $N = 200$ sites and $\Delta = 1$. The first row show the μ-t plane for $u = 0$ (no coupling at the borders) while the second row is for $u = 1$. Trivial gapped phases are characterized by $E_1 > 0$ and $E_2 - E_1 \sim 0$, while non-trivial gapped phases have $E_2 - E_1 > 0$; which indicates that the energy E_1 is separated from the bulk band. The dark blue lines in the pictures on the left indicate closure of the gap. In the first row we also find a region with $E_1 \sim 0$ and $E_2 - E_1 > 0$, which indicates the presence of zero modes. By confronting it with the second row, we see that these zero modes acquires a mass when a small coupling at the border is added.

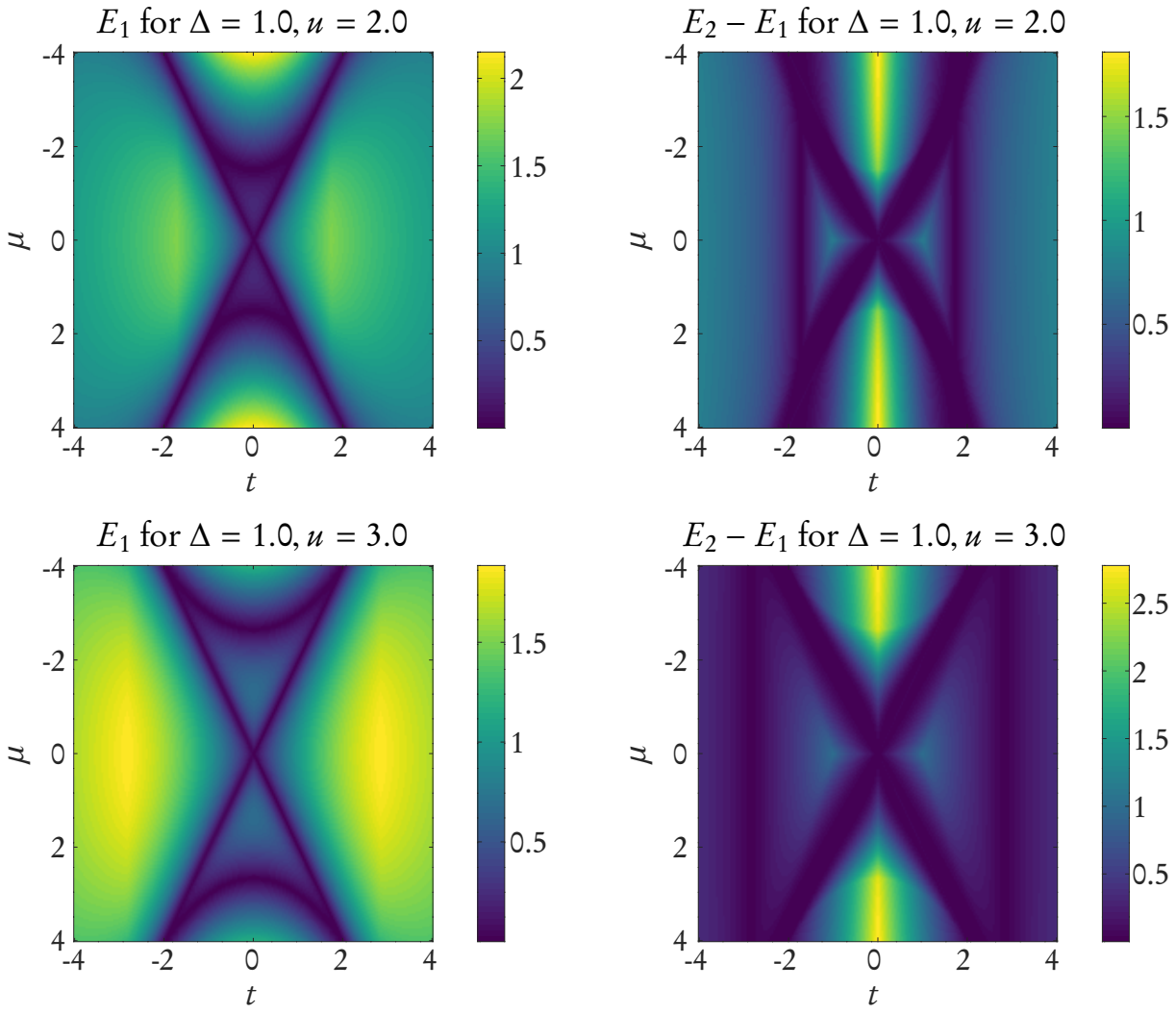

Figure 4.3: Like in Fig. 4.2, here we different plots of the μ-t plane for the lowest energy E_1 (left column) and for the difference $E_2 - E_1$ (right column), for $N = 200$ sites and $\Delta = 1$ but now with $u = 2$ (first row) and $u = 3$ (second row). Trivial gapped phases are characterized by $E_1 > 0$ and $E_2 - E_1 \sim 0$, while non-trivial gapped phases have $E_2 - E_1 > 0$; which indicates that the energy E_1 is separated from the bulk band. The dark blue lines in the pictures on the left indicate closure of the gap. In this case there are no zero modes and the structure of the phase diagram is richer when u increases

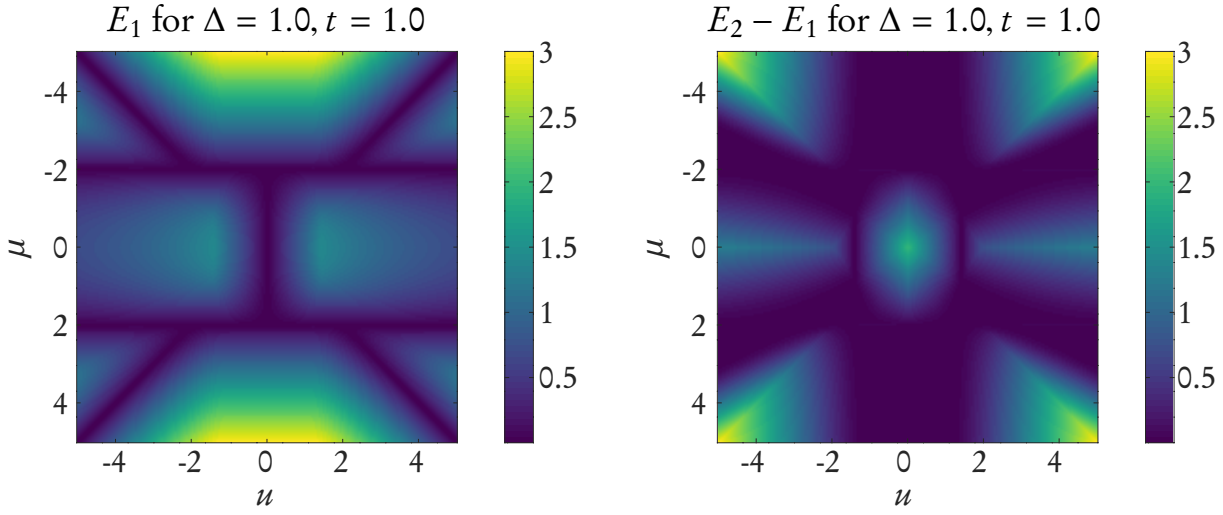

Figure 4.4: These two graphs represent the values of the lowest energy E_1 (on the left) and the difference $E_2 - E_1$ (on the right) in u-μ plane for $\Delta = t = 1$ for $N = 200$ sites. In the first picture we only see the lines where the energy closes (the dark blue lines). Meanwhile on the second picture it's possible to distinguish regions trivial gapped regions, in dark blue, and non-trivial gapped regions where the E_1 is separated from the bulk band, i.e. $E_2 - E_1 > 0$.

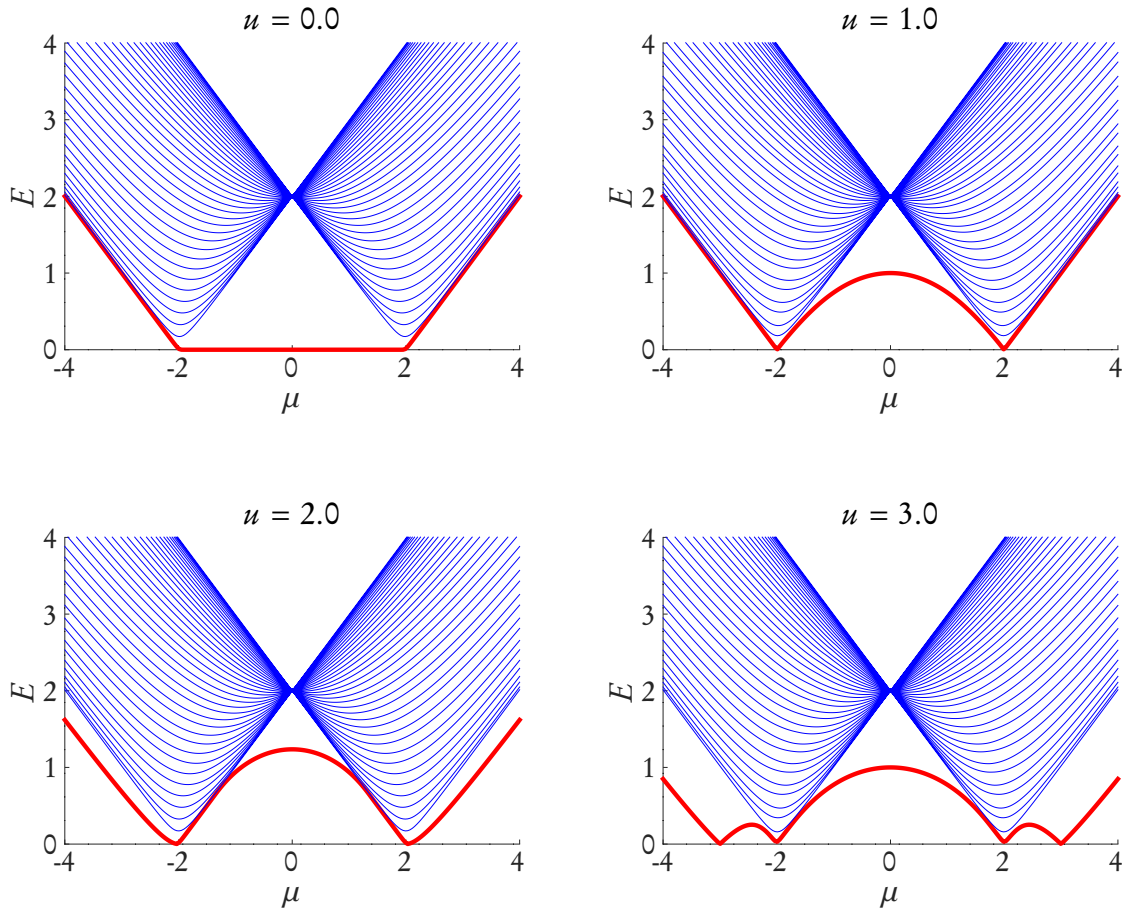

Figure 4.5: Plot of the energy levels as a function of the chemical potential μ, for fixed u. The parameters t and Δ have been set to 1. The lowest energy level is drawn in red while the bulk band is in blue. The graph in the top left kernel represent the Kitaev model without the coupling at the end of the chains, where is possible to see the zero mode for $|\mu| < 2$. With coupling at the borders, the edge mode is no longer a zero mode, it has become massive. In Fig. 4.6 is possible to verify that it is indeed an edge mode.

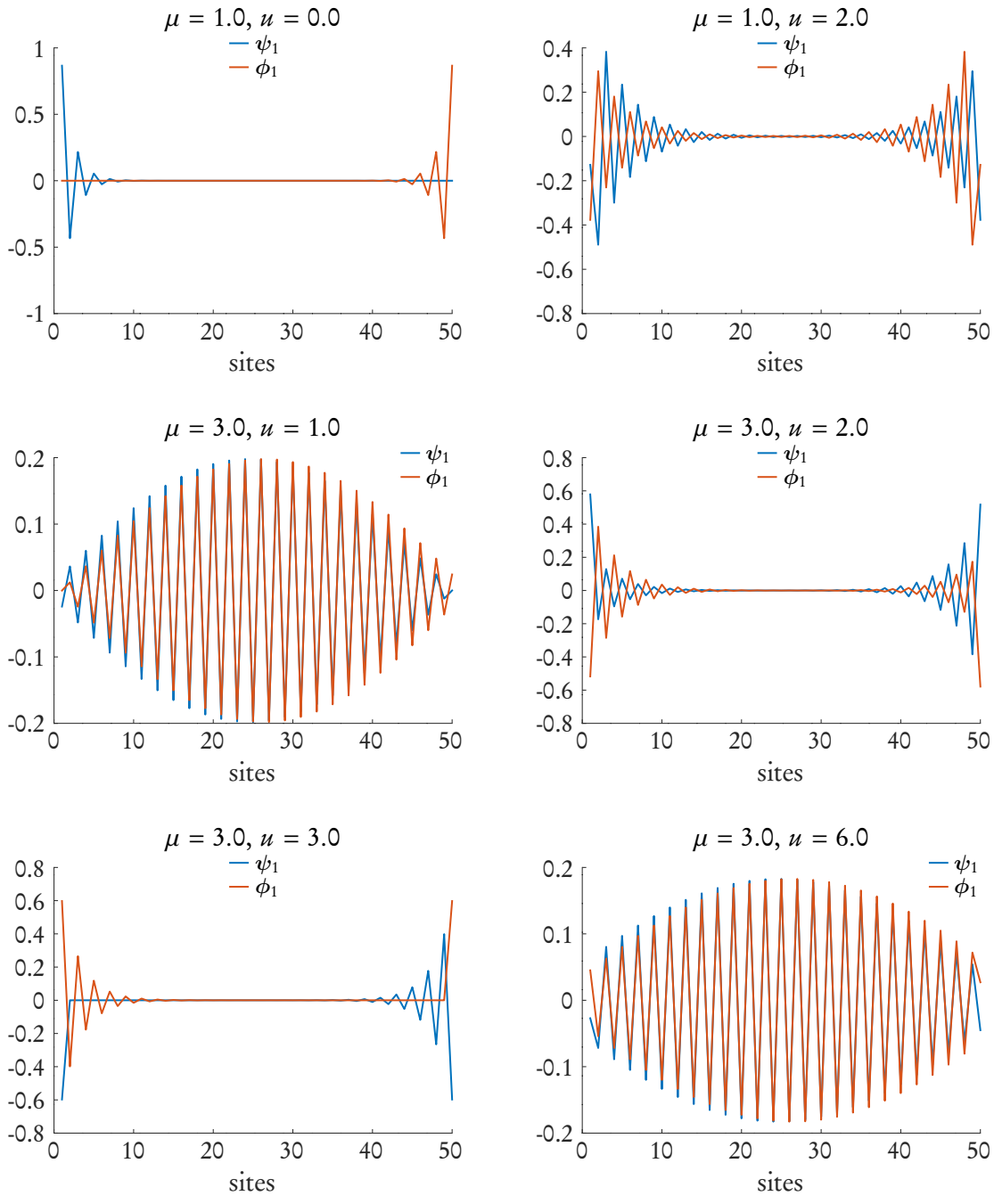

Figure 4.6: The wavefunctions ψ_1 and ϕ_1, i.e. the lowest energy solutions of the LSM equations, of the Kitaev chain with coupling at the ends have been plotted for different values of μ and u. We can clearly distinguish between edge states and bulk states. To be more specific, for $\mu < 2$ we only have edge states but, more interestingly, for $\mu > 2$ we can pass from a state without edge states to a state with them, or vice versa, without closure of the gap.

4.2 Another kind of coupling at the boundaries

In this section we investigate another kind of coupling at edges, that let us transition continuously from open boundaries to periodic boundary condition. The Hamiltonian of this model can be written as follows:

$$H = -t\sum_{i=1}^{N-1}\left(c_i^\dagger c_{i+1} + c_{i+1}^\dagger c_i\right) - \mu\sum_{i=1}^{N}\left(c_i^\dagger c_i - \frac{1}{2}\right) + \frac{\Delta}{2}\sum_{i=1}^{N-1}\left(c_i c_{i+1} + c_{i+1}^\dagger c_i^\dagger\right) - xt\left(c_1^\dagger c_N + c_N^\dagger c_1\right) + x\Delta\left(c_1 c_N + c_N^\dagger c_1^\dagger\right) \quad (4.13)$$

where the real parameter x can vary in the interval $[0, 1]$. For $x = 0$ we have open boundaries, whereas for $x = 1$ we have periodic boundary conditions. The matrices of the LSM method are now

$$A = \begin{pmatrix} -\mu & -t & \dots & 0 & -xt \\ -t & -\mu & \dots & \dots & 0 \\ \vdots & \vdots & \ddots & & \vdots \\ 0 & \vdots & & \ddots & -t \\ -xt & 0 & \dots & -t & -\mu \end{pmatrix} \quad \text{and} \quad B = \begin{pmatrix} 0 & \Delta & \dots & \dots & -x\Delta \\ -\Delta & 0 & \dots & \dots & 0 \\ \vdots & \vdots & \ddots & & \vdots \\ \vdots & \vdots & & \ddots & \Delta \\ x\Delta & 0 & \dots & -\Delta & 0 \end{pmatrix} \quad (4.14)$$

Therefore, the spectrum is encoded in the following matrix

$$A + B \equiv T_N^x = \begin{pmatrix} -\mu & -t+\Delta & \dots & 0 & -x(t-\Delta) \\ -t-\Delta & -\mu & \dots & \dots & 0 \\ \vdots & \vdots & \ddots & & \vdots \\ 0 & \vdots & & \ddots & -t+\Delta \\ -x(t+\Delta) & 0 & \dots & -t-\Delta & -\mu \end{pmatrix} \quad (4.15)$$

From now on, we are going to assume $\Delta = t = 1$.

For $\mu < 2$, we know that massless edge states should appear if we are in an open chain, whereas for a closed and periodic chain no edge state should be present, because there is no edges. Therefore, for x that varies from 0 to 1, in the phase $-2 < \mu < 2$, we expect that the massless state acquires a mass, if $x \neq 0$, until it disappears in the bulk band for $x = 1$. In fact, this is exactly what we observe in Fig. 4.7. We further confirm that these are indeed edge states, by looking at their wavefunction in Fig. 4.8. The trivial phase $|\mu| > 2$ is not even touched by the presence of the coupling.

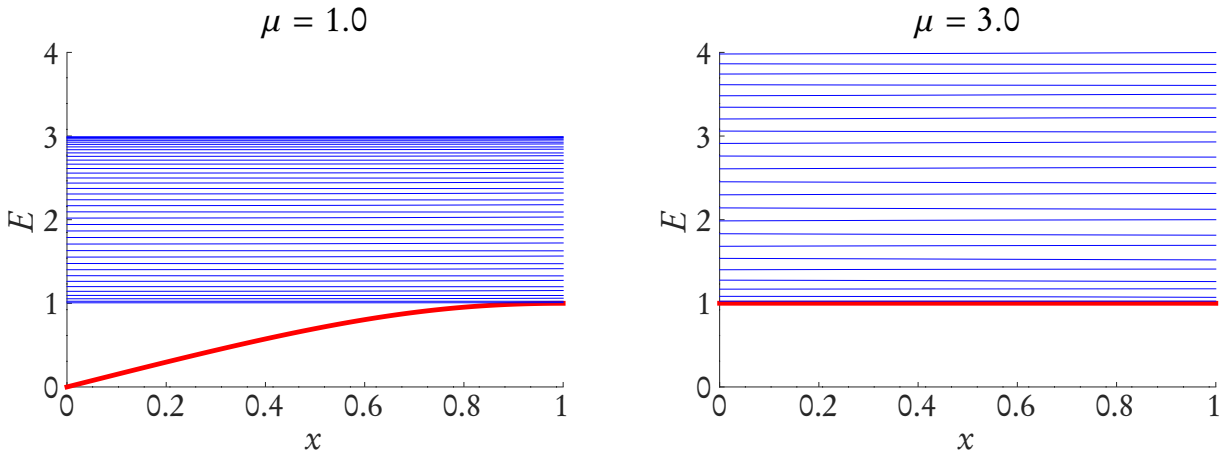

Figure 4.7: The graph represents the different energy levels with variable x and fixed μ for $N = 200$ sites. The lowest energy E_1 is pictured in red while the bulk band is in blue. We can clearly see that in the topological phase $|\mu| < 2$, the edge state vanishes in the periodic boundary condition, i.e. $x = 1$. The trivial phase is insensible to the presence of the coupling.

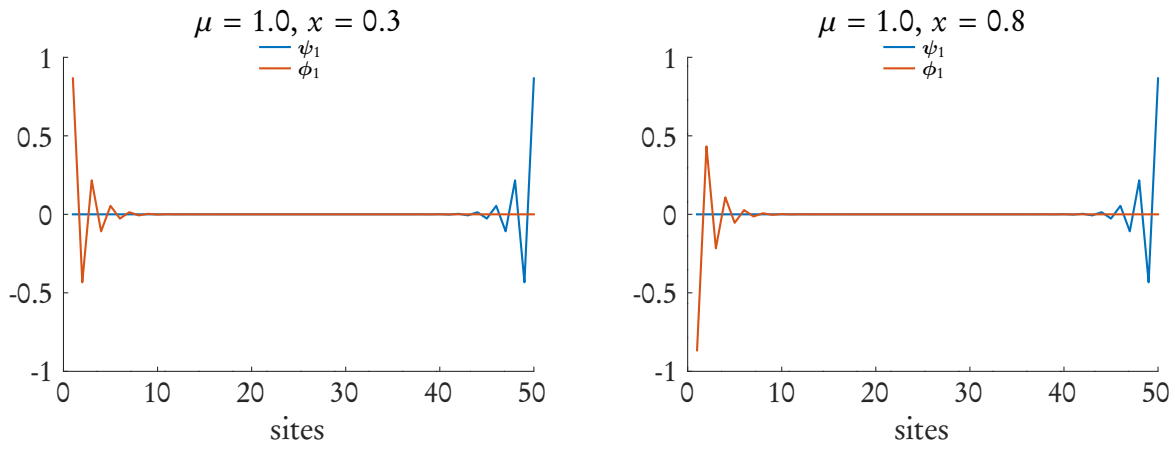

Figure 4.8: The two graphs are plots of the wave function of the massive states of the Kitaev chain with x-coupling, in the phase $|\mu| < 1$ for $N = 50$ sites. The wavefunctions are clearly localized at the edges and the lowest energy state is indeed an edge state for $x < 1$.

4.3 Long-range Kitaev model

In this section we present some qualitative analysis of the long-range Kitaev (LRK) model with open boundaries and propose a conjecture about the existence of massive edge states for systems with topological singularities. The Hamiltonian of LRK chain, with open boundaries, can be written as follows

$$H = \sum_{j=1}^{N} \left[-\left(c_j^\dagger c_{j+1} + c_{j+1}^\dagger c_j \right) - \mu \left(c_j^\dagger c_j - \frac{1}{2} \right) \right] + \frac{1}{2} \sum_{i,j=1}^{N} \frac{i-j}{|i-j|^{\alpha+1}} \left(c_i c_j + c_j^\dagger c_i^\dagger \right) \tag{4.16}$$

where we have put $\Delta = t = 1$ for simplicity, and also ignore any $c_{i>N}$. In this instance, the matrix A of the LSM equations (3.23) and (3.24) is just

$$A_{ij} = \begin{cases} -1 & i - j = \pm 1 \\ -\mu & i = j \\ 0 & \text{otherwise} \end{cases} \tag{4.17}$$

while B is a bit more complicated

$$B_{ij} = \frac{i-j}{|i-j|^{\alpha+1}}. \tag{4.18}$$

The matrix A is symmetric while B is antisymmetric but both are real, as required by the LSM method. With open boundaries, A and B are both pure Toeplitz matrices and, in this case, the symbol for $A - B = T_N(g_\alpha)$ is

$$g_\alpha(e^{ik}) = -2\cos k - \mu - i f_\alpha(k) \tag{4.19}$$

where $f_\alpha(k) = -i(\mathrm{Li}(e^{ik}) - \mathrm{Li}(e^{-ik}))$, which is the same function that appears in (3.99).

The symbol g_α, in particular the function f_α, is divergent at $k = 0$ for $\alpha < 1$. This makes the analysis of the symbol, and as a consequence the analysis of the operator $T(g_\alpha)$, much more complicated, especially for $\alpha < 1$ where there are supposed to be the massive Dirac edge mode (see Sec. 3.5.4).

The divergence can be explained in the following way. The polylogarithm function $\mathrm{Li}_\alpha(z)$ admits the series expansion in (A.2) for non-integer order α. If we put $z = e^{ik}$,

the series expansion of $\mathrm{Li}_s(z)$ in (A.2) becomes

$$\mathrm{Li}_s(e^{ik}) = \Gamma(1-\alpha)(-ik)^{\alpha-1} + \sum_{n=0}^{\infty} \zeta(\alpha-n)\frac{(ik)^n}{n!} \qquad 0 \le k < 2\pi \tag{4.20}$$

The dominant term for $k \to 0$ is then

$$\mathrm{Li}_\alpha(e^{ik}) \sim \Gamma(1-\alpha)\frac{(-i)^{\alpha-1}}{k^{1-\alpha}} \qquad k \to 0 \tag{4.21}$$

Consequently, for $\alpha < 1$ the function $\mathrm{Li}_\alpha(e^{ik})$ diverges as $1/k^{1-\alpha}$. The same goes for $\mathrm{Li}_\alpha(e^{-ik})$. Thus, the symbol g_α is not L^∞, which makes $T(g_\alpha)$ *an unbounded operator*. If we lose the boundedness of the Toeplitz operator, then we lose many of the theorems in Chap. 2. Then, the question arises whether or not the symbol g_α can still be used as a tool to detect the different phases of the chain. At the end of this chapter we are going to propose a conjecture about how we can still use the symbol g_α for detecting topological phases. First of all, we proceed with some numerical analysis of the LRK chain, as way to gain physical intuition about the problem in hand.

4.3.1 Numerical analysis of LRK

Similarly to Sec. 4.1.1, the lowest energy E_1 and the difference $E_2 - E_1$ of the LRK chain in Fig. 4.11–4.12, both for fixed α and variable μ, and also fixed μ and variable α. First thing first, for $\alpha \lesssim 1.5$ the distribution of the energy levels is radically different from that of the short-range Kitaev chain; whereas already for $\alpha = 2$ and $\alpha = 3$, the distribution is practically similar to the short-range case. This is a signal that indeed the sector $\alpha > 3/2$ is topologically equivalent to the short-range model, where we clearly have zero modes for $|\mu| < 2$ while $|\mu| > 2$ is trivial, with closure of the gap at $\mu = \pm 2$ (see Fig. 4.11).

However, it is more interesting to observe what happens in the Dirac sector $\alpha < 1$. We notice that there is an asymmetry with respect to the point $\mu = 2$. For $\mu > 2$, the phase is rather trivial, with no energy level inside the gap. For $\mu < 2$ instead, the lowest energy is clearly gapped, and separated from the bulk band as well; this means we have a massive state, which is also an edge states, as confirmed by the plots of the wavefunctions in Fig. 4.14. So far so forth we have confirmed the phase diagram in Fig. 3.6.

Furthermore, also the crossover sector $1 < \alpha < 3/2$ of [39] is worth of interest. From the graphs in 4.11, it appears that the edge mass vanishes for $0 < \mu < 2$, while it is slightly above zero in the interval $-2 < \mu < 0$. For $\mu < -2$, the gap between the edge state and the bulk band slowly goes to zero until $\alpha = 3/2$, where the edge state vanishes

into the bulk band. We will come back to this at the end of the next section.

In conclusion, the phase diagram in Fig. 3.6 seems to be mostly confirmed by the numerical analysis conducted here, in particular in the Dirac and Majorana sector, as it can also be viewed in Fig. 4.13, where both E_1 and $E_1 - E_2$ have been plotted as function of μ and α. In the crossover sector, the agreement with Fig. 3.6 is not totally faithful; this can be an issue of numerical computation, as the symbol g_α is not quite smooth in this sector, especially for $k \to 0$.

4.3.2 Winding number and the unconventional phase transition

It is established knowledge that the topological invariants that characterize a phase can only change if there is a phase transition, which implies a closure of the energy gap. Moreover, In Sec. 3.4.3 we already argued that $\mathrm{wind}(g, 0)$ has the properties necessary for being a good topological invariant. Then, one must ask what happens to $\mathrm{wind}(g_\alpha, 0)$ when we pass from the Majorana sector to the Dirac sector.

Given the divergence of g_α for $\alpha < 1$, we have that the image $g_\alpha(\mathbb{T})$ becomes an open curve that goes to infinity. This phenomenon is showcased in Fig 4.9, where we have plotted the curve $g_\alpha(\mathbb{T})$ for different values of α.

Case $\alpha > 1$ For $\alpha > 1$, $f_\alpha(k)$ is finite for every k. Thus, the curve $g(\mathbb{T})$ is limited and continuous, and $\mathrm{wind}(g_\alpha, 0)$ is a well defined number. The parameters t and Δ influence only the width of the curve along the real and imaginary axes of complex plane, respectively. Therefore, without loss of generality, t and Δ can be fixed to 1. On the other hand, the chemical potential μ has the effect of shifting the whole curve along the real axis. Hence, by varying μ, we can have different situations of $g(\mathbb{T})$ with respect to the origin of the complex plane; as a matter of fact, for $|\mu| < 2$ the winding number is non-zero, which corresponds to a topological phase, because, basically, the zero is inside the curve $g_\alpha(\mathbb{T})$.

Case $\alpha < 1$ In the Dirac sector there are two different phases: the massive phase and the trivial phase. The former phase has the origin on the left side, while the latter of the right side, of the curve $g_\alpha(\mathbb{T})$. To be more precise, the curve g_α divide the plane in two regions, a convex one and a concave one, and we *conjecture* that *the massive edge states are present only if the origin belongs to the convex region.* Going further, we identify the *essential range* $\mathcal{R}(g_\alpha)$ with the image of g_α, because it does not presents any isolated points, and the convex half of the plane with $\mathrm{conv}\,\mathcal{R}(g_\alpha)$, the convex hull of $\mathcal{R}(g_\alpha)$. Therefore, we formulate our hypothesis as follows

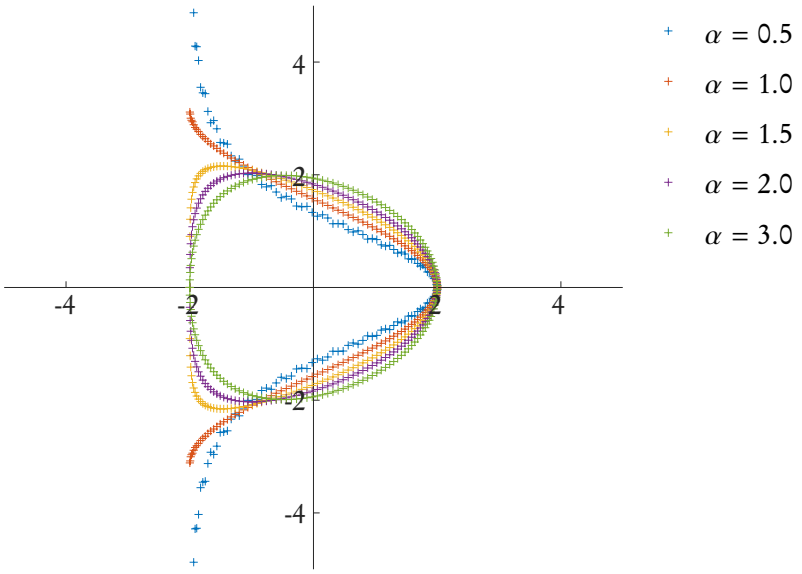

Figure 4.9: Graphs of the function g_α in the complex plain, for $\mu = 0$ and different values of α. It is possible to see that for $\alpha < 1$, the curve opens and diverges to infinity. In this case the left and right regions are convex and concave, respectively.

Conjecture. *A system with a* topological singularity, *e.g. the LRK chain, is in a topological phase with* massive edge states *only if* $0 \in \operatorname{conv} \mathcal{R}(g)$, *where* g *is the symbol of the unbounded Toeplitz matrix that encodes the spectrum of the system.*

This conjecture is further corroborated, at least in the LRK case, by the fact that if we invert the sign of t, then the curve must open on the right side. Therefore, the critical line is $\mu = -2$ and massive edge states should be present only for $\mu > -2$ and $\alpha < 1$, and indeed such a behaviour is reported in Fig 4.13 for $t = -1$. Of course it has to be noted that when α transitions from $\alpha < 1$ to $\alpha > 1$, the set $\operatorname{conv} \mathcal{R}(g_\alpha)$ abruptly changes from an infinite set to a finite one. In this case, the topological singularity vanishes and $\operatorname{wind}(g_\alpha, 0)$ is once again a well defined quantity. Hence, the mass of the edge state could be related to the finiteness of the set $\operatorname{conv} \mathcal{R}(g_\alpha)$.

Remark on the crossover region Based on our analysis, *we don't expect any crossover region*. The polylogarithm function $\mathrm{Li}_\alpha(e^{ik})$, and therefore also $f_\alpha(k)$, in the sector $1 < \alpha < 3/2$, presents a steep but continuous behaviour for $k \to \infty$, which is it hard to capture numerically. Nonetheless, $f_\alpha(k)$ is still L^∞, which means $wind(g_\alpha, 0)$ remains a well defined number. Thus, *there should not be any difference between the Majorana sector*

and the crossover sector. For this reason, we argue that the massive edge states observed in latter sector are just artifacts of the finite size scaling. By increasing the precision of the numerical analysis conducted here, for $1 < \alpha < 3/2$ we should expect to find massless state across the interval $-2 < \mu < 2$ and no massive states whatsoever, while outside it the phase is trivial.

An unconventional phase transition Supposing our conjecture is true, we can now find a mechanism that would explain the unconventional phase transition, from a massless topological phase to a trivial one, without the closure of the gap. All the steps are illustrated in Fig. 4.10. In the trivial Majorana phase, the curve $g_\alpha(\mathbb{T})$ is closed ($\alpha > 1$) and the winding number is $\mathrm{wind}(g_\alpha, 0) = 1$. Moving to $\alpha < 1$, the curve opens up and $\mathrm{wind}(g_\alpha, 0)$ is no longer well defined. This let us, by lowering the chemical potential, to shift the curve in the real positive direction and move the origin away, without intersecting the curve itself. In this way is possible to avoid any critical phase, which are characterized by $0 \in g_\alpha(\mathbb{T})$. When we are in a state with $\mu < -2$, we can then again increase the power α and reobtain a closed curve. When, finally, the transition to $\alpha > 1$ has happened, we end up with $\mathrm{wind}(g_\alpha, 0) = 0$, which implies a trivial phase. As a final remark, we notice that our conjecture is compatible with the ones of [1, 2], where the long-range Kitaev chain has been studied by calculating the entanglement entropy, by means of the study of the determinant of Toeplitz matrix. Long-range pairing systems are described by matrices that do not usually fall in the application domain of the most important theorems of Toeplitz operator.

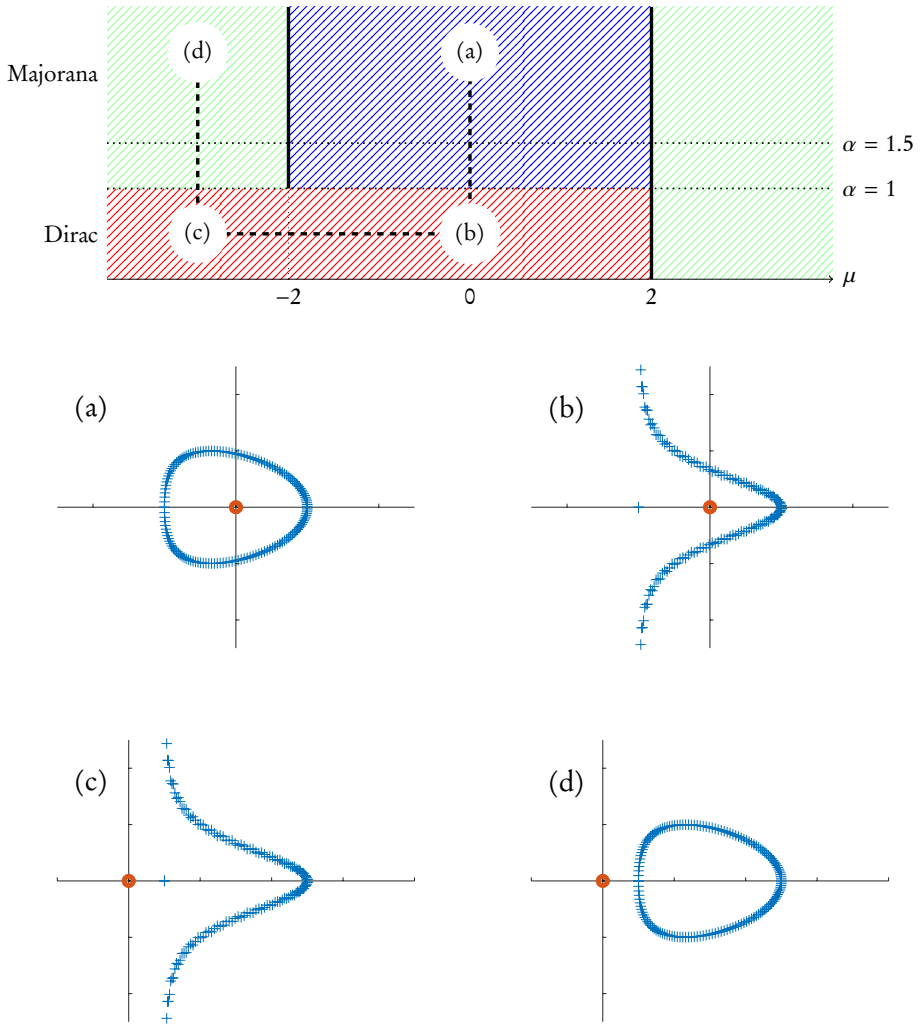

Figure 4.10: We have illustrated the different steps, in terms of the curve $g_\alpha(\mathbb{T})$, of the path the connect the topological phase to the trivial phases, in the Majorana sector. We reported how the shape of $g_\alpha(\mathbb{T})$ changes in relationship with the origin of the complex plane.

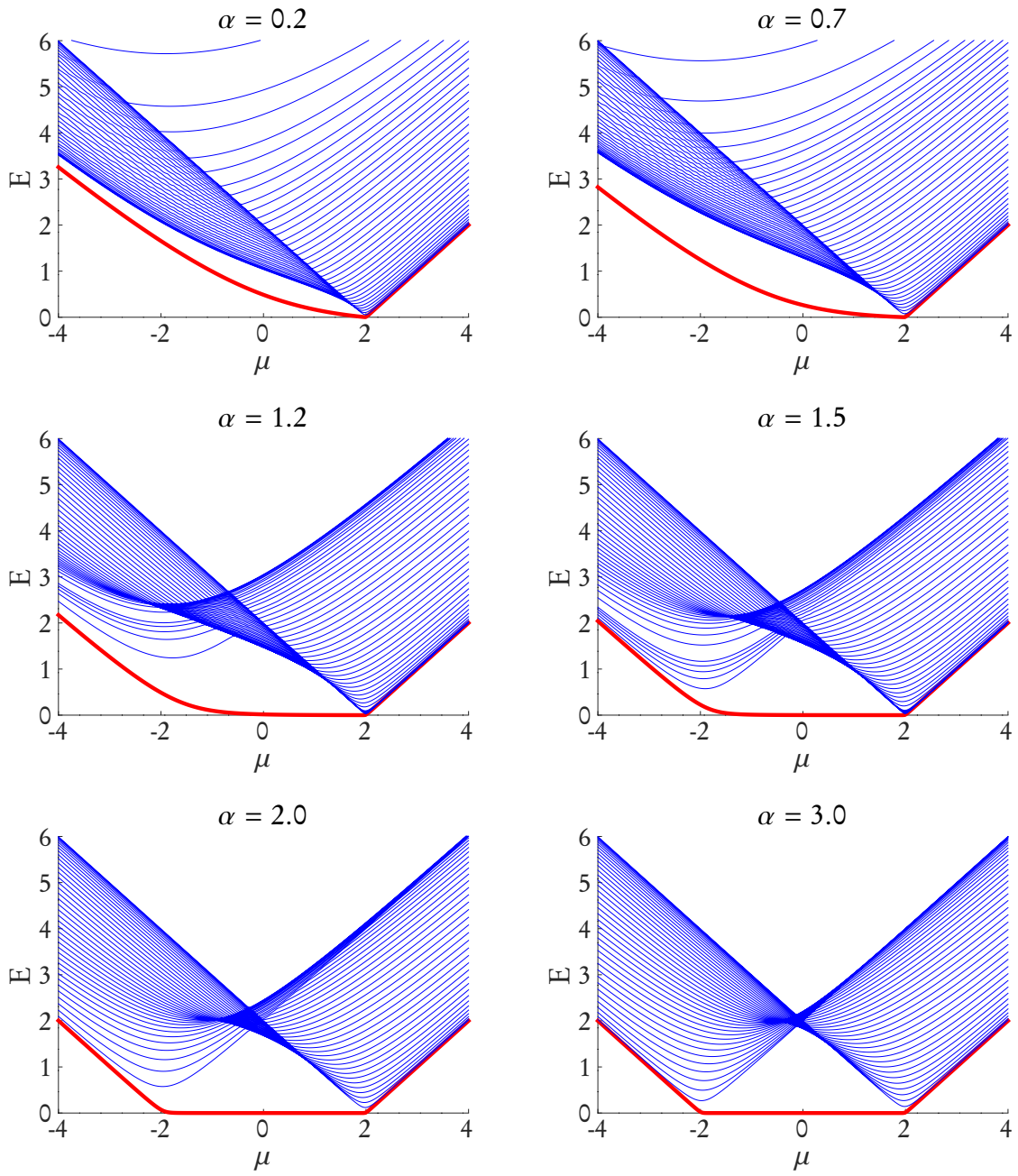

Figure 4.11: We have plotted the energy bands of the LRK with variable chemical potential μ and fixed power α for $N = 200$. In all the graphs the parameters t and Δ have been fixed to 1. It has to be noticed that not all the 200 energy levels have been plotted, but only every 5. In particular, in some cases ($\alpha = 1.2$ and $\alpha = 1.5$) all the first five levels of the band have been plotted, in order to give a real sense of the gap in the case they were not closely distributed.

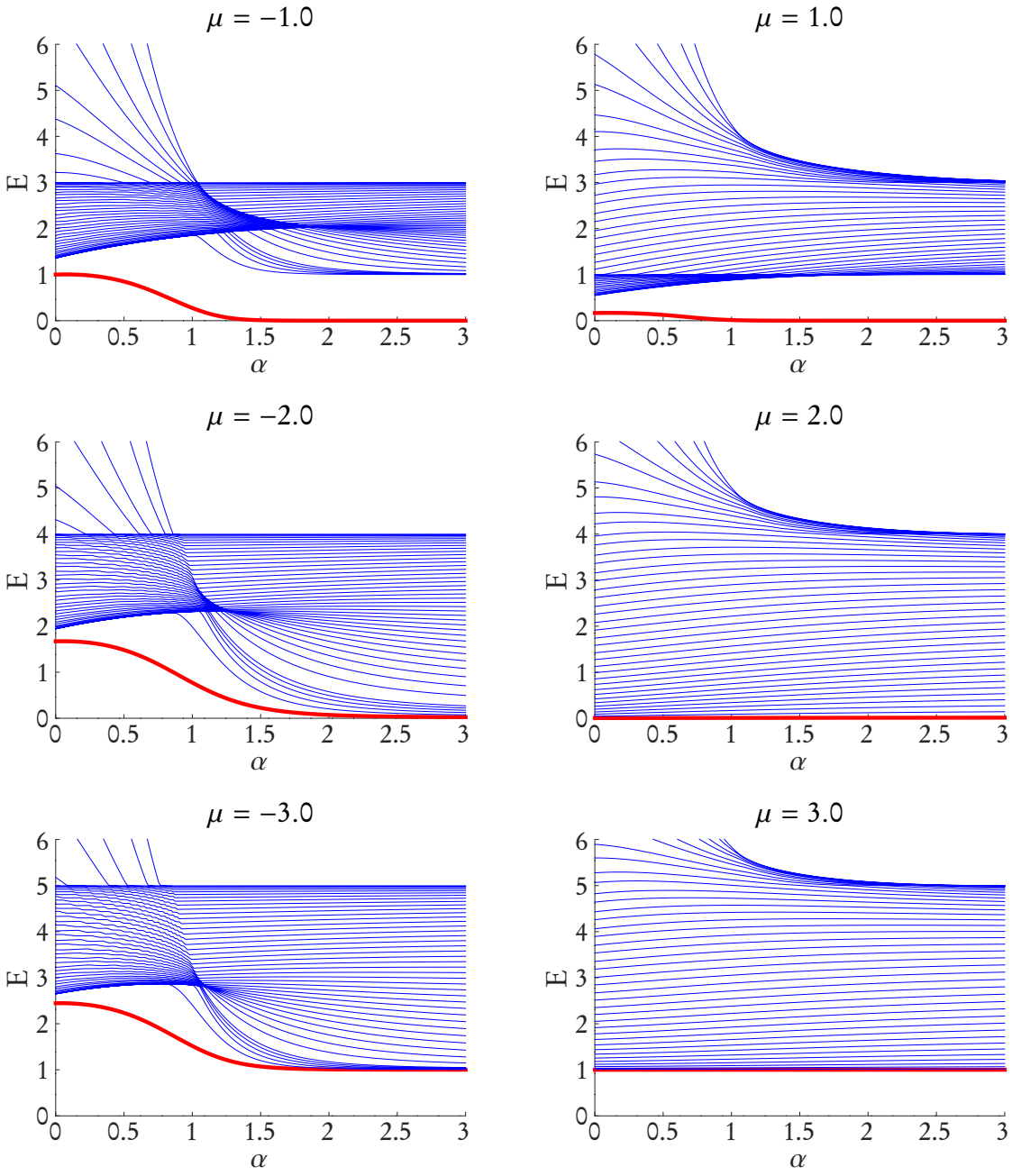

Figure 4.12: We have plotted the energy bands of the LRK with variable chemical potential μ and fixed power α for $N = 200$ sites. In all the graphs the parameters t and Δ have been fixed to 1. Analogously to Fig. 4.11, only every other 5 levels is shown. Only in the case of negative μ, also the first 5 energies are shown.

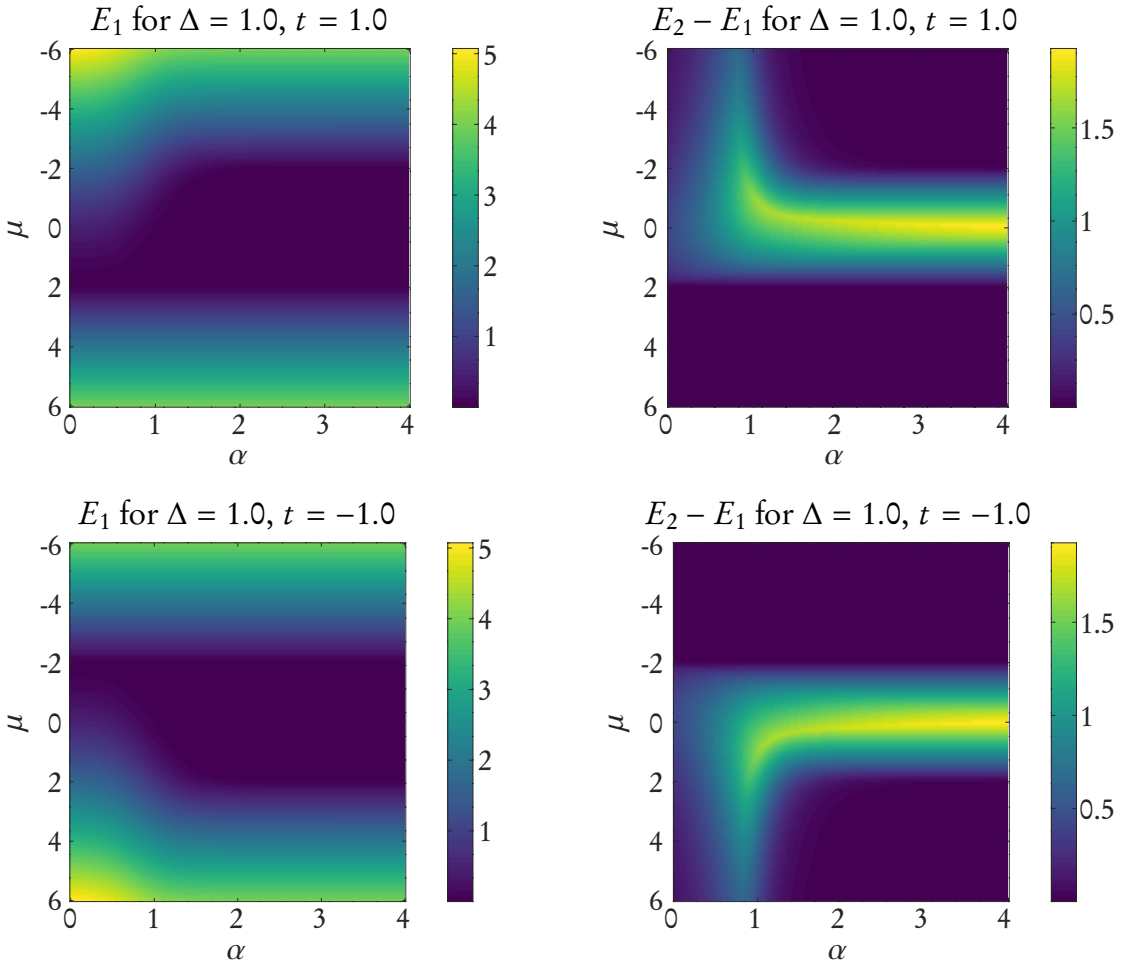

Figure 4.13: The two images report the plots of E_1 (left) and $E_2 - E_1$ (right) as function of both μ and α, for $t = 1$ (first row) and $t = -1$. In both cases the plots have calculated for $\Delta = 1$ and $N = 200$ sites.

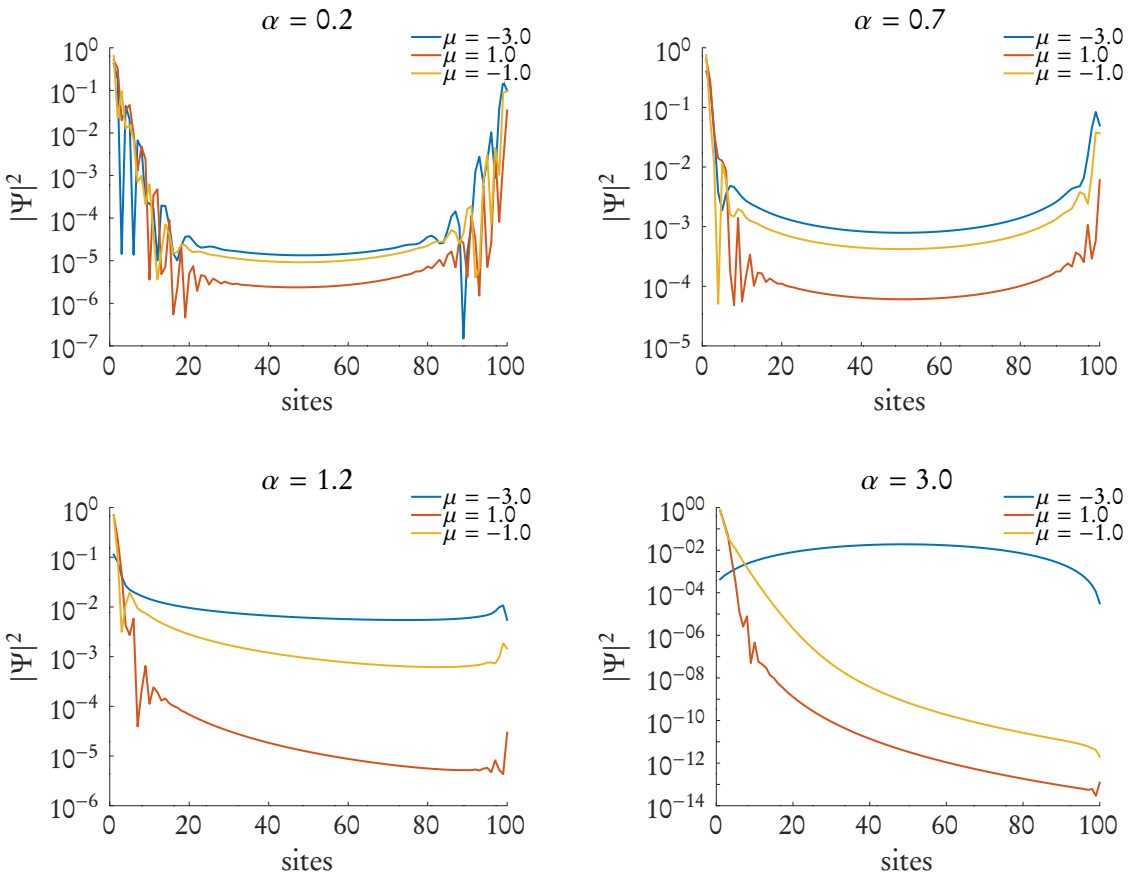

Figure 4.14: Here the wavefunctions for the LRK for different values of the power α and the chemical potential μ for $N = 200$ sites is presented. The parameters t and Δ have been fixed to 1.

Conclusion and outlooks

In this thesis we showed how the theory of Toeplitz matrices is effective for the description of short-range systems and how known facts of Topological Matter, like the bulk-edge correspondence, are already encoded in it. On the other hand, when we move to the realm of long-range systems, like LRK, most of the assumptions we took for granted for Toeplitz matrices fall short. In the case of LRK in Sec 3.5 and Sec. 4.3, we lost the boundedness of the matrix that encodes the spectrum. Hence, as consequence, the "Toeplitz version" of the bulk-edge correspondence was lost. Therefore, one was obliged to look for other topological invariants that could characterize the different phases.

For this reason in Sec 4.3 we looked at the set $\operatorname{conv}\mathcal{R}(g_\alpha)$. The transition from the inside of $\operatorname{conv}\mathcal{R}(g_\alpha)$ to its outside necessarily requires the crossing of the curve $R(g_\alpha)$, which is equivalent to a phase transition. Indeed, the fact that $0 \in R(g_\alpha) = \operatorname{sp}_{\text{ess}} T(g_\alpha)$ implies the closure of the bulk gap. Therefore, the property of the zero belonging or not to $\operatorname{conv} R(g_\alpha)$ appeared as a good candidate for the replacement of the winding number $\operatorname{wind}(g_\alpha, 0)$ being zero or not.

Based on our analysis, the crossover region of [39] should not be present. From the geometry of $\operatorname{conv}\mathcal{R}(g_\alpha)$ and $\mathcal{R}(g_\alpha)$, there should not be any reason why massive edge states should be present in the sector $1 < \alpha < 3/2$. For this reason, in Sec. 4.3, we argued that they were artifacts of the finite-size of the systems.

We want to conclude with a remark about the necessity to expand the theory of Toeplitz operator beyond what was its standard domain of application. This fact is also evident from the works of Ares et al. in [1, 2], where the entanglement entropy of the LRK chain has been investigated through the determinant of Toeplitz matrices. In particular, they found out that the Toeplitz matrix that describes the entanglement, which has the same origin as the matrix $T(g_\alpha)$ we used in our analysis, does not fall into the domain of application of the Strong Szegö Theorem of the Fisher-Hartwig conjecture. These theorems are one of the most important results in the theory of the determinants and spectrum distributions of Toeplitz matrices. In the instance of this thesis, what is needed is an investigation of the properties of unbounded Toeplitz matrices and their

distribution of eigenvalues.

Henceforth, the study of topological phases of long-range systems through the lens of Toeplitz theory requires much more development and understanding of the latter, but also of topological phases as a whole. In fact, the unconventional phase transition was unconventional for a reason, because we should not expect to move between those that are considered topologically different phases, in the short-range case at least, without closure of the gap. This is a signal that, maybe, we are in front of a new kind of phase transition and we hope to clearly understand it one day.

APPENDIX A

POLYLOGARITHM FUNCTION

The *polylogarithm* function $\mathrm{Li}_s(z)$ of order (real or complex) s and variable z is defined as

$$\mathrm{Li}_s = \sum_{n=1}^{\infty} \frac{z^n}{n^s} = \frac{z}{1^s} + \frac{z^2}{2^s} + \frac{z^3}{3^s} + \dots \tag{A.1}$$

For each fixed complex s the series defines an analytic function of z for $|z| \leq 1$. The series also converges when $|z| = 1$, provided that $\mathrm{Re}\, s > 1$. For other values $\mathrm{Li}_s(z)$ is defined via analytic continuation [30].

Integral representation For $s = n = 1, 2, \dots$ we have

$$\mathrm{Li}_n(z) = \int_0^z \frac{\mathrm{Li}_{n-1}(z)}{z} \mathrm{d}z$$

and for the special case $n = 2$

$$\mathrm{Li}_2(z) = -\int_0^z \frac{\log(z-1)}{z} \mathrm{d}z.$$

This integral relation let us extend the polylogarithm function to z outside the unit disk $|z| = 1$ for integral order [28].

Another integral representation is possible

$$\mathrm{Li}_s(z) = \frac{z}{\Gamma(s)} \int_0^{\infty} \frac{x^{s-1}}{e^x - z} \mathrm{d}z$$

which is valid for $\mathrm{Re}\, s > 0$ and $\left|\arg(1-z)\right| < \pi$, or $\mathrm{Re}\, s > 1$ and $z = 1$ [30]. Here $\Gamma(s)$ is the Gamma function of s.

Asymptotic expansion The polylogarithm can be expended as

$$\mathrm{Li}_s(z) = \Gamma(1-s)\left(\ln\frac{1}{z}\right)^{s-1} + \sum_{n=0}^{\infty}\zeta(s-n)\frac{(\ln z)^n}{n!}, \qquad s \neq 1, 2, 3\ldots, \ |\ln z| < 2\pi \quad \text{(A.2)}$$

where $\zeta(s)$ is the Riemann zeta function $\zeta(s) = \sum_{n=1}^{\infty} n^{-s}$. Furthermore,

$$\mathrm{Li}_s(e^{2\pi i a}) + e^{\pi i s}\,\mathrm{Li}_s(e^{-2\pi i a}) = \frac{(2\pi)^s e^{\pi i s/2}}{\Gamma(s)} \quad \text{(A.3)}$$

for $\mathrm{Re}\, s > 0$, $\mathrm{Im}\, a > 0$ or $\mathrm{Re}\, s > 1$, $\mathrm{Im}\, a = 0$.

Special values The function $\mathrm{Li}_s(z)$ reduces to the Riemann zeta function for $z = 1$

$$\mathrm{Li}_s(1) = \zeta(s).$$

Moreover, for $\alpha = 0$ and $\alpha = 1$ we can get the closed expression

$$\mathrm{Li}_0(z) = \frac{z}{1-z} \qquad \mathrm{Li}_1(z) = -\log(1-z)$$

which clearly are only valid for $z \neq 1$. This means we can the following expression for the function $f_\alpha(k)$ that enters the dispersion relation

$$f_1(k) = \pi - k \qquad f_0(k) = \cot\frac{k}{2}. \quad \text{(A.4)}$$

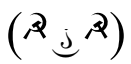

List of Figures

Bibliography

[1] F. Ares, J. G. Esteve, F. Falceto, and A. R. de Queiroz, "Entanglement entropy in the long-range Kitaev chain", Physical Review A **97**, 062301, 062301 (2018).

[2] F. Ares, J. G. Esteve, F. Falceto, and Z. Zimborás, "Sublogarithmic behaviour of the entanglement entropy in fermionic chains", arXiv e-prints, arXiv:1902.07540, arXiv:1902.07540 (2019).

[3] J. K. Asbóth, L. Oroszlány, and A. Pályi, "A Short Course on Topological Insulators", Lecture Notes in Physics **919** (2016).

[4] J. Bardeen, L. N. Cooper, and J. R. Schrieffer, "Microscopic theory of superconductivity", Physical Review **106**, 162 (1957).

[5] E. Barouch and B. M. McCoy, "Statistical Mechanics of the X Y Model. II. Spin-Correlation Functions", Physical Review A **3**, 786 (1971).

[6] A. Bernevig and T. Neupert, "Topological Superconductors and Category Theory", arXiv e-prints (2015).

[7] B. A. Bernevig and T. L. Hughes, *Topological insulators and topological superconductors* (Princeton university press, 2013).

[8] M. V. Berry, "Quantal phase factors accompanying adiabatic changes", Proc. R. Soc. Lond. A **392**, 45–57 (1984).

[9] N. N. Bogoljubov, "On a new method in the theory of superconductivity", Il Nuovo Cimento (1955-1965) **7**, 794–805 (1958).

[10] A. Boöttcher and S. M. Grudsky, *Spectral properties of banded Toeplitz matrices*, Vol. 96 (Siam, 2005).

[11] A. Böttcher and S. M. Grudsky, *Toeplitz matrices, asymptotic linear algebra and functional analysis*, Vol. 67 (Springer, 2000).

[12] A. Böttcher and B. Silbermann, *Introduction to large truncated Toeplitz matrices* (Springer Science & Business Media, 2012).

[13] A. Böttcher and B. Silbermann, *Analysis of Toeplitz operators* (Springer Science & Business Media, 2013).

[14] X. Chen, Z.-C. Gu, and X.-G. Wen, "Local unitary transformation, long-range quantum entanglement, wave function renormalization, and topological order", Phys. Rev. B **82**, 155138 (2010).

[15] P. Deift, A. Its, and I. Krasovsky, "Toeplitz matrices and Toeplitz determinants under the impetus of the Ising model: some history and some recent results", Communications on pure and applied mathematics **66**, 1360–1438 (2013).

[16] R. G. Douglas, *Banach algebra techniques in operator theory*, Vol. 179 (Springer Science & Business Media, 2012).

[17] R. M. Gray, "Toeplitz and circulant matrices: A review", Foundations and Trends® in Communications and Information Theory **2**, 155–239 (2006).

[18] M. Z. Hasan and C. L. Kane, "Colloquium: topological insulators", Reviews of modern physics **82**, 3045 (2010).

[19] A. R. Its, B. .-.-Q. Jin, and V. E. Korepin, "Entropy of XY Spin Chain and Block Toeplitz Determinants", eprint arXiv:quant-ph/0606178 (2006).

[20] A. R. Its, F. Mezzadri, and M. Y. Mo, "Entanglement Entropy in Quantum Spin Chains with Finite Range Interaction", Communications in Mathematical Physics **284**, 117–185 (2008).

[21] H. Kamerlingh Onnes, "The resistance of pure mercury at helium temperatures", Commun. Phys. Lab. Univ. Leiden, b **120** (1911).

[22] C. Kane, "Topological Band Theory and the $\mathbb{Z}_2$ Invariant", in *Contemporary Concepts of Condensed Matter Science*, Vol. 6 (Elsevier, 2013), pp. 3–34.

[23] J. P. Keating and F. Mezzadri, "Random Matrix Theory and Entanglement in Quantum Spin Chains", Communications in Mathematical Physics **252**, 543–579 (2004).

[24] A. Y. Kitaev, "Unpaired Majorana fermions in quantum wires", Physics Uspekhi **44**, 131 (2001).

[25] A. Kitaev, "Periodic table for topological insulators and superconductors", in AIP Conference Proceedings, Vol. 1134, 1 (AIP, 2009), pp. 22–30.

[26] K. v. Klitzing, G. Dorda, and M. Pepper, "New Method for High-Accuracy Determination of the Fine-Structure Constant Based on Quantized Hall Resistance", Phys. Rev. Lett. **45**, 494–497 (1980).

[27]M. Leijnse and K. Flensberg, "Introduction to topological superconductivity and Majorana fermions", Semiconductor Science Technology **27**, 124003, 124003 (2012).

[28]L. Lewin, "Polylogarithms and associated functions", (1981).

[29]E. Lieb, T. Schultz, and D. Mattis, "Two soluble models of an antiferromagnetic chain", Annals of Physics **16**, 407–466 (1961).

[30]F. W. Olver, D. W. Lozier, R. F. Boisvert, and C. W. Clark, *NIST handbook of mathematical functions* (Cambridge University Press, 2010).

[31]X.-L. Qi and S.-C. Zhang, "Topological insulators and superconductors", Reviews of Modern Physics **83**, 1057 (2011).

[32]A. P. Schnyder, S. Ryu, A. Furusaki, and A. W. W. Ludwig, "Classification of topological insulators and superconductors in three spatial dimensions", Phys. Rev. B **78**, 195125 (2008).

[33]J. R. Schrieffer, *Theory of superconductivity* (CRC Press, 2018).

[34]S.-Q. Shen, *Topological insulators*, Vol. 174 (Springer, 2012).

[35]J. C. Teo and C. L. Kane, "Topological defects and gapless modes in insulators and superconductors", Physical Review B **82**, 115120 (2010).

[36]D. J. Thouless, M. Kohmoto, M. P. Nightingale, and M. den Nijs, "Quantized Hall Conductance in a Two-Dimensional Periodic Potential", Phys. Rev. Lett. **49**, 405–408 (1982).

[37]D. Tong, "Lectures on the Quantum Hall Effect", arXiv e-prints (2016).

[38]J. G. Valatin, "Comments on the theory of superconductivity", Il Nuovo Cimento (1955-1965) **7**, 843–857 (1958).

[39]O. Viyuela, D. Vodola, G. Pupillo, and M. A. Martin-Delgado, "Topological massive Dirac edge modes and long-range superconducting Hamiltonians", Phys. Rev. B **94**, 125121 (2016).

[40]D. Vodola, L. Lepori, E. Ercolessi, A. V. Gorshkov, and G. Pupillo, "Kitaev Chains with Long-Range Pairing", Physical Review Letters **113**, 156402, 156402 (2014).

[41]D. Vodola, L. Lepori, E. Ercolessi, and G. Pupillo, "Long-range Ising and Kitaev models: phases, correlations and edge modes", New Journal of Physics **18**, 015001, 015001 (2016).

[42]D. Vodola, "Correlations and Quantum Dynamics of 1D Fermionic Models: New Results for the Kitaev Chain with Long-Range Pairing", PhD thesis (alma, Feb. 2015).